



COMILLAS
UNIVERSIDAD PONTIFICIA

ICAI

MÁSTER UNIVERSITARIO EN INGENIERÍA INDUSTRIAL

TRABAJO FIN DE MÁSTER

**EXPERIMENTAL ANALYSIS ON THE INFLUENCE
OF AMBIENT TEMPERATURE ON THE
MECHANICS OF LITHIUM-ION CELL MODULES**

Autor: Jaime Gutiérrez Galindo

Director: M.Sc. Maximilian Altmann

Madrid

Agosto de 2019

AUTHORIZATION FOR DIGITALIZATION, STORAGE AND DISSEMINATION IN THE NETWORK OF END-OF-DEGREE PROJECTS, MASTER PROJECTS, DISSERTATIONS OR BACHILLERATO REPORTS

1. Declaration of authorship and accreditation thereof.

The author Mr. /Ms. Jaime Gutiérrez Galindo

HEREBY DECLARES that he/she owns the intellectual property rights regarding the piece of work: Experimental Analysis on the Influence of Ambient Temperature on the Mechanics of Lithium-Ion Cell Modules that this is an original piece of work, and that he/she holds the status of author, in the sense granted by the Intellectual Property Law.

2. Subject matter and purpose of this assignment.

With the aim of disseminating the aforementioned piece of work as widely as possible using the University's Institutional Repository the author hereby **GRANTS** Comillas Pontifical University, on a royalty-free and non-exclusive basis, for the maximum legal term and with universal scope, the digitization, archiving, reproduction, distribution and public communication rights, including the right to make it electronically available, as described in the Intellectual Property Law. Transformation rights are assigned solely for the purposes described in a) of the following section.

3. Transfer and access terms

Without prejudice to the ownership of the work, which remains with its author, the transfer of rights covered by this license enables:

- a) Transform it in order to adapt it to any technology suitable for sharing it online, as well as including metadata to register the piece of work and include "watermarks" or any other security or protection system.
- b) Reproduce it in any digital medium in order to be included on an electronic database, including the right to reproduce and store the work on servers for the purposes of guaranteeing its security, maintaining it and preserving its format.
- c) Communicate it, by default, by means of an institutional open archive, which has open and cost-free online access.
- d) Any other way of access (restricted, embargoed, closed) shall be explicitly requested and requires that good cause be demonstrated.
- e) Assign these pieces of work a Creative Commons license by default.
- f) Assign these pieces of work a HANDLE (*persistent URL*), by default.

4. Copyright.

The author, as the owner of a piece of work, has the right to:

- a) Have his/her name clearly identified by the University as the author
- b) Communicate and publish the work in the version assigned and in other subsequent versions using any medium.
- c) Request that the work be withdrawn from the repository for just cause.
- d) Receive reliable communication of any claims third parties may make in relation to the work and, in particular, any claims relating to its intellectual property rights.

5. Duties of the author.

The author agrees to:

- a) Guarantee that the commitment undertaken by means of this official document does not infringe any third party rights, regardless of whether they relate to industrial or intellectual property or any other type.

- b) Guarantee that the content of the work does not infringe any third party honor, privacy or image rights.
- c) Take responsibility for all claims and liability, including compensation for any damages, which may be brought against the University by third parties who believe that their rights and interests have been infringed by the assignment.
- d) Take responsibility in the event that the institutions are found guilty of a rights infringement regarding the work subject to assignment.

6. Institutional Repository purposes and functioning.

The work shall be made available to the users so that they may use it in a fair and respectful way with regards to the copyright, according to the allowances given in the relevant legislation, and for study or research purposes, or any other legal use. With this aim in mind, the University undertakes the following duties and reserves the following powers:

- a) The University shall inform the archive users of the permitted uses; however, it shall not guarantee or take any responsibility for any other subsequent ways the work may be used by users, which are non-compliant with the legislation in force. Any subsequent use, beyond private copying, shall require the source to be cited and authorship to be recognized, as well as the guarantee not to use it to gain commercial profit or carry out any derivative works.
- b) The University shall not review the content of the works, which shall at all times fall under the exclusive responsibility of the author and it shall not be obligated to take part in lawsuits on behalf of the author in the event of any infringement of intellectual property rights deriving from storing and archiving the works. The author hereby waives any claim against the University due to any way the users may use the works that is not in keeping with the legislation in force.
- c) The University shall adopt the necessary measures to safeguard the work in the future.
- d) The University reserves the right to withdraw the work, after notifying the author, in sufficiently justified cases, or in the event of third party claims.

Madrid, on ...26th... ofAugust....., 2019.

HEREBY ACCEPTS

Signed..........

Reasons for requesting the restricted, closed or embargoed access to the work in the Institution's Repository

Declaro, bajo mi responsabilidad, que el Proyecto presentado con el título **“Experimental Analysis on the Influence of Ambient Temperature on the Mechanics of Lithium-Ion Cell Modules”** en la ETS de Ingeniería - ICAI de la Universidad Pontificia Comillas en el curso académico 2018/19 es de mi autoría, original e inédito y no ha sido presentado con anterioridad a otros efectos. El Proyecto no es plagio de otro, ni total ni parcialmente y la información que ha sido tomada de otros documentos está debidamente referenciada.



Fdo.: Jaime Gutiérrez Galindo

Fecha: ...26.../ ...08.../ ...2019...

Autorizada la entrega del proyecto

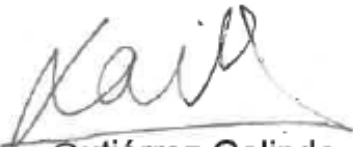
EL DIRECTOR DEL PROYECTO



Fdo.: Maximilian Altmann

Fecha: 26 / 08 / 2019

I hereby declare, under my own responsibility, that the Project presented under the title "**Experimental Analysis on the Influence of Ambient Temperature on the Mechanics of Lithium-Ion Cell Modules**" at the ETS de Ingeniería - ICAI of the Universidad Pontificia Comillas in the academic year 2018/19 is of my authorship, original and unpublished and has not been presented previously for other purposes. The Project is not plagiarism of another, neither totally nor partially and the information that has been taken from other documents is duly referenced.



Signed.: Jaime Gutiérrez Galindo

Date: ...26.../ ...08.../ ...2019...

Project submission authorized

THE DIRECTOR OF THE PROJECT



Signed.: Maximilian Altmann

Date: 26 / 08 / 2019



COMILLAS

UNIVERSIDAD PONTIFICIA

ICAI

MÁSTER UNIVERSITARIO EN INGENIERÍA INDUSTRIAL

TRABAJO FIN DE MÁSTER

**EXPERIMENTAL ANALYSIS ON THE INFLUENCE
OF AMBIENT TEMPERATURE ON THE
MECHANICS OF LITHIUM-ION CELL MODULES**

Autor: Jaime Gutiérrez Galindo

Director: M.Sc. Maximilian Altmann

Madrid

Agosto de 2019

ANÁLISIS EXPERIMENTAL DE LA INFLUENCIA DE LA TEMPERATURA AMBIENTE SOBRE LA MECÁNICA DE LOS MÓDULOS DE CÉLULAS ION-LITIO

Autor: Gutiérrez Galindo, Jaime.

Director ICAI: Linares Hurtado, José Ignacio.

Entidad Colaboradora: The BMW Group.

RESUMEN DEL PROYECTO

Introducción

La industria del automóvil está viviendo actualmente uno de los cambios tecnológicos más importantes de su historia. Desde sus primeros indicios a finales del siglo XX, el concepto de *electromobilidad* es la transición más sonada que nuestro mundo parece necesitar en estos momentos.

El imparable calentamiento de la capa atmosférica por las emisiones de dióxido de carbono, los elevados niveles de contaminación en zonas urbanas y la hasta ahora exclusiva dependencia en los combustibles fósiles por parte de la industria del transporte son los principales factores que han impulsado el rechazo a los motores de combustión y el nacimiento de una nueva industria, que quizás está llegando con demasiada prisa.

La realidad de la industria automovilística moderna es que se ha convertido en una intensa carrera tecnológica, estimulada tanto por los gobiernos como por los propios consumidores finales, necesitada de numerosas y creativas soluciones para poder transformar el parque circulante en un tiempo inferior al que parece posible. Esta situación ha fomentado el espíritu científico en la industria, respaldado por los enormes presupuestos que las empresas del sector están invirtiendo en I+D.

Las incertidumbres tecnológicas, la falta de infraestructura y el miedo al cambio son los obstáculos que están ralentizando esta transformación tan solicitada por todos. Uno de los problemas derivados del coche eléctrico es el peligro que traen las baterías y las altas corrientes necesitadas para poner el vehículo en movimiento. La transformación de esta

industria pasa primero por enfrentarse y controlar esta nueva fuente de problemas, inexistente en la era de los motores tradicionales, que pone en peligro la seguridad de los usuarios de una forma que hasta ahora nunca había tenido que ser abordada.

Y no sólo es la energía eléctrica el objeto de estudio en el ámbito de la seguridad operacional. Los nuevos diseños de componentes derivados de la arquitectura del vehículo eléctrico también deben ser enfocados desde el punto de vista mecánico. Los problemas relacionados con las vibraciones, tanto acústicos como de fatiga y resonancia, deben ser de nuevo analizados, en un área ya perfectamente controlada en el campo de los motores de combustión.

Un factor añadido del vehículo eléctrico, derivado de la carrera tecnológica tan intensa y veloz que supone, es la gran variedad de distintos diseños de los sistemas de almacenamiento de energía y de los materiales que los constituyen. Esto hace que los posibles problemas que van apareciendo sean abordados de una forma más individualizada, demanden más tiempo y que las soluciones aportadas sólo puedan ser aplicadas a determinadas estructuras.

Una forma de entender la estructura y los componentes propios de un vehículo eléctrico es a través de su clasificación en tres niveles energéticos. En el nivel más elemental se encuentran las células, encargadas de realizar los procesos electroquímicos que proporcionan la energía eléctrica necesaria a través de reacciones químicas entre los materiales activos que contienen. Las que mayor alcance comercial tienen en la actualidad son las de ion-litio, de mayor tamaño que las empeladas

en los dispositivos móviles y capaces de entregar un voltaje de unos 3.7V. En un nivel inmediatamente superior se encuentran lo que se conoce como módulos. Un módulo es simplemente un conjunto de células empaquetadas, generalmente a modo de caja. Su tamaño, peso y forma depende esencialmente del número de células que contienen, representativo de su nivel energético. Las células dentro de un módulo se agrupan y son conectadas en serie y paralelo, en función del voltaje y corriente que se desea obtener, respectivamente. Además de las células, ciertos elementos estructurales son necesarios para proteger y aislar las células de agentes como la temperatura, la humedad y partículas, además de para juntar las células ocupando el mínimo espacio posible. En el nivel más superior estaría el sistema de almacenamiento de energía eléctrica, más comúnmente conocido como batería. Estos sistemas consisten en la agrupación de varios módulos hasta formar un sistema de alto voltaje, del orden de 400-800V. También se constituyen de todo el cableado que conecta con el motor eléctrico, el freno regenerativo, los distintos módulos y el Battery Management System (BMS), encargado de controlar y monitorizar los niveles de carga y voltaje de cada célula.

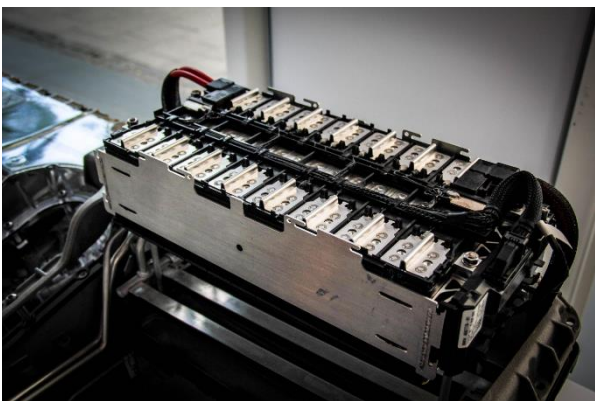


Figure 1. Arquitectura de la generación actual de los módulos de BMW

El comportamiento mecánico de estos componentes ha sido objeto de estudio reciente en la industria. El foco se ha puesto en el comportamiento vibratorio y dinámico de los componentes de mayor interés, bajo las distintas condiciones operacionales que se pueden dar. Tres agentes físicos se han clasificado como los agentes operacionales de mayor influencia: el estado de carga de la

batería (SOC, por sus siglas en inglés), el estado de salud de la batería; debido al desgaste por el número de ciclos de carga y descarga (SOH), y la temperatura (T).

Estudios recientes [HOOP15, POPP18] han abordado análisis sobre la influencia del SOC y SOH en el comportamiento vibratorio de células conocidas como *pouch-cells*, presentes en muchos dispositivos electrónicos del día a día. La técnica de estudio vibratorio más comúnmente implementada es el análisis modal, el cual permite determinar los modos vibratorios y las frecuencias naturales de vibración propias del objeto de estudio. El análisis modal experimental se lleva a cabo por medio de dos técnicas: ensayo de impacto con martillo modal, o *impact testing*, o ensayo de vibraciones inducidas por un *shaker*. Las aplicaciones de cada técnica son muy dependientes del tamaño y morfología del objeto de estudio y del rango de vibraciones que se desea analizar.

Lo que los estudios actuales no han sido aún capaces de cuantificar es la influencia que tiene la temperatura sobre el comportamiento vibratorio de estos elementos. Más desconocido aún es el mismo análisis llevado al nivel del módulo. Los muy diferentes diseños de módulos de células y la privacidad con la que estos se mantienen desde el lado de las compañías es la causa de que no haya ninguna evidencia científica sobre este tema.

El objeto principal de estudio de este trabajo es precisamente analizar el impacto que tiene la temperatura en el comportamiento vibratorio de un módulo de células de ion-litio. Este estudio se aborda por medio de la técnica de análisis modal. Además de ello, se busca justificar los cambios de comportamiento observados a nivel módulo desde un nivel inferior, a nivel material, por medio del ensayo de los materiales del módulo propensos a sufrir cambios por el efecto de la temperatura. Un último objetivo es el desarrollo de un método o técnica que permita abordar este estudio de una manera más estandarizada, aplicable a otras arquitecturas de módulos, e incluso llevable al nivel superior energético de los sistemas de almacenamiento de alto voltaje.

Se estudiaron diferentes técnicas de ensayo de materiales para abordar el impacto de la

temperatura. Se eligió la técnica del *Dynamic Mechanical Analysis* (DMA) por su relación con las propiedades dinámicas y mecánicas de los materiales y la posibilidad que ofrece de realizar ensayos con variación constante de la temperatura. Los conceptos teóricos y las descripciones de las magnitudes viscoelásticas propias de la técnica fueron comprendidas y consideradas muy representativas del objetivo de estudio que se pretende [AVIT09].

Metodología

Este trabajo ha sido realizado en colaboración con The BMW Group en Múnich, Alemania. El objeto de estudio es un módulo de células conocido como “dummy”, sin carga alguna para evitar los peligros de operar con componentes eléctricos, el cual ha sido proporcionado por la empresa como parte del proceso de desarrollo e investigación de componentes eléctricos.

El primer paso fue realizar un profundo análisis de los distintos componentes presentes en el módulo, con el fin de detectar aquellos que puedan verse seriamente afectados por el efecto de la temperatura. Tres elementos de materiales poliméricos fueron seleccionados con la intención de llevar a cabo un análisis a nivel material. Estos componentes se recogen bajo los nombres TCE, SA y HCA.

El segundo paso consiste en el diseño y planificación de los ensayos modales bajo el efecto de la temperatura. Los ensayos fueron diseñados para realizarse en una cámara climática que permita simular distintos escenarios de temperaturas de operación y por medio de la técnica del *impact testing* con martillo modal. Según la norma de transporte de bienes peligrosos y del manejo de baterías de ion-litio [UN38, KORT13], se establecieron los límites del rango de temperaturas de estudio de -40°C a $+50^{\circ}\text{C}$. Este rango permite asegurar el estudio de las temperaturas operacionales que se pueden encontrar bajo servicio, incluyendo condiciones realmente extremas.

A continuación se diseñaron y valoraron tres diferentes estrategias de medida en cámara climática. Por motivos de seguridad en condiciones extremas, se eligió una estrategia

con apertura de puerta, que sin embargo mantuviera una estabilidad de la temperatura aceptable durante todo el ensayo. La validez de esta estrategia fue asegurada a través del registro de la temperatura en diversos puntos de módulos por medio de la instalación de varios termopares. Se llevaron a cabo con éxito hasta cuatro ensayos: a -20°C , 0°C , $+20^{\circ}\text{C}$ y $+40^{\circ}\text{C}$. Para el caso más extremo de estudio, el de -20°C (debido al mayor desnivel de temperatura con la apertura de puerta), se registra un desnivel de temperatura menor de 5°C entre la mayor y la menor temperatura registrada por cualquiera de los termopares. Este rango se considera suficientemente aceptable.

Previo a los ensayos modales, se diseñó un sistema de soporte del módulo que permitiera simular el *free-free state* necesario para recoger las frecuencias naturales propias únicamente del objeto de estudio [HOOP15]. Los ensayos modales se llevaron a cabo con un martillo modal comercial de PCB Piezotronics, para el cual se evaluó la punta que permitiera obtener una mayor precisión hasta una frecuencia de 2.5kHz de interés de estudio. La respuesta vibratoria fue medida con un acelerómetro colocado en el eje longitudinal del módulo, asegurándose de no coincidir con un nodo en ninguno de los modos de vibración observables. El colector de señales MKII y el software PAK fueron empleados para la interpretación de las señales.

Los ensayos modales tuvieron una duración de unas dos horas cada uno, con una malla de medida de un total de 20 puntos de medición. Las funciones de respuesta en frecuencia (FRF) y de coherencia (CF) fueron analizadas para recolectar las frecuencias naturales de vibración y para asegurar la correcta relación causa-efecto de las señales recogidas, respectivamente. Este proceso fue realizado de manera similar para los cuatro escenarios de temperatura.

A nivel material, se diseñaron y llevaron a cabo tres ensayos mecánicos dinámicos (DMA), uno por cada elemento de estudio, con el fin de recoger la influencia de la temperatura sobre las propiedades dinámicas elásticas de los tres materiales. El tipo de ensayo DMA se realizó a tensión, el cual permite recoger el valor del *Storage Modulus* (capacidad de almacenar la energía elásticamente), *Loss Modulus* (capacidad de disipar la energía o comportamiento viscoso) y *Tan Delta* (amortiguamiento o ratio del segundo entre el primero); magnitudes viscoelásticas muy representativas del comportamiento vibratorio de materiales [AVIT09]. Los ensayos DMA se diseñaron en un rango de temperaturas de interés de -40°C a $+50^{\circ}\text{C}$, con un intervalo de confianza de 10°C extra en cada extremo debido a las fases transitorias al principio y final del ensayo.

Para poder llevar a cabo los ensayos de DMA se diseñaron unas probetas de medida para cumplir con la geometría de ensayo requerida por la propia técnica. Para los elementos SA y HCA se llevó a cabo un proceso de preparación de probetas a partir de los materiales almacenados en depósitos. Para el caso del TCE, esto no fue necesario. El proceso fue llevado a cabo con éxito para los dos materiales, de los cuales se obtuvieron entre 8 y 12 probetas de cada uno. El diseño del proceso de obtención de probetas se validó para futuros ensayos.

Resultados

A nivel módulo, se recogieron y analizaron con éxito las frecuencias naturales del primer modo de vibración para los cuatro escenarios de temperatura. Para ello, se computaron las frecuencias naturales de cada punto de medición por medio del análisis de varianza (ANOVA), con el fin de mostrar también la dispersión de los puntos de medida y la precisión de los resultados mostrados.

Los resultados muestran una notable disminución de la frecuencia natural de vibración con el aumento de la temperatura. Una regresión exponencial muestra una tendencia bastante marcada a nivel cualitativo. El número de puntos no permite sin embargo

un preciso estudio a nivel cuantitativo, más allá de la regresión de ajuste mostrada.

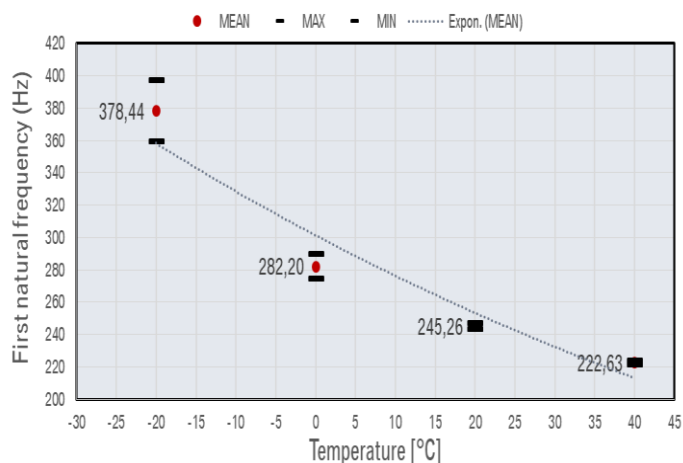


Figure 2. Análisis de varianza y representación de las frecuencias naturales del primer modo de vibración en el plano de temperaturas de interés

A nivel material, se llevaron a cabo exitosamente los ensayos dinámicos mecánicos de los tres materiales poliméricos de interés. El rango de temperaturas de interés fue correctamente registrado con la parametrización implementada en cada uno de los tres ensayos. Los resultados muestran una caída sustancial del *Storage Modulus* a medida que aumenta la temperatura. Este comportamiento se observa de manera muy notable para los tres materiales, con especial prominencia del TCE, el cual se encuentra en un orden de magnitud superior a los otros dos.

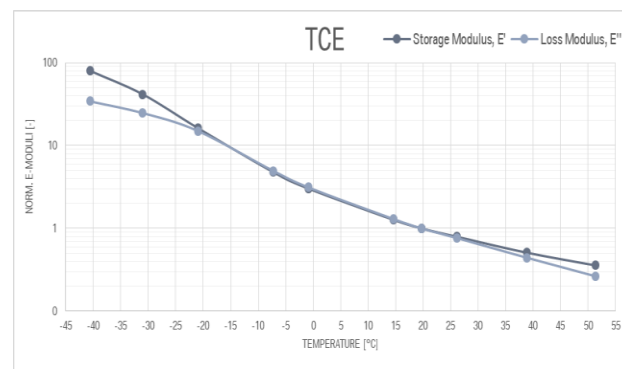


Figure 3. Representación del Storage Modulus del espécimen TCE en el rango de temperatura

Conclusiones

El ANOVA sobre la primera frecuencia natural de los cuatro escenarios de temperatura muestra una caída, aproximadamente exponencial, de la frecuencia natural con el aumento de la temperatura. Los resultados muestran una mayor dispersión de los datos cuanto mayor es la diferencia de temperatura entre el interior de la cámara climática y el ambiente al abrir la puerta. Las diferencias de frecuencia son muy notables para el rango de temperaturas estudiado, lo que supone un comportamiento vibratorio de los módulos de células muy diferente en función de la temperatura de operación. Este aspecto es considerado de suma importancia en la fase de diseño de estructuras y los resultados arrojan información muy interesante en este ámbito. Se sugiere un análisis similar sobre módulos reales, cargados eléctricamente, que puedan confirmar los resultados aquí vistos.

A nivel material, la presencia de estos componentes poliméricos en la estructura del módulo de celdas puede tener una gran influencia en el comportamiento vibratorio de la estructura completa, ya que se observa una caída de más del 95% en las magnitudes dinámicas de importancia en aspectos vibratorios de estos materiales. Estos datos arrojan información muy útil en la fase de diseño y producción estructural de estos módulos al tener en cuenta los materiales adhesivos que se vayan a usar.

Por último, las técnicas implementadas para el estudio de la influencia de la temperatura sobre las propiedades mecánicas de los módulos de células de ion-litio han sido ampliamente confirmadas para su posterior aplicación en el estudio de otras arquitecturas de módulos y materiales estructurales propios de ellos. Se ha

establecido también una relación, únicamente a nivel cualitativo, entre los comportamientos vibratorios del módulo y la variación de los valores de ciertas propiedades viscoelásticas de materiales de interés presentes en el módulo de células de estudio.

Este proyecto no confirma, sin embargo, que los resultados observados en la primera frecuencia natural de vibración sean también observados en las sucesivas frecuencias naturales propias del objeto de estudio. Tampoco está clara la realidad del comportamiento vibratorio del módulo real, al haberse implementado la técnica sobre un módulo sin carga eléctrica alguna.

Queda para objeto de estudio complementario la confirmación de los resultados aquí arrojados en un módulo real con carga eléctrica, así como el análisis del efecto de la temperatura sobre los modos de vibración del módulo de células en frecuencias más altas.

Referencias

- [AVIT09] – P. Avitabile, Sound & Vibration Magazine.
- [HOOP15] - Hooper J.M., Marco J. - Experimental Modal Analysis of Lithium-Ion Pouch Cells.
- [KORT13] – Reiner Korthauer, 2013, „Handbuch Lithium-Ionen Batterien“ (Springer Vieweg).
- [POPP18] - Popp H., Glanz G. - Mechanical Frequency Response Analysis of LIBs.
- [UN38] – European Union, Transportation of Dangerous Goods, 5th revised edition.

EXPERIMENTAL ANALYSIS ON THE INFLUENCE OF AMBIENT TEMPERATURE ON THE MECHANICS OF LITHIUM-ION CELL MODULES

Introduction

The automotive industry is currently experiencing one of the most important technological changes in its history. Since its first steps at the end of the 20th century, the concept of electromobility has become the most demanded transition that our world seems to need at this time.

The unstoppable warming of the atmosphere by carbon dioxide emissions, high levels of pollution in urban areas and the hitherto exclusive dependence on fossil fuels by the transport industry are the main factors that have driven the rejection of combustion engines and the birth of a new industry, which is perhaps arriving in too great a hurry.

The reality of the modern automobile industry is that it has become an intense technological race, stimulated both by governments and by end consumers themselves, in need of numerous and creative solutions to be able to transform the circulating fleet in a time less than it seems possible to. This situation has fostered the scientific spirit in the industry, backed up by the enormous budgets that companies in the sector are investing in R&D.

Technological uncertainties, lack of infrastructure and fear of change are the obstacles that are slowing down this much-needed transformation. One of the problems arising from the electric car is the danger brought by the batteries and the high currents needed to put the vehicle into motion. The transformation of this industry is first to face and control this new source of problems, non-existent in the era of traditional engines, which endangers the safety of users in a way that until now had never had to be addressed.

And it is not only the electrical energy what is being studied in the field of operational safety. New component designs derived from the architecture of the electric vehicle must also be approached from the mechanical point of view. The problems related to vibrations, both acoustic as well as fatigue and resonance, must

be re-analyzed, in an area already perfectly controlled in the field of combustion engines.

An added factor of the electric vehicle, derived from the intense and fast technological race that it represents, is the great variety of designs of energy storage systems and the materials that constitute them. This means that the possible problems that arise are addressed in a more individualized way, require more time and that the solutions provided can only be applied to certain structures.

One way of understanding the structure and components of an electric vehicle is through its classification into three energy levels. At the most elementary level are the cells, in charge of carrying out the electrochemical processes that provide the demanded electrical energy through chemical reactions between the active materials they contain. The ones with the greatest commercial influence in the automotive industry nowadays are lithium-ion cells, which are bigger than those similar ones used in mobile devices and capable of delivering a voltage of around 3.7V. At an immediately higher level are what are known as modules. A module is simply a set of packaged cells. Their size, weight and shape depends essentially on the number of cells they contain, representative of their energy level. The cells within a module are grouped and connected in series and parallel, depending on the voltage and current to be obtained, respectively. In addition to the cells, certain structural elements are necessary to protect and isolate the cells from agents such as temperature, humidity and particles, as well as to bring the cells together in the smallest possible space. At the highest level would be the electrical energy storage system, more commonly known as battery. These systems consist of the grouping of several modules into a high voltage system, at an order of 400-800V. They also include all the wiring that connects to the electric motor, the regenerative brake, the various modules and the Battery Management System (BMS), responsible for

controlling and monitoring the current and voltage of each cell.

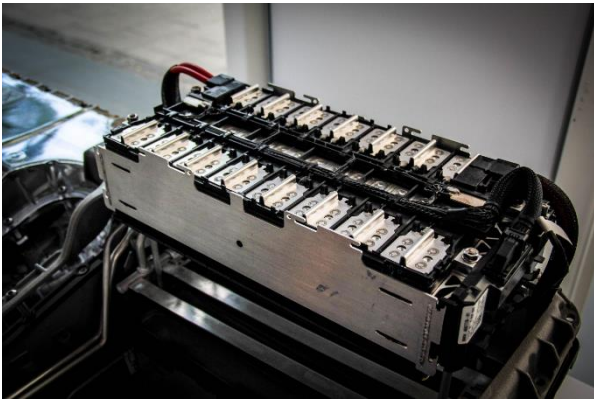


Figure 4. BMW's current generation of cell modules

The mechanical behavior of these components has been the subject of recent study in industry. The focus has been placed on the vibratory and dynamic behavior of the components of greatest interest, under the different operational conditions that can occur. Three physical agents have been classified as the most influential operational agents: the state of charge of the battery (SOC), the state of health of the battery; due to wear by the number of charge and discharge cycles (SOH), and temperature (T).

Recent studies [HOOP15, POPP18] have undertaken several analyses of the influence of SOC and SOH on the vibratory behavior of the so-called pouch-cells, present in many everyday electronic devices. The most commonly implemented technique is modal analysis, which allows for the determination of the vibratory modes and natural frequencies of the object of study. Experimental modal analysis is carried out by means of two techniques: impact testing with a modal hammer, or vibration testing by the use of a shaker, known as shaker test. The applications of each technique are highly dependent on the size and morphology of the object of study and the range of vibrations to be analyzed.

What current studies have not yet been able to quantify is the influence that temperature has on the vibratory behavior of these elements. Even more unknown is the same analysis carried out at the module level. The very different designs of cell modules and the privacy with which they are maintained from

the side of the companies is the reason why there is no scientific evidence on this subject.

The main object of study of this work is in fact to analyze the impact that temperature has on the vibratory behavior of a lithium-ion cell module. This study is approached by means of the modal analysis technique. In addition, it seeks to justify changes in behavior observed at the module level from a lower level, at the material level, by testing module materials prone to change due to the effect of temperature. A final objective is the development of a method or technique that allows this study to be approached in a more standardized manner, applicable to other module architectures, and even transferable to the higher energy level of high-voltage storage systems.

Different materials testing techniques were studied to address the impact of temperature. The Dynamic Mechanical Analysis (DMA) technique was chosen because of its close relationship with the dynamic and mechanical properties of the materials and the possibility it offers of carrying out tests with constant variation of the temperature. The theoretical concepts and descriptions of the viscoelastic magnitudes of the technique were understood and considered very representative of the objectives of this work [AVIT09].

Work Methodology

This work has been carried out in collaboration with The BMW Group in Munich, Germany. The object of study is a cell module known as "dummy", without any load, to avoid the dangers of operating with electrical components, which has been provided by the company as part of the process of development and research of electrical components.

The first step was to carry out an in-depth analysis of the different components present in the module, in order to detect those that could be seriously affected by the effect of temperature. Three elements of polymeric materials were selected with the intention of carrying out a material level analysis. These components are collected under the names TCE, SA and HCA.

The second step consists of the design and planning of modal tests under the effect of temperature. The tests were designed to be carried out in a climatic chamber to simulate different operating temperature scenarios and by means of the impact testing technique with a modal hammer. According to the regulations for the transport of dangerous goods and the handling of lithium-ion batteries [UN38, KORT13], the limits of the study temperature range of -40°C to $+50^{\circ}\text{C}$ were established. This range allows to ensure the study of the operational temperatures that can be found under service, including really extreme, yet feasible conditions.

Three different strategies for climatic chamber measurement were designed and evaluated. For safety reasons in such extreme conditions, a door-opening strategy was chosen, which nevertheless provided acceptable temperature stability throughout the test. The validity of this strategy was ensured by recording the temperature at various module points by installing several thermocouples. Up to four tests were successfully carried out: at -20°C , 0°C , $+20^{\circ}\text{C}$ and $+40^{\circ}\text{C}$. For the most extreme case study, that of -20°C (due to the higher temperature difference with the door opening), a temperature difference of less than 5°C is recorded between the higher and the lower temperature by any of the thermocouples. This range is considered sufficiently acceptable.

Prior to the modal tests, a module support system was designed to simulate the free-free state necessary to collect the natural frequencies only from the object of study [HOOP15]. Modal tests were carried out with a commercial PCB Piezotronics modal hammer, for which the tip was evaluated in order to obtain a higher precision up to a frequency of 2.5 kHz of study interest. The vibratory response was measured with an accelerometer placed on the longitudinal axis of the module, making sure not to meet a node in any of the observable vibration modes. The MKII signal collector and PAK software were used to interpret the signals.

The modal tests lasted about two hours each, with a measuring mesh of a total of 20 measuring points. The frequency response

(FRF) and coherence (CF) functions were analyzed to collect the natural vibration frequencies and to ensure the correct cause-effect relationship of the collected signals, respectively. This process was done in a similar way for the four temperature scenarios.

At material level, three dynamic mechanical tests (DMA) were designed and carried out, one for each element of study, in order to collect the influence of temperature on the elastic dynamic properties of the three materials. The type of DMA test was performed under tension, which allows to collect the value of the Storage Modulus (ability to elastically store energy), Loss Modulus (ability to dissipate energy, representative of the viscous behavior) and Tan Delta (damping or ratio of the Loss to the Storage Moduli); viscoelastic magnitudes that are very representative of the vibratory behavior of materials [AVIT09]. The DMA tests were designed in a temperature range of interest from -40°C to $+50^{\circ}\text{C}$, with an extra 10°C at each end due to the transient phases at the beginning and end of the test.

In order to carry out the DMA experiments, test samples were designed to comply with the test geometry required by the technique itself. For the SA and HCA elements, a preparation process of specimens was carried out from the materials stored in tanks. In the case of TCE, this was not necessary. The process was successfully carried out for the two materials, of which between 8 and 12 specimens were obtained from each component. The design of the specimen preparation process was also validated for future trials.

Results

At the module level, the natural frequencies of the first vibration mode for the four temperature scenarios were successfully collected and analyzed. For this purpose, the natural frequencies of each measurement point were computed by means of the analysis of variance (ANOVA), in order to show also the dispersion of the measurement points and the accuracy of the displayed results.

The results show a substantial decrease in the natural frequency of vibration with increasing temperature. An exponential regression shows a quite marked trend at a qualitative level. The number of points, however, does not allow a precise quantitative study beyond the adjustment regression shown.

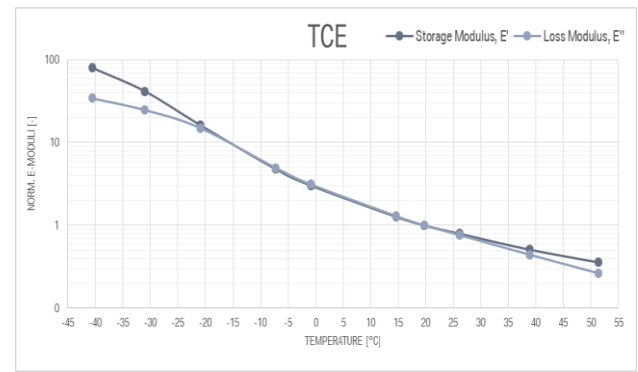


Figure 4. Storage Modulus of the TCE sample over temperature

Conclusions

The ANOVA on the first natural frequency of the four temperature scenarios shows a much exponential decay of the natural frequency with increasing temperature. The results show a greater dispersion of the data the greater the temperature difference between the inside of the climatic chamber and the environment. The frequency differences are very noticeable for the temperature range studied, which results in a very different vibratory behavior of the cell modules depending on the operating temperature. This aspect is considered of great importance in the design phase of structures and the results give very interesting information in this field. A similar analysis is suggested on real, electrically charged modules that can confirm the results seen here.

At the material level, the presence of these polymeric components in the cell module structure may have a great influence on the vibratory behavior of the entire structure, since a decrease over 95% is observed in the dynamic magnitudes of importance in vibrating response of these materials. This data provides very useful information in the design and structural production phase of these modules when considering the kind of adhesive materials to be used.

Finally, the techniques implemented for the study of the influence of temperature on the mechanical properties of lithium-ion cell modules have been widely confirmed for subsequent application in the study of other module architectures and their own structural materials. A relationship has also been established, only at a qualitative level, between the vibratory behaviors of the module and the

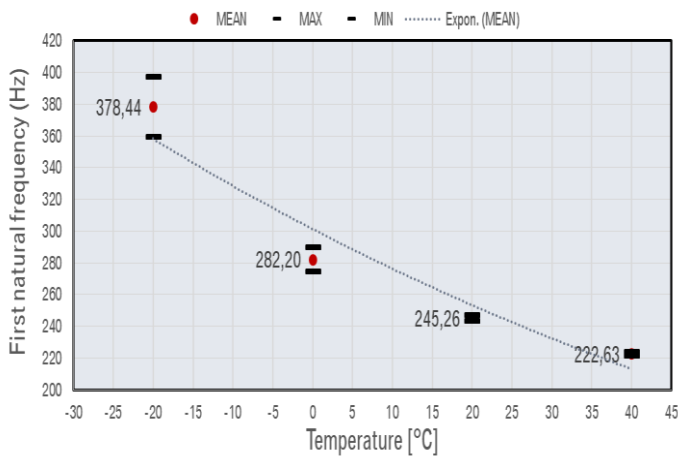


Figure 5. Analysis of variance and representation of the natural frequencies of the first mode of vibration in the temperatures of interest.

At the material level, the dynamic mechanical tests of the three polymeric materials of interest were successfully carried out. The temperature range of interest was correctly recorded with the parameterization implemented in each of the three tests. The results show a substantial decrease of the Storage Modulus as temperature increases. This behavior is very noticeable for the three materials, with special prominence of the TCE, whose change experienced is at one order of magnitude over the other two.

variation of the values of certain viscoelastic material properties of interest present in the cell modules.

This project does not confirm, however, that the results observed in the first natural frequency of vibration are also observed in the successive natural frequencies characteristic of the object of study. It is also not clear what the vibrating behavior of real modules may be, since the technique was implemented on a module without any electrical charge.

The confirmation of the results shown here to be evaluated in a charged module, as well as the analysis of the effect of the temperature on the cell module's modes of vibration in higher frequencies, remains as object of complementary study.

References

- [AVIT09] – P. Avitabile, Sound & Vibration Magazine.
- [HOOP15] - Hooper J.M., Marco J. - Experimental Modal Analysis of Lithium-Ion Pouch Cells.
- [KORT13] – Reiner Korthauer, 2013, „Handbuch Lithium-Ionen Batterien“ (Springer Vieweg).
- [POPP18] - Popp H., Glanz G. - Mechanical Frequency Response Analysis of LIBs.
- [UN38] – European Union, Transportation of Dangerous Goods, 5th revised edition.

Table of Contents

List of Tables	i
List of Figures.....	iii
Symbols.....	vii
Abbreviations.....	ix
Acknowledgements.....	xi
1. INTRODUCTION	1
2. STATE OF THE ART	9
2.1 ELECTROMOBILITY: A NEW ERA IN THE AUTOMOTIVE INDUSTRY	11
2.1.1 Storage systems and energy levels	11
2.1.1.1 Cell	11
2.1.1.2 Module.....	12
2.1.1.3 High Voltage Storage System (HVSS)	13
2.1.2 Current research on the influence of the operational conditions.....	14
2.2 POLYMERIC MATERIALS	17
2.2.1 Introduction.....	17
2.2.2 Classification of polymers	17
2.2.3 Use of polymers within the engineering industry and properties of interest	19
2.3 MODAL ANALYSIS	21
2.3.1 Introduction to Modal Analysis.....	21
2.3.2 Experimental Modal Analysis (EMA)	22
2.3.2.1 Frequency Response Function (FRF)	22
2.3.2.2 Coherence Function (CF)	24
2.3.3 The Modal Model.....	24
2.3.3.1 Single Degree of Freedom (SDOF)	25
2.3.3.2 Multiple Degree of Freedom (MDOF)	29
2.3.4 Practical approach to EMA	30
2.3.4.1 Contribution from Avitabile.....	30
2.3.4.1.1 The free plate: an illustrative example.....	31
2.3.4.1.2 Performing EMA.....	34
2.3.4.1.3 Reality of EMA and aspects of interest	36
2.3.5 Impact of vibrations on the industry	39
2.4 DMA.....	41
2.4.1 Introduction to DMA.....	41
2.4.1.1 First steps into oscillatory experiments	41
2.4.1.2 Contribution from Menard	41
2.4.2 Foundations and basic principles	41

2.4.3 Theory and governing equations	44
2.4.4 Instrumentation	49
2.4.5 Working principles	50
2.4.6 Material Experimentation: Why DMA	51
3. WORK METHODOLOGY	53
3.1 CELL MODULES.....	55
3.1.1 Components of interest for the analysis of the influence of temperature.....	55
3.2 MODAL ANALYSIS	57
3.2.1 Equipment.....	57
a) Input tool: Impact Hammer (tip).....	57
b) Output tool: Accelerometer	57
c) MKII – Signal acquisition system.....	57
d) Measurement Software PAK.....	57
3.2.3.4 Design of the test frame and bearing mechanism.....	58
A) Test frame design	58
B) Bearing mechanism.....	59
3.2.3 Measurement Technique and Strategies.....	61
3.2.3.1 Climatic chamber testing strategy	63
3.2.3.1.1 Designed measurement strategies in the climatic chamber.....	63
A) Test method with closed chamber	63
B) Test methods with door opening	64
B1) Sequential test with door opening.....	64
B2) Point-by-point (PbP) Test with door opening	64
3.2.3.2 Positioning and fastening of the test object inside the climatic chamber	67
3.2.3.3 Placement of the test frame and the test object inside the climatic chamber	67
3.3 DMA.....	69
3.3.1 Measurement equipment	69
3.3.1.1 Instrumentation.....	69
3.3.1.2 Software.....	70
3.3.2 Test conditions and settings	70
3.3.3 Preparation of test specimens	71
3.3.3.1 Experimental guidelines	72
a) Purpose	72
b) Process steps.....	72
3.3.3.2 Geometry of the specimens	75
4. ANALYSIS OF RESULTS	77
4.1 MODAL ANALYSIS	79
4.1.1 Overview.....	79

4.1.2 Reality in the climatic chamber	79
4.1.3 First natural frequency of vibration.....	81
4.1.4 Applications of the designed measurement strategies	82
4.2 DMA.....	83
4.2.1 TCE	85
4.2.2 SA	87
4.2.3 HCA.....	88
4.2.4 General findings	91
4.2.5 Overview.....	91
5. CONCLUSIONS.....	93
5.1 GENERAL FINDINGS	95
5.2 WORK METHODOLOGY	96
5.2.1 Module level.....	96
5.2.2 Material level.....	96
5.3 RESULTS	97
5.3.1 Module level.....	97
5.3.2 Material level.....	97
5.4 FURTHER WORK	98
6. BIBLIOGRAPHY.....	101
7. APPENDIX	105

List of Tables

Table 1. Testing strategy matrix	66
Table 2. Technical data of the DMA GABO EXPLEYOR 500N	69
Table 3. DMA GABO EPLEXOR® 8 Software features	70
Table 4. Temperature-Sweep experimental settings	71
Table 5. ANOVA on the first natural frequency at the four tested scenarios.....	81
Table 6. DMA data of interest from the TCE experiment	85
Table 7. DMA data of interest from the SA experiment.....	87
Table 8. DMA data of interest from the HCA experiment.....	89
Table 9. DMA Parameters of the TCE experiment	109
Table 10. DMA parameters of the SA experiment.....	110
Table 11. DMA Parameters of the HCA experiment	111
Table 12. DMA test data of the TCE experiment.....	119
Table 13. DMA test data of the SA experiment.....	121
Table 14. DMA test data of the HCA experiment	123

List of Figures

Figure 1. Arquitectura de la generación actual de los módulos de BMW	II
Figure 2. Análisis de varianza y representación de las frecuencias naturales del primer modo de vibración en el plano de temperaturas de interés.....	IV
Figure 3. Representación del Storage Modulus del espécimen TCE en el rango de temperatura.....	IV
Figure 4. BMW's current generation of cell modules.....	VIII
Figure 5. Analysis of variance and representation of the natural frequencies of the first mode of vibration in the temperatures of interest.	X
Figure 6. EV, BEV and PHEV sales comparison between China and The US.....	3
Figure 7. BMW i3 (2013) HVSS. Source: Mestmotor	4
Figure 8. BMW i3 (2013) at different environmental scenarios. Source: BMW.	5
Figure 9. Energy levels within an EV and Voltage range	11
Figure 10. How to arrange a group of cells, following the two connection principles of Parallel (left) and Series (right)	12
Figure 11. Current generation of cell module design from The BMW Group. Source: BMW	13
Figure 12. BMW i3's 100kWh HVSS. Source: BMW.....	13
Figure 13. Molecular and chain structure of Polyethylene (PE)	17
Figure 14. Monomers arrangement of (from left to right): Thermoplastics, Elastomers and Thermosets.....	18
Figure 15. Transition temperatures and material regions	19
Figure 16. Modes of vibration of an airframe. Source: Application of pilot models to study trajectory based manoeuvres, Mudassir, 2012	21
Figure 17. Time domain to Laplace domain transformation.....	24
Figure 18. SDOF spring-damper-mass system.....	26
Figure 19. Effect of Lehr's damping factor on the amplitude and phase on a SDOF system	28
Figure 20. Vibration response of a second-order damped system	29
Figure 21. Example of a two-DOF spring-damper-mass system	29
Figure 22. A MDOF system represented as the superposition of multiple SDOF systems ...	30
Figure 23. Free-free plate test illustration and output signal representation [Avitab]	31
Figure 24. Process of the FFT. Source: NTi Audio	32
Figure 25. Overlay of the Time and Frequency responses.....	32
Figure 26. Modes and frequencies of vibration of the free plate	33
Figure 27. Overview of the modal response analysis process	33
Figure 28. Gain matrix with one indicated drive FRF (left) and two cross FRFs (middle and right)	35
Figure 29. First bending mode shape of the free plate.....	35
Figure 30. Key decisions on EMA.....	36
Figure 31. EMA process and sources of error.....	39

Figure 32. The Tacoma Narrows Bridge disaster, 1940. Source: [GUIL00].....	39
Figure 33. Modal analysis of a car body [GUIL00]	40
Figure 34. Relationship between input and output on DMA	42
Figure 35. Stress-Strain curve and Young's Modulus for elastic behavior	43
Figure 36. Triangular relationship of the complex Moduli.....	43
Figure 37. Energy diagram of the bounce of a tennis ball	44
Figure 38. Mass-spring system	45
Figure 39. Dashpot.....	46
Figure 40. Stress and strain curves as a function of temperature	49
Figure 41. Sectional view of a DMA and its parts	49
Figure 42. Physical magnitudes present within a DMA and their process.....	50
Figure 43. Explosion view of a cell module architecture.....	55
Figure 44. Piezotronics 086C03 Impulse Hammer: tips assortment response curves	58
Figure 45. Taste frame and module setup	59
Figure 46. Spring-mass relationship for frequency estimation of the springs	60
Figure 47. DMA GABO EXPLEXOR 500N	69
Figure 48. Image (left) and sketch (right) of the Teflon-coated plates.....	72
Figure 49. Image (left) and sketch (right) of round plate with spacers	73
Figure 50. Correct application of injected material.....	73
Figure 51. Geometry of the HCA sample	75
Figure 52. Geometry of the TCE sample.....	75
Figure 53. Geometry of the SA sample	75
Figure 54. Temperature record inside the climatic chamber at the -20°C measurement	80
Figure 55. Distribution of the first natural frequency of the cell module over temperature ...	81
Figure 56. Normalized moduli over temperature for the TCE experiment	86
Figure 57. Tan delta over temperature for the TCE experiment.....	86
Figure 58. Normalized moduli over temperature for the SA experiment.....	87
Figure 59. Tan delta over temperature for the SA experiment.....	88
Figure 60. Normalized moduli over temperature for the HCA experiment.....	89
Figure 61. Tan delta over temperature for the HCA experiment	90
Figure 62. Comparison of varying behavior of the three materials over temperature.....	91
Figure 63. Expected result of the -40°C EMA test.....	98
Figure 64. FRF and CF of the measurement at -20°C.....	107
Figure 65. FRF and CF of the measurement at 0°C.....	107
Figure 66. FRF and CF of the measurement at +40°C	108
Figure 67. FRF and CF of the measurement at +20°C	108
Figure 68. NETZSCH GABO EPLEXOR Series technical data.....	112
Figure 69. Engineering drawing of the Piezotronics 086C03 Impact Hammer.....	113
Figure 70. Data sheet of the Piezotronics 086C03 Impact Hammer	114

Figure 71. Temperature data record of the EMA experiment in the climatic chamber at -20°C	115
Figure 72. Temperature data record of the EMA experiment in the climatic chamber at 0°C	116
Figure 73. Temperature data record of the EMA experiment in the climatic chamber at +20°C	117
Figure 74. Temperature data record of the EMA experiment in the climatic chamber at +40°C	118

Symbols

c	Damping coefficient $\left[\frac{N.s}{m}\right]$
ε	Strain [-]
E'	Storage modulus [MPa]
E''	Loss modulus [MPa]
E^*	Complex modulus [MPa]
f	Force [N]
δ	Delta [$^\circ, x\pi$]
g	Gravitational acceleration $\left[9.81 \frac{m}{s^2}\right]$
k	Stiffness $\left[\frac{N}{m}\right]$
m	Mass [kg]
N	Newton $\left[kg * \frac{m}{s^2}\right]$
σ	Stress [Mpa]
$\tan\delta$	Tan delta [-]
T_G	Glass-transition temperature [$^\circ\text{C}$, K]
T_M	Melting temperature [$^\circ\text{C}$, K]

Abbreviations

ADC	Analog to Digital Converter
BEV	Battery Electric Vehicle
BMS	Battery Management System
CF	Coherence Function
DMA	Dynamic Mechanical Analysis
DMA	Dynamic Mechanical Analyzer
DOF	Degree Of Freedom
ECU	Electronic Control Unit
EMA	Experimental Modal Analysis
EV	Electric Vehicle
FEM	Finite Element Model
FFT	Fast Fourier Transform
FRF	Frequency Response Function
HCA	Heat-Conducting Adhesive
HVSS	High Voltage Storage System
LTI	Linear Time-Invariant
LVDT	Linear Variable Differential Transformer
MA	Modal Analysis
MDOF	Multiple Degree Of Freedom
PHEV	Plug-in-Hybrid Electric Vehicle
RH	Relative Humidity
SA	Structural Adhesive
SDOF	Single Degree Of Freedom
SISO	Single Input Single Output
SOC	State Of Charge
SOH	State Of Health
T	Temperature
TCE	Tolerance Compensator Element

Acknowledgements

This work is the result of the inestimable patience and dedication of more people that I can mention, which sadly will end up hidden under the author's name. My gratitude to all of those who came across my path and listened to my story.

The first person and the one I need to thank the most is my supervisor. Thank you, Max, for your guidance, knowledge, creativity, perseverance and for your immense effort on making this work out. Half of this work should have your name in it.

To Michael Fromm, for having to deal with a newbie to modal analysis for countless days at the Laboratories for Vibration and Acoustic. My special recognition to Gunter Schröter, for showing interest on my culture while acting as a professor in Materials Science week after week.

A very sincere thank you to Dominik Mittelmann, for making my testing days in the climatic chamber an unforgettable experience and to the operators in the prototype production line, for having always a yes for me.

To all my colleagues from the department of Protection, Test and Simulation of HVSS of the BMW Group. No project could have been done without the splendid work atmosphere they are guilty of. The warm time I had as part of the group makes it easier to survive the winter in Munich.

And lastly, to my people, my sister and my parents. Their invisible yet unbroken support have written most of the pages here presented.

1. INTRODUCTION

Electromobility: the technological race.

With the increasing need of reducing local and global emissions along with sustainability in the world of mobility, the development and usage of the electric vehicle (EV) has become a priority for the automotive industry.

The development of EVs has become a technological race, reinforced by both governments and customers, who are well aware and concerned about the emission issues and related fees that the automotive industry has been dealing with. This technological race has fostered the scientific spirit and automotive companies are now investing an enormous budget into “electromobility”, as they try to position themselves above their competitors within the electric vehicle market.

Electromobility is no longer a premise, but already a fact. There is unquestionably sufficient data from the last ten years that shows a substantial, steady increase in the market share of EVs in their full electric and plug-in-hybrid forms, as well as an important expansion in the infrastructure needed for electromobility to happen [STAT18]. This trend is already happening worldwide, with its most impact across the three major markets: Europe, The US and China [VPSO19]. A few different studies have recently arisen, which show the evolution of electromobility within these three markets [BABO18, MCCA19].

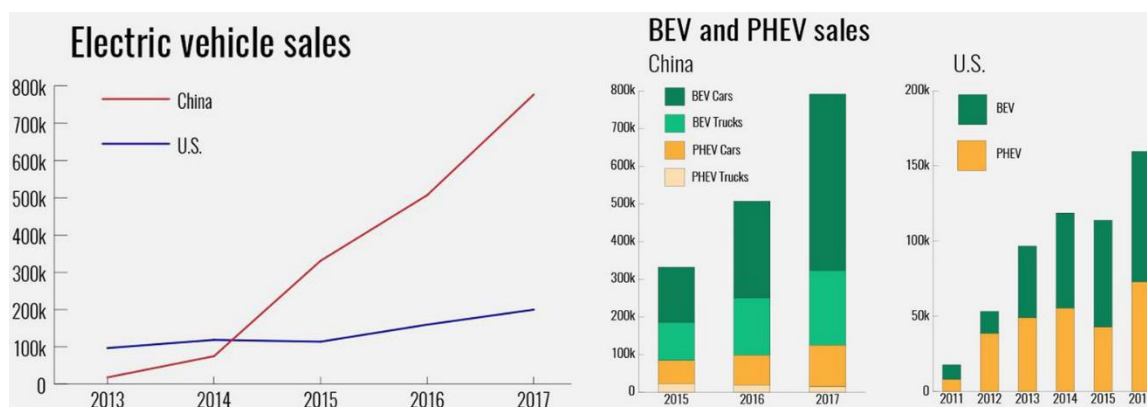


Figure 6. EV, BEV and PHEV sales comparison between China and The US

The automotive industry is going through one of its biggest technological changes and whoever has not come aboard yet will be surely left out of this competitive race the automotive industry is currently facing [VPSO19].

And with a new technology, new challenges come as a consequence. Numerous variants and different designs of EV-components are being developed at a very high rate. It is therefore the task of the engineers to ensure that the new models and electric components that are coming up in the market comply with the safety and sustainability requirements within the automotive industry. Since the technological race of EVs is developing very quickly, this has become a very urgent task to undertake.

Furthermore, all this comes into more importance by considering the potential new dangers that electromobility brings with it. This means that there may be new, earlier unknown threats regarding the EVs that can compromise the safety of both the developers and the final clients. The swelling force experimented by lithium-ion cells as they load up during charge-discharge cycles is just an example of the new concerns that the automotive industry is currently dealing with [KYOH16]. Temperature is a strong actor, which definitely has a big impact on the mechanical behavior of the various components of electric cars. Additionally, the mere failure of a single cell or another small component within an electric engine or storage device can lead to the collapse of the whole system, sometimes causing irreversible damage. And if that happens during service, the safety concept is under enormous risk.

What's more, electromobility is bringing new materials into the vehicles, which may be prone to undergo changes in their mechanical behavior under the influence of temperature. It is therefore the duty of engineers, in order to produce safe batteries, to understand the impact that the dynamic environment has on their mechanics and that of their components [HOOP15]; which is not an easy task to do.

These potential new dangers that compromise the safety, and which were not a concern in the years of combustion engines are demanding the development of robust, standard methods and techniques in order to both qualitative and quantitative determine their influence and to come across ways to reduce and control their impact on the concept of security and safety. This is one of the main tasks automotive engineers are currently working on and also an excellent chance for the fields of scientific research and engineering to go hand in hand.

New technology, new challenges.

There has been a rising amount of experiments, papers and general research studies undertaking safety matters related to EVs during the recent years. However, the quick growth of electromobility that is being demanded by everyone involved in the industry requires such an amount of new technologies to be developed and perfected, that there are currently many open questions to be undertaken yet.

After the very first models that have come out in the market, the safety and durability of the recently developed components has become a main, if not the most important, task for automotive engineers. Besides that, the new, upcoming designs and approaches may differ from the ones that currently exist: this technological race is driven by drastic, innovative ideas, which may also call into question the existing methods but provide as well new solutions to the current topics of concern. The result is a wide range of research possibilities for the scientific field, and the urgent need for answers from the engineering development and production side.

With respect to high voltage storage systems or, for short within this topic, HVSS, it is useful to distinguish between the three concept levels: high voltage batteries as the whole energy system, cell modules as the main blocks constituting them and, at the lowest level of energy: the cells, the single, elementary components responsible for the energy storage and distribution throughout the whole system.



Figure 7. BMW i3 (2013) HVSS. Source: Mestmotor

It is imperative for automotive engineers to undertake research and develop improvements at all three levels of energy, as well as to fully understand the connection and relationships between each other. Hence, the need to focus by all developers to work on each of the three levels thoroughly.

In regard to the cells, their active materials or the so-called “cell chemistry” is the biggest current matter of research. The energy density and also their recyclability rely mostly on them and therefore new chemistries are constantly coming up in the market. The one that has stand out the most and that is currently being used as the energy source for the future of the transport industry are the lithium-ion cells. There are different variations regarding the size and geometry of the cells being used by automotive companies: Tesla is well known for their cylinder cells, whereas German constructors such as the BMW Group have heretofore bet for prismatic ones. With respect to active materials, the lithium ions are the active components in charge of conducting the chemical processes related to the flowing of an electrical current inside the cell. Meanwhile, the cation and the anion electrodes within the cell are responsible for collecting the current and transferring it into the active materials. The cation, or the positive material, is mostly made of materials like nickel, cobalt, manganese and lithium oxide, whereas the negative component currently on scene are graphite anions.

To investigate how the behavior and the properties of these materials evolve over the lifetime and the different environment and usage conditions is of crucial importance to ensure the durability and safe service of the components of an electric battery. Particularly, stable mechanical properties of these components are required for such batteries to be able to provide electric energy under all environmental, transportation conditions worldwide. Within this matter, there are three main factors that conform what is considered as the operating conditions: the state of charge (SOC), the state of health (SOH) and the temperature (T).



Figure 8. BMW i3 (2013) at different environmental scenarios. Source: BMW.

The effects of the operating conditions on pouch cells has recently been studied [HOOP15], with an approach to analyze the effects of the SOC by performing modal analysis on a certain sample of pouch Lithium-ion pouch cells. This work has been further developed by some others [POPP18], who have proven the effect that SOC has on the mechanics of this kind of cells.

These recent results, which were just published a year ago, provide a slight insight of how strong can be the effect of temperature on the stiffness and vibrational behavior on these lithium-ion cells. However, there are still some open questions and studies to be made regarding the real effect of temperature. There is still no exact evidence of which effect, not only at qualitative but also at quantitative level, has the temperature solely on these lithium-ion cells. A further mission is to study this effect of temperature not only on the cell structures used in the automotive industry but also at a higher level, at the module level, and how it affects the mechanical properties of all its components. This will be the aim of the work described here.

After all, research is undertaken and changes have to be made from lower to higher levels and following this upwards process will lead to the robust study of how the environment really affects the behavior of the current electric batteries and how they can be improved in search for the maximal security in service.

What refers to the scope of this work comes into place, as its ultimate research field, at the broad topic of electromobility. It is imperative for engineers working in the field to ensure the full understanding of the behavior of every component of the batteries and at all levels of construction: the cell, the module and finally the whole storage system.

As far as electromobility has come, there are still some open questions at the lower levels that urgently need to be undertaken prior to ensuring the correct functionality of the new designs and technologies being demanded. Regarding the references to recent work done within the field, the effect of temperature on lithium-ion cells has not been yet fully evaluated, and neither has been approached the mechanical behavior at the higher level, the cell module, and how it may change under different service temperature conditions. This topic is of huge importance for the automotive industry in order to being capable of developing as well as producing the safe-functioning cells, modules and electric storage devices that the current scene of electromobility is demanding, which need to be serviceable under all possible transportation conditions worldwide.

The approach of going from the lower, elemental levels of energy components up to the higher levels, where the whole system is entirely considered, has the following reason: the whole system's mechanical behavior can only be understood by decomposing it into its most elementary blocks (or components), and then by fully acknowledging how the different operating conditions impact each of the components. The second and final step is to move upwards from lower to higher levels, ultimately reaching the whole system considered: the high voltage storage system. Reaching the highest level here means being able to transferring the impact of the operating conditions on specific battery components up to the whole system, and therefore allowing for the necessary conceptual changes in design or production processes on the affected components, as well as isolating those which do not have any proved impact on the higher levels. This approach follows the guidelines of system dynamics and ensures a final, desired state at which every single component or piece of the whole puzzle is accounted, controlled and known.

Project goals and methodology.

The general purpose of this work is to measure, quantify and to analyze the influences that different operating temperature scenarios have on the mechanical behavior of a state-of-the-art cell module, as well as to find out the main source of those changes that is, which components -lower level- of the module are responsible for these changes seen at the middle, module level. The latter purpose of this work is to serve as a guideline for further experiments regarding the topic of temperature influence on the mechanics of energy storage systems, as well as becoming an outline or a pattern to be followed for the analysis of future module designs or specifications. This work will be done in collaboration with The BMW Group, in their head laboratories for prototype development in Munich, Germany.

To put it into a few words, the aim is to provide precise insight on the currently uncertain mechanical behavior of EV-cell modules at different temperature scenarios, as well as the main causes to such changes that can be taken into account at the early design phase. The whole point of this scientific work is addressed to collect valuable information for the current, big concern on electric vehicle safety.

These different operating temperature scenarios are considered to go from extreme cold conditions (-40°C) up to a very high temperature state (+50°C), also accounting for temperature scenarios found in-between these two limits. As a result of a solid series production and the worldwide established transport sector, for convenience reasons, cell modules (as well as every

vehicle component) have to be designed for functionality in all known environment scenarios, and all of their components should therefore be serviceable under this broad temperature range.

The idea of the here studied temperature range is to emulate what in service vehicles may encounter all around the world: the coldest temperatures which have to be faced in northern areas, such as the North European countries; while the warmest case-scenarios will represent dramatic high temperatures as found, for instance, in Central America. The two most extreme temperatures within the range of study are also designed to comply with the European norm on transportation of goods [UN38].

Once the temperature analysis at cell module level has been executed, the initial hypothesis is that the results will show different vibrating states in terms of the natural frequencies of the cell module. This is due to the fall on the values of some mechanical properties, for instance, the stiffness, with increasing temperature. The aim is to quantify these falls and to see if there may be a linear (or any other) behavior that allows to, qualitative as well as quantitative, frame these changes under the influence of temperature. For the cell module tests, “dummy”, and not-charged cells will conform the so called “dummy modules” that will be subject to test.

The second goal of this work is to strive to justify these changes and to find the most elementary sources that cause them by performing a different kind of mechanical analysis. There are some components of the cell module expected to be more prone to experimental mechanical changes caused by the influence of temperature, which are those conforming the joining techniques.

The purpose of this second analysis is to study or subject the different joining materials of a new generation state-of-the-art cell module under mechanical testing, in isolation to one another. That means, to study every bonding technique separately –at material level-, in order to find the ones that may face the biggest changes, which may then be the explanation to the different vibration behaviors seen at cell module –component- level.

Finally, the third and final goal of this work is to set or develop a valid, applicable method that allows for evaluation of the influences of changing temperatures on the vibrating behavior of cell modules, as well as for detecting the individual component or components that may be the main cause for such changes. Once a solid method is achieved and its functionality is proven, it would be then possible to relate and link the test results with the input vibration data which is documented as what vehicles may face during in service activities or usage [HOOP15].

The initial idea of analyzing the dynamic mechanical properties of cell modules is done through modal analysis. This technique consists of subjecting the test component to a controlled vibratory state, allowing to obtain the natural frequencies and the different modes of vibration, which are essentially intrinsic characteristics of the component. Just as colour, density or geometry are intrinsic and unique properties of a body, so are the natural frequencies and their respective modes of vibration. These vibratory properties belong to the family of mechanical properties of the component, and their values are connected to other mechanical properties such as, for instance, stiffness.

This system, when subjected to a force that does not go further the limits of the spring, will vibrate at its natural frequency, which is commanded by the relationship between its mass and stiffness. The damping has no influence on the value of the frequency itself, but rather on the amplitude of the sinusoidal movement and the duration of it, as energy is gradually dissipated. Needless to say that this single, first order scheme is just an introduction to the dynamics that govern the behavior of every linear vibrating system, and what really dictates the behavior of the system studied here is a very complex, various orders system which is but fundamentally composed of several single spring-mass systems and their relationships to one another.

To put it into context, performing modal analysis consists of putting the body under evaluation into a vibratory, known state, so its mode shapes and natural frequencies can be excited and recognized, as they get amplified due to resonance. This will be the first engineering technique

employed within this work of study. The different desired scenarios will be achieved by performing modal analysis inside a climatic chamber, where temperature can be chosen and controlled during the measurements.

The different temperature scenarios will be replicated inside a climate chamber and the component under test and test setup will be located inside it. It is of crucial importance that the temperature inside the climate chamber is at all times controlled and known. Otherwise, the results of the tests would not be valid from a scientific point of view.

Along with modal analysis, a second mechanical testing technique is selected for the analysis of the properties of the different materials conforming the bonding technologies of the studied cell module. This technique is the DMA technique, which stands for “Dynamic Mechanical Analysis”. The components of the module that might be prone to changing their behavior due to effect of temperature will be analyzed by means of this technique. The whole idea is to provide some insight from the lower, material level, which may explain to a certain degree the behavior seen at the higher level, the module level.

2. STATE OF THE ART

2.1 ELECTROMOBILITY: A NEW ERA IN THE AUTOMOTIVE INDUSTRY

2.1.1 Storage systems and energy levels

Due to their huge impact on the smart phone industry, the lithium-ion batteries are known to be small devices, just the size of current smartphones, with some kind of flat-prismatic geometry and not many distinguishable components. They are planar and often called “pouch cells”. Under normal conditions, they usually operate between 3.7 and 4.2 volts (V) and can be fully charged within 2 to 3 hours. Other parameters like the number of cycles and cycle duration of use between charges are difficult to enclose, as they highly depend on the level of use and particular phone model.

However, the concept of the batteries installed on EVs can be expected to differ from the ones on smartphones. To operate an EV, an enormous amount of energy and power is demanded, several orders above that of a smartphone. EVs need dozens to thousands

The different terminologies that have arisen as the world of EV-batteries has been expanding are found to be sometimes confusing and need to be clarified. The most common approach is to divide them by the energy level they belong to, by going from a lower to a higher energy level as follows:

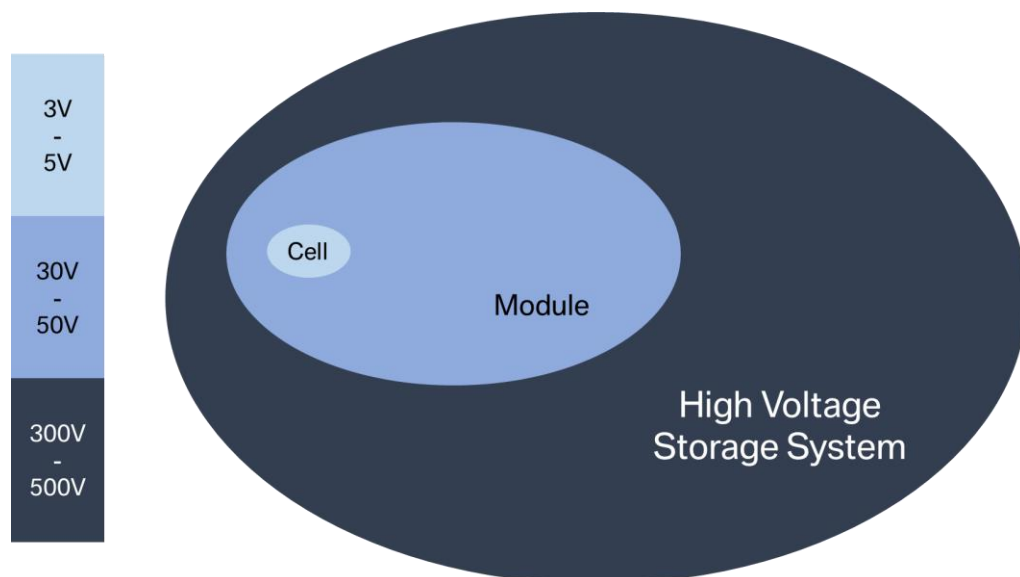


Figure 9. Energy levels within an EV and Voltage range

2.1.1.1 Cell

Most elementary unit of energy within an EV, they contain active materials, in charge of the electrochemical reactions as the source of electrical energy through reduction and oxidation processes that take place in the cathode and the anode.

They can be considered as the similar battery elements characteristic of smartphones, but are found in a variety of many different shapes and geometries: Tesla, for instance, is well known for their cylindrical cells, whereas other constructors, such as BMW or Toyota, opt for prismatic ones. Their design and use of materials is in constant change, as the market demands for more autonomy, serviceable life and faster charging.

The purposes of analysis within this work does not wade into the different cell designs. Due to safety concerns, the here analyzed EV-components do not have any active materials that may

cause harm and be responsible of an accident that compromises the whole prospective work. All elements are safe from electric currents and should be handled safely, accounting only for the dangers that may arise from their heavy weights and sharp edges. The cells present in the studied modules are the so-called “dummy” cells, which are made of aluminum and imitate the weight and geometry of the original cells.

2.1.1.2 Module

A cluster of cells make up a module, which is also made up of other components like the structuring parts and the connecting elements between batteries. They are also called “packs” of cells.

Modules are essentially a battery assembly put into a frame by combining a certain number of cells together, protecting them from heat, external shocks and vibrations. The frame mostly consist of plates and tie rods made of aluminum or other light but stiff materials, which allow for the construction of a robust, safe structure to cover the cells.

The connecting elements between the cells play also an important role. The cell-layout within the modules is designed to guarantee the required supply of current and voltage. Depending on the values required of these magnitudes, cells can be connected in groups, by following a specific series-to-parallel arrangement:

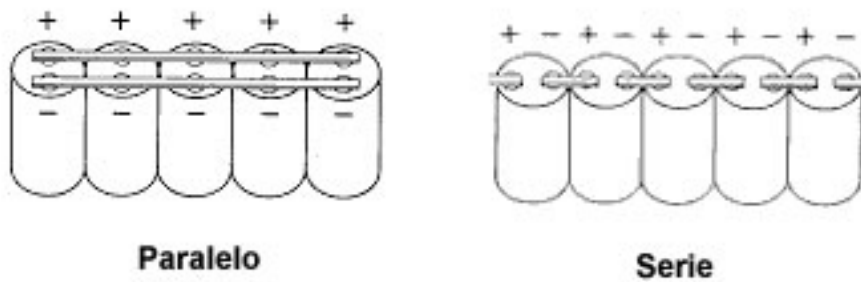


Figure 10. How to arrange a group of cells, following the two connection principles of Parallel (left) and Serie (right)

- a) Parallel connection: connects the cells into a same voltage, so the currents of each cell are added up to achieve a desired value. Terminals of the same sign are connected to each other to achieve this distribution.
- b) Serie connection: cells are connected into a sequence, by alternating positive and negative terminals between cells. This way, the same current flows through all cells, adding up their voltages. The connection is always set between the positive terminal of one cell to the negative terminal of another cell. The positive and negative terminals of the same cell should never be connected to each other, as it will result in a shortcut and cause a huge current to flow over a very short period of time with no resistance, probably causing an unsafe release of electrical energy.

The physical appearance of a state-of-the-art cell module can be seen below. It is, essentially, an aluminum block, inside which the cells have been arranged together in a compact fashion. The size of a module is clearly dependent on the number of cells it has, or put it into other words, bigger modules have usually a higher capacity.

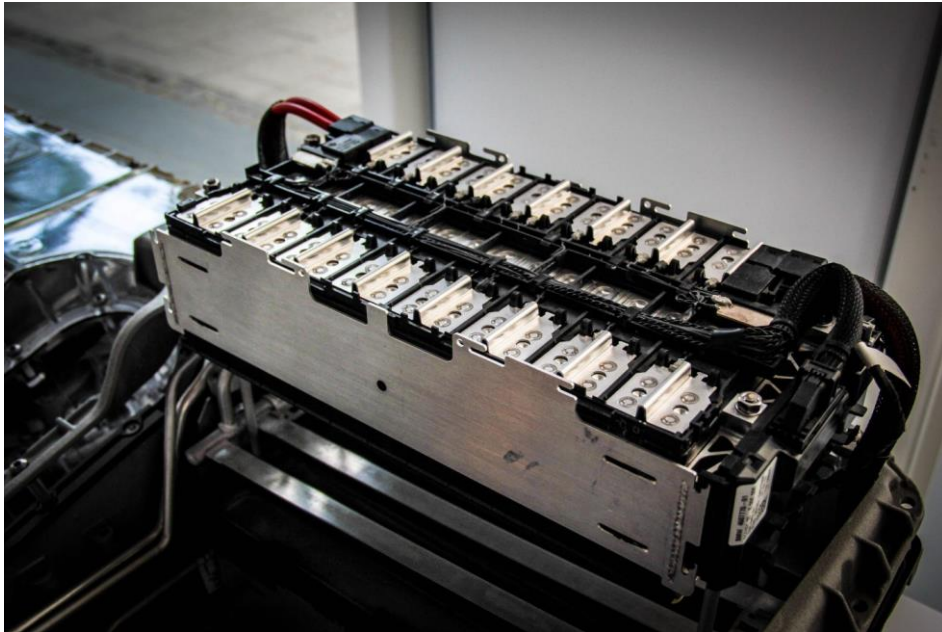


Figure 11. Current generation of cell module design from The BMW Group. Source: BMW

The endless layout options of a cell module make it possible to consider very different architectures at the design phase. That means, targeting a particular design and accounting for all of its specifications is not found to be a good approach for the analysis discussed within this work. The focus is then on the components present on most designs and the materials they are made from.

2.1.1.3 High Voltage Storage System (HVSS)

As a final structuring level, modules are put together and arranged into a specific way, which will at the end fit into the vehicle structure. The current and most seen trend is to place them on the floor.

This final cluster of cell modules, along with other components of the electrical circuit, such as the connections to the electric engine or the inverter form what it is known as the HVSS.

These systems, commonly called the “battery” of the vehicle, also vary a lot in size and shape, depending on the vehicle architecture, type of EV and capacity of the battery itself. Their size can go up to occupy the whole vehicle floor and some early geometries mimic that of eagle-wings.

The layout of the HVSS and their specifications differ a lot from the manufacturer. Following the technological race of electromobility, very different designs are found in each new project, with the intention to provide the best performance with the minimum size and weight.

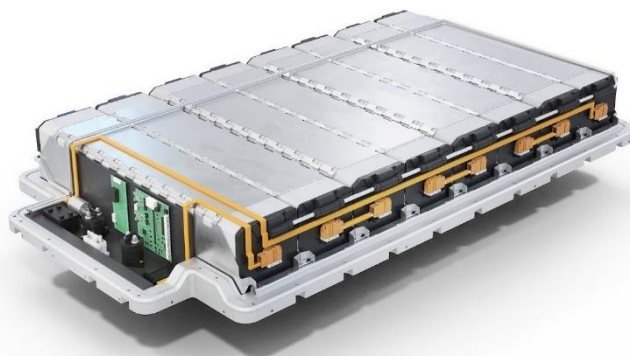


Figure 12. BMW i3's 100kWh HVSS. Source: BMW

An essential component of a HVSS is the Battery Management System (BMS), as it controls the voltage levels of the modules and cells, by accounting for and monitoring important parameters, such as the operating temperature, the electrical current and the voltage levels. The BMS regulates the voltage of each cell, and stops the flow of energy when the battery is fully charged. It balances out the charge level of each module or cell pack.

Due to design and production tolerances, not all cells within a battery are perfectly equal. Some may take slightly higher values of voltage than others, or may last a bit longer. The BMS is especially important to manage these operational differences and to ensure an efficient, safe performance and durability of the HVSS.

It is also in charge of the communication with other control units, like the one of the electric engine and the regenerative break, or the Electronic Control Unit (ECU).

2.1.2 Current research on the influence of the operational conditions

The rapid development of electromobility has brought several concerns on the performance and durability of the HVSS elements under different operational conditions. Unlike the world of combustion engines, the EV is yet far from being completely controlled and established within the automotive industry. Many safety concerns have arisen due to the new dangers that electromobility brings with, essentially by having high electric currents flowing and stored within the vehicle, under the influence of many environmental changing factors when operating them.

The main focus has been put on the cells, as they are the most elemental level of energy and the main source of system failure.

Recent research has targeted the three main actors classified as operational conditions of interest: the Temperature (T), the State of Charge (SOC) and the State of Health (SOH).

Hooper and Marco experimented with the natural vibration response of pouch cells in 2015 through the technique of modal analysis, as the impact of mechanical vibration on the vehicle's electrical components and subsystems is known to be a major cause of in-market durability failure [HOOP15]. They implemented an experimental method by the use of the impulse excitation technique to testing the natural frequencies of pouch cells at different values of their SOC. Although they could not conclude any influence of the SOC that could overpower the effect of the geometrical differences among the tested cells [R5], their experimental technique would be the starting point for further analyses.

Almost two years later, Popp (et al) published in 2018 their research on the correlation of the SOC and the SOH on mechanical parameters of pouch cells, such as the stiffness and the damping [POPP18]. Their idea was to find a method for monitoring the changes of the mechanical parameters, highly important during construction of battery systems. Despite the explained limitations of their method, they found an interesting indicator of the influence of the temperature, and suggested that a further analysis on the matter.

This recent field of research provided sufficient insight to assert that the technique of modal analysis may provide the answer to the here intentioned scope of analysis, as it has been endorsed as the most effective, non-destructive method for mechanical testing in such field of research.

The findings on pouch cells cannot, however, be directly transferred to the electrical elements present in EVs. Not only because the cells are not the same, but because the research done only undertakes the first elemental energy level. The addition of other components and the arrangement of several cells together done at the next energy level may well

As for the automotive industry, the influence of the three main operational actors on the mechanical behavior of the electrical components in an EV is yet a subject on course. The most research is done by the manufacturers themselves as part of the validation for production processes and there is naturally no existent field of research available. Additionally, the large variety of module and HVSS designs creates the problematic of having analyses that are applicable to only a specific architecture, as contrary to what happens to the finer developed pouch cells market.

This situation gives rise to a challenging, yet very interesting topic of research within the automotive industry. The influence of the temperature on the natural vibrating response of a higher energy level, the cell module, might provide a better insight to the mechanical dangers and operational failure that electromobility has currently to deal with.

In order to undertake such analysis, so that it can take on the problem with the diversity of architectures and comply with the operational demands of the automotive industry, the analysis of the different components within a module is at this point necessary. A thorough understanding of the potential elements, prone to changing their mechanical behavior under the influence of temperature follows as the first step into this idea of research.

2.2 POLYMERIC MATERIALS

2.2.1 Introduction

The word polymer is made up of the Greek terms “poly-“ (many) and “-meros” (part) and essentially refer to a large molecule, or macromolecule, composed of -many- subunits, the mers, which are smaller molecules extensively repeated in the form of chains.

These monomers are carbon-based molecules fundamentally composed of Carbon, C, Hydrogen, H, and Oxygen, O. Other elements within the periodic chart, such as halogens like Chlorine, Cl, are also commonly seen as part of these chains and allow for very different structures, properties and physical appearance.

Polymeric materials are then a bundle of chains, made up of organic molecules, which are bonded to each other and arranged into the three-dimensional space through a process called “polymerization”. Among all these bonds between molecules and chains, some are found to be very strong, like the covalent bonds between two carbons, but there are also hydrogen bonds, a much weaker type of bond that forms a dipole within the molecule.

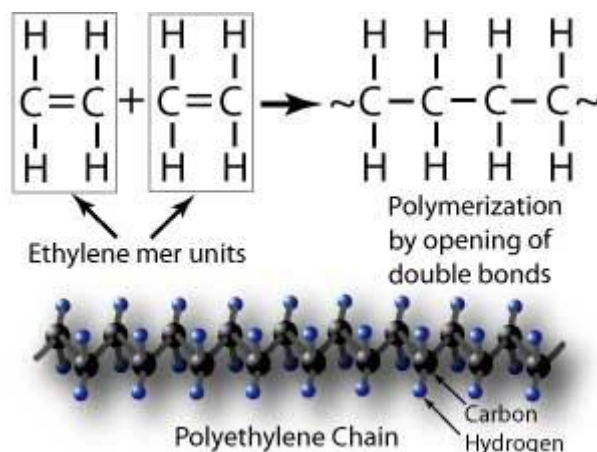


Figure 13. Molecular and chain structure of Polyethylene (PE)

As it can be predicted, such broad layout assortment of chains, bond typing and molecular structures forming the polymeric chains support an enormous variety of very different materials, properties and performances. That is why polymeric materials are so widely established and commonly found within many industries. They form a large piece of all commercial and industrial materials available and have had a massive impact on the development of the automotive industry.

This type of materials are often, yet sometimes wrongly referred to as “plastics”, due to the plastic behavior most of them exhibit when handling or testing them, although not necessarily all polymeric material behave this way. The term used within this work to address this type of materials will still rely on the original name “polymer”, to avoid any confusion.

2.2.2 Classification of polymers

There are several ways into which polymers can be classified. To name a few, polymers can be classified by [GOWA15](#):

- Origin: being natural or synthetic.
- Monomer variety: having polymers made up of identical or several different monomers.
- Method of synthesis: as there are different processes of polymerization, such as addition and condensation.
- Structure: linear, branched and cross-linked polymers.

- Crystallinity: monomers arranged in an ordered way form crystalline polymers, whereas a random arrangement of monomers is specific of amorphous ones.
- Tacticity: orientation of monomer units in a polymer molecule with respect to the main chain. They can be isotactic (head-to-tail), syndiotactic or atactic.
- Applications and physical properties: fibers, plastics and rubbers.

A special way to classify polymers used within the industry is by how they respond under thermal excitation, or simply put, by their thermal behavior. The heat can cause the relaxation of the molecules, changing the internal structures and the bonding among chains. This can also be seen as based on their molecular forces and is the most common classification within the industry, as the thermal response of materials has been always a prior object of characterization. There are three main groups within this classification [\[BILL84, KISS02\]](#):

a) Thermoplastics: easily molded in desired shapes, becoming soft by heating and hard by cooling. They are usually linear or slightly branched polymers and become moldable into different shapes above a specific temperature. Held together by relatively weak intermolecular forces, they can be repeatedly softened by heating and then solidified by cooling and have therefore a wide range of applications. Examples are polyethylene (PE), polystyrene (PS), polypropylene (PP) and polyvinylchloride (PVC)

b) Thermosets: contrary to thermoplastics, thermosetting polymers are highly cross-linked and branched polymers. They are soft solids that change irreversibly into non-moldable polymers on heating, hard and infusible, cannot be reshaped and are not reusable. Strong and durable, they are widely used within in automobiles and construction. A typical example is Bakelite.

c) Elastomers: solids with rubber-like elastic properties. Their polymeric chains are held together by weak intermolecular forces, like hydrogen bonds, which allow them to be stretched. Highly amorphous in nature, they have the ability to recover to their original position after the stretching ceases. Natural and vulcanized rubber are common examples.

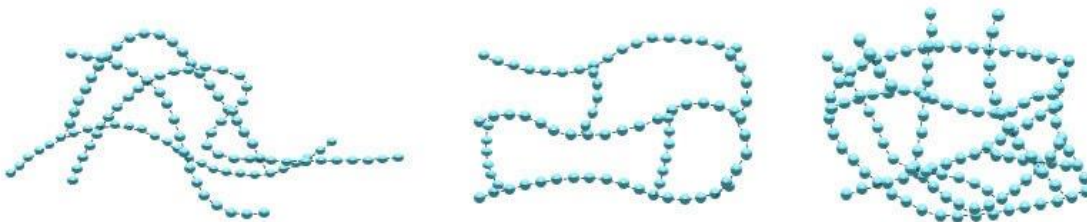


Figure 14. Monomers arrangement of (from left to right): Thermoplastics, Elastomers and Thermosets

There is one very useful magnitude to characterize polymers by their thermal behavior: the glass-transition temperature, known as T_G . It is the temperature, at which the physical properties of polymers change to from those of a rigid glassy-like, crystalline material to of a soft (not melted), rubbery-like material, and obviously below the melting temperature, T_M .

It is also the reason why Thermoplastics are often divided into crystalline and amorphous, depending on whether their glass-transition temperature is above or below room temperature, respectively.

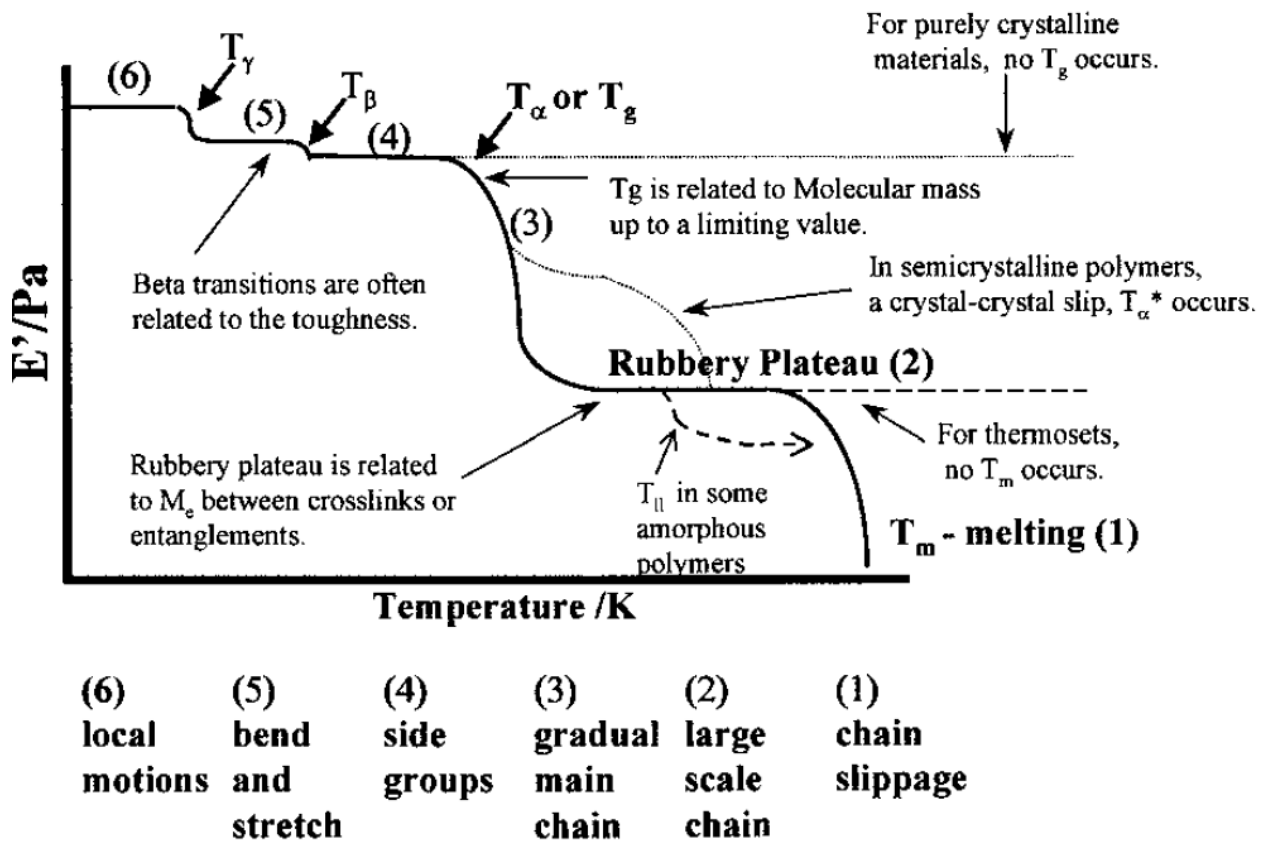


Figure 15. Transition temperatures and material regions

The T_G helps to characterize specific polymers by its thermal behavior. However, the exact temperature to transition is sometimes very difficult to say, as this is seen within a temperature range in which the stiffness decays steeply. The glass-transition temperature can therefore be characterized by the Modulus too, but should not be looked up to as an exact value, as for example the melting temperature, but more as a range. Although it does not provide an exact value where the characteristics of the material can be said to have drastically changed at one point, it is used to characterize an area where the material will start to behave very differently. It is a very handy concept in Engineering and very practical for the characterization of polymeric materials within the industry.

Other transition temperatures like the beta and the gamma transitions are especially interesting to explain the inter- and intramolecular changes that a material experiences due to the effect of temperature. The scope of this work is, however, slightly away from the area of research that the analysis of these transitions may provide to characterizing the behavior of materials under several environmental conditions. The temperatures, at which these transitions usually occur for most industrial polymers, are too low in comparison with the field of study within this work. They will be therefore left for further analysis, and not elaborated here.

2.2.3 Use of polymers within the engineering industry and properties of interest

The immense polymer assortment, as much as naturally found or artificially synthesized, and their diverse characteristics along with their abundant availability on the planet have made possible to perfect their production processes. They have become a notably cheap and versatile group of materials, highly used within all industries.

Depending on the purpose of use, some properties or others may be of interest for certain industries. Polymers are used as adhesives, thermal or electrical insulation elements, for light-weight structuring and even for very stiffer ones, like fibers are.

Polymeric materials cover most of the demands of the automotive and construction industries and are progressively acquiring more focus, as they become cheaper and easier to produce and transport.

The usual properties of interest in the automotive industry are high resistance, lower density, electrical conductivity or insulation, thermal response, stiffness, toughness, hardness, heat conductivity or insulation and , to name a few. Essentially, they highly rely on their microstructure and type of bonding. Most of them can be classified as mechanical properties, and the alteration of these properties due to some physical factor has been always a subject in the engineering field.

The vibrating response of a structure is highly dependent on the mechanical properties. Therefore, it is of no doubt that the changing vibrating behavior of such structural element as the cell module will highly rely on the mechanical properties of the polymers present in it. This is the basis for the mechanical analysis of the mentioned materials, as the second object of study in this project of work. A broader argumentation is elaborated in the following two sections.

2.3 MODAL ANALYSIS

2.3.1 Introduction to Modal Analysis

The mechanical evaluation technique of Modal Analysis (MA) studies the vibrational behavior of structures. It is widely used in the aeronautical and civil engineering field and becomes an essential part in the design and examination of structures, as it helps identify weaknesses and areas where improvement is needed.

To begin with, modal analysis is composed of the two equally-important experimental and simulation parts.

Simulation has been a crucial tool in the engineering sphere for a long time on. The development of Finite Element Model (FEM) tools has had an unquantifiable value on the study of structural dynamics. The models implemented by sophisticated software configurations allow to emulate all kinds of different scenarios and operational conditions in a very lesser cost- and much quicker manner. They rely on the theoretical groundings and heavy mathematics behind, but also from the data collected during experimentation. FEMs and analytical models work together by correlating and correcting each other in an iterative process. Without data collection, there is no evidence of sufficient proximity to reality, which is, at the end, the whole purpose of simulation.

Experimental modal analysis reaches the area of study of two types of systems: mechanical systems, in which the input is usually a force (N) and the output an acceleration (g); and acoustical systems, where inputs and outputs are normally expressed as volume acceleration, also called acoustic force (Q) and sound pressure (p or SPL), respectively. As the components studied within work act as mechanical systems, it is at this point clear that modal analysis covers the demands of the here pretended analysis.

In accordance with the experimental approach this project is set to follow, the experimental part of modal analysis and its theoretical foundations will be the focus of attention within this section.

The extent to which modal analysis can be implemented goes far beyond the purposes of this work. The technique is frequently used to analyze the modes of vibration of complex structural systems, in which several inputs and many more outputs are present.

A good example is the use of modal analysis when studying the fluttering of airplane wings [GUIL00] during flight-like scenarios. In the construction field, modal analysis is the to-go technique to analyze the behavior of large structures under operational conditions.

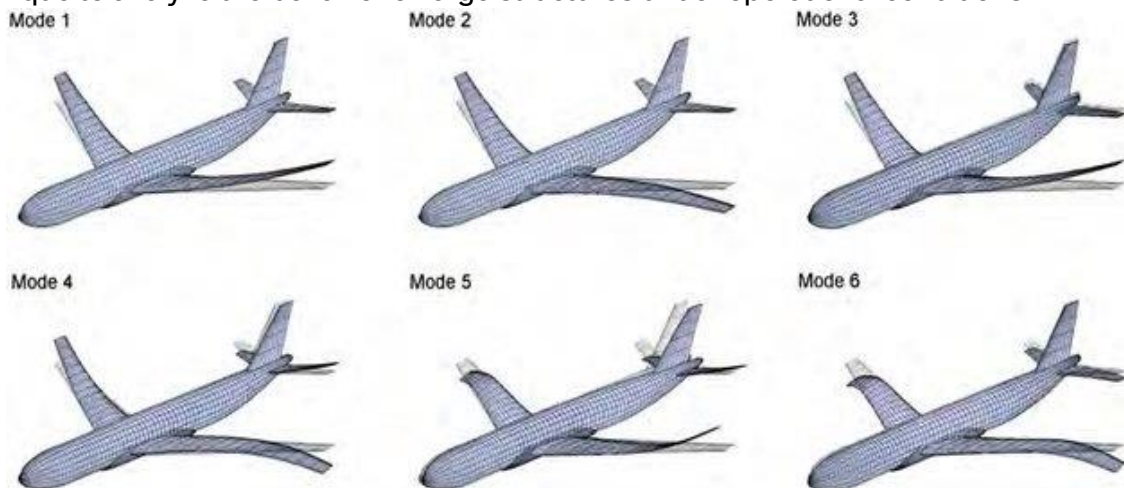


Figure 16. Modes of vibration of an airframe. Source: Application of pilot models to study trajectory based manoeuvres, Mudassir, 2012

With respect to the test object and the principal aim of this work, the scope to which modal analysis can be realized becomes too complex to be fully implemented here. The mathematical foundations of this technique can eventually turn into an unnecessarily confusing area and will be only elaborated to a certain reach. The necessary comprehension of the technique of modal analysis to follow the work done in this project stays away from these complex foundations, as it has been found to disturb and drive away the focus on the steps followed and the decisions made during the experimentation process within this work.

Therefore, only the basic foundations of modal analysis are explained in this section. In the need for a deeper theoretical background, the references used for the here done elaboration of the concepts behind modal analysis can be consulted.

2.3.2 Experimental Modal Analysis (EMA)

Vibrational, experimental tests are carried out at the design phase of structures and allow to estimate the natural (or resonance) frequencies and damping magnitudes by measuring the input force and output deformation curves when exciting the structure to a controlled vibrational state.

The physical signals are interpreted by transducers, which transform the readings on the input tool (usually an impact hammer or a shaker) and the accelerometers into electrical signals. A signal acquisition device interprets the signals and translates the physical data collection into time or frequency-based curves, with the help of the right software. These curves are then related to each other by the so-called Frequency Response Function (FRF).

The measure on to which degree the input is the cause of the output (in other words, how much the input and the output re related to each other) is defined by the Coherence Function (CF), which is especially useful when performing the experiments.

These two functions play a crucial role in the experimental modal analysis of the vibrational behavior of the structure or object of evaluation and are the main focus of study when performing such experiments.

2.3.2.1 Frequency Response Function (FRF)

The FRF is an essential element in experimental modal analysis. It shows the relationship between the input and the output in the frequency domain and is used to identify resonant frequencies, damping and mode shapes. It is sometimes called “Transfer Function”, and mathematically described as the ratio of the output to the input in Laplace domain:

$$Y(s) = H(s) * X(s); \quad H(s) = \frac{Y(s)}{X(s)} \quad (1)$$

where:

- $X(s)$ is the input function in Laplace domain.
- $Y(s)$ is the output function in Laplace domain.
- $H(s)$ is the FRF or transfer function in Laplace domain.

As perceived from its own definition as the ratio between two curves in the frequency domain, the FRF is a complex number, with a real and an imaginary part. The most common representation of the FRF is yet described by its magnitude and phase, which entirely characterize the dynamics of the studied system:

$$H(j\omega) = H(s)_{s=j\omega} \quad (2)$$

- ω is the angular frequency, in rad/s.
- Gain: $|H(j\omega)|$
- Phase: $\angle H(j\omega)$

A representation of the gain and the phase of the FRF in the frequency domain results in a complete representation of the dynamics of the system.

Experimental modal analysis has, however, a restrictive assumption: it considers the component under evaluation to be a Linear Time-Invariant (LTI) system [HOOP15]:

- “Linearity” states that the component follows the Law of Superposition, which is described as follows:

If two inputs $x_1(t)$ and $x_2(t)$ produce the outputs $y_1(t)$ and $y_2(t)$, respectively:

$$x_1(t) \rightarrow y_1(t); \quad x_2(t) \rightarrow y_2(t) \quad (3)$$

then:

$$ax_1(t) + bx_2(t) \rightarrow ay_1(t) + by_2(t) \quad (4)$$

- “Time Invariant” stands for a non-variation of the relationship between input and output over time:

If the input $x_1(t)$ produces the output $y_1(t)$:

$$x_1(t) \rightarrow y_1(t) \quad (5)$$

The input $x_1(t - T)$ then produces the same output delayed in time by a value of T :

$$x_1(t - T) \rightarrow y_1(t - T) \quad (6)$$

This comes at the end to say that the vibrating behavior of a component can be studied by means of experimental modal analysis as long as it acts as a LTI system.

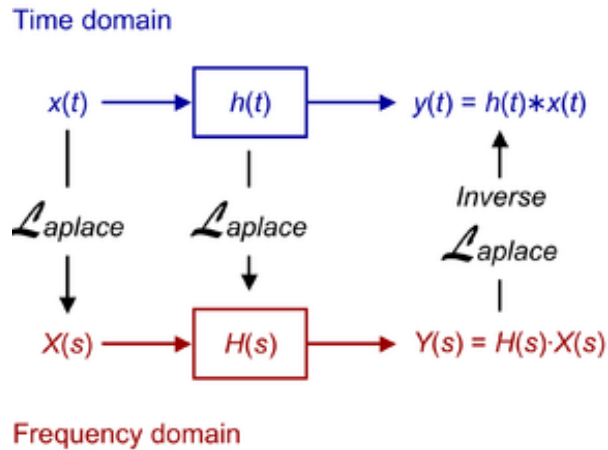


Figure 17. Time domain to Laplace domain transformation

2.3.2.2 Coherence Function (CF)

The CF simply indicates the portion of the output energy that is caused by the input energy and is defined in the frequency domain as follows:

$$G_{xy}(f) = \frac{|G_{xy}(f)|^2}{G_{xx}(f) * G_{yy}(f)} \quad (7)$$

where:

- $G_{xy}(f)$ represents the cross-spectral density between the input and the output.
- $G_{xx}(f)$ is the auto-spectral density of the output signal.
- $G_{yy}(f)$ is the auto-spectral density of the input signal.

The CF is always measured as a value between zero and unity; 0 meaning that none of the output is caused by the input at the given frequency, and a value of 1 meaning that all of the response energy is due entirely to the stimulus signal. A CF value greater than 0.9 is representative of a valid measurement point [HOOP15].

It then allows to identify potential uncertainty between both signals and excessive noise caused by an external factor or an incorrect measurement procedure. It comes very handy when performing the experiments and is an essential feature to ensuring a fine measurement.

A more accurate definition of the mentioned terms of auto- and cross-spectral density can be found on A. Bilošová [[BILO11](#)].

2.3.3 The Modal Model

The previously mentioned modes of vibration, natural frequencies and damping factors are all related to each other and collected in what is known as the “Modal” Model.

The development of a modal model is a mathematical process, which uses data (modal data) to determine the effects of modifications in the system characteristics due to physical structural changes.

This model describes each mode shape (or mode of vibration) of an object of study by its modal parameters: the natural frequency, also called resonant or modal frequency; the modal damping and the mode shape.

These modal parameters are inherent of the object of study, just as its colour or density, and are defined by the elastic and inertial properties of the materials within the object, for instance the mass and the stiffness. The boundary conditions of the object also play a role when defining the modal parameters. If either its material properties or boundary conditions change, so will the modal parameters, the mode shape and the vibrating behavior of the object of study. By attaching the object to a vertical surface as a cantilever or by including an additional mass anywhere in its structure, the boundary conditions and material properties have been respectively changed and so have therefore the vibrational behavior [GUIL00].

How the alteration of these actors affects the modes of vibration of a body can be interpreted by the description of two physical systems.

2.3.3.1 Single Degree of Freedom (SDOF)

A mechanical SDOF system described by means of modal analysis is represented as a spring-damper-mass system of a single element, where the mass is only allowed to move in one direction.

The dynamic properties of the system: the mass, m [kg]; the stiffness, k [N/m]; and the damping coefficient, c [$N \cdot s/m$] define its structural dynamics. They are all related to the and the total force in the direction of movement, f [N]; by the following equation:

$$f(t) = m\ddot{x}(t) + c\dot{x}(t) + kx(t) \quad (8)$$

Where $x(t)$ stands for the position of the mass with respect to its equilibrium point, $\dot{x}(t)$ to the velocity and $\ddot{x}(t)$ to the acceleration, at any point in time. Four force-like terms can be identified from the model [GUIL00.]:

- Externally applied force: $f(t)$
- Inertial force: $-m\ddot{x}(t)$
- Viscous or damping force: $-c\dot{x}(t)$
- Restoring force: $-kx(t)$

The mentioned equilibrium point is the value of $x(t)$ at which $f(t) = 0$.

By transforming equation (8) to the Laplace domain and assuming zero initial conditions for simplification, the relationship of the four mentioned terms is now described as follows:

$$F(s) = Z(s) * X(s) \quad (9)$$

Which has an analog structure as that of the FRF described above. This means that, being:

- $F(s)$ the applied force in Laplace domain, or input to the system
- $X(s)$ the subsequent position of the mass in Laplace domain, or output of the system

The term $Z(s)$ is called the dynamic stiffness and also the inverse of the transfer function of the system in Laplace domain, which is a second-order system. The dynamic stiffness is described as:

$$Z(s) = ms^2 + cs + k \quad (10)$$

which means that the transfer function of the spring-damper-mass SDOF system here described is defined as:

$$H(s) = \frac{X(s)}{F(s)} = \frac{1}{Z(s)} = \frac{1}{ms^2 + cs + k} \quad (11)$$

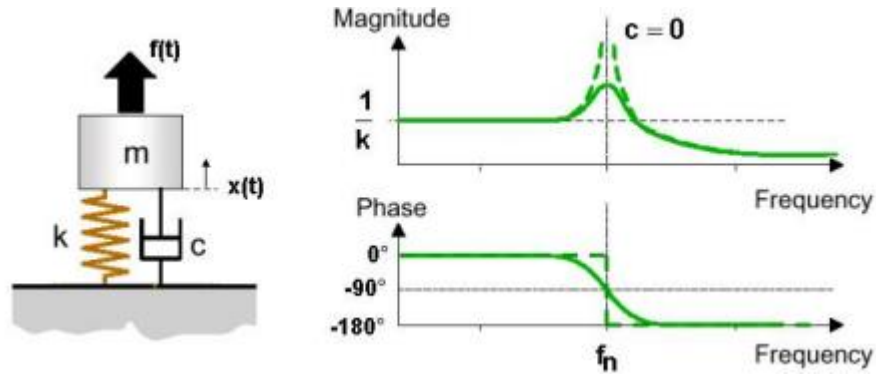


Figure 18. SDOF spring-damper-mass system

The roots of the dynamic stiffness (denominator of the transfer function) are subsequently the poles of the system, that is, the values at which the denominator polynomial becomes zero.

When solving for $Z(s) = 0$, the poles of the system are defined by the physical parameters of the spring-mass-damper model as follows:

$$s = \frac{-c \pm \sqrt{c^2 - 4mk}}{2m} = \frac{-c}{2m} \pm \frac{\sqrt{c^2 - 4mk}}{2m} \quad (12)$$

Considering the imaginary number $j = \sqrt{-1}$, the equation (12) can be then rearranged into its real and imaginary parts:

$$s = \frac{-c}{2m} \pm j \frac{\sqrt{4mk - c^2}}{2m} = \frac{-c}{2m} \pm j \sqrt{\frac{k}{m} - \left(\frac{c}{2m}\right)^2} \rightarrow s = -\delta \pm j\omega_d \quad (13)$$

being:

- Modal damping: $\delta = -Re\{s\} = \frac{c}{2m}$.
- Modal frequency: $\omega_d = Im\{s\} = \sqrt{\frac{k}{m} - \left(\frac{c}{2m}\right)^2}$, as the imaginary part.

This shows that for a system with no damping, $c = 0$, its poles will result in a complex pair of poles:

$$s = \pm j \sqrt{\frac{k}{m}} \quad (14)$$

And by recalling that $s = j\omega$, the value of the natural frequency of the undamped system, ω_n , is essentially that relationship between the stiffness and the mass:

$$j\omega = \pm j \sqrt{\frac{k}{m}} \rightarrow \omega|_{c=0} = \omega_n = \sqrt{\frac{k}{m}} \quad (15)$$

The stiffer the material, the higher the frequency at which it naturally vibrates. On the other hand, larger and heavier structures of the same material (same stiffness) will naturally vibrate at a lower frequency.

The natural frequency is especially important for mechanical structures, as they usually have very low damping coefficients when compared to the other magnitudes. That is, when considering a weakly damped system, the modal frequency can be approximated to the natural frequency:

$$c \approx 0 \rightarrow \omega_d \approx \omega_n \quad (16)$$

As both the modal damping and the natural frequency of vibration of the system are described, these two magnitudes can be arranged to describe the natural damped vibration of the system as follows [KOKA10]:

$$\omega_d = \text{Im}\{s\} = \sqrt{\frac{k}{m} - \left(\frac{c}{2m}\right)^2} = \sqrt{\omega_n^2 - \delta^2} \quad (17)$$

The FRF of a SDOF spring-damper-mass system can then be described in the frequency domain by substituting $s = j\omega$ and rearranging the components as follows:

$$H(j\omega) = \frac{1}{-m\omega^2 + jc\omega + k} = \frac{1}{(k - m\omega^2) + jc\omega} \quad (18)$$

By simply substituting the values of frequency and damping coefficient for the case of the non-damped system, it can be seen that the value of the transfer function goes to infinity. This idea is related to the phenomenon of resonance explained in a subsequent section.

There are two magnitudes that help minimize the dimensions used within the formulas and that allow for a representation with relative values:

- Lehr's Damping ratio (sometimes referred to as damping grade, D): $\zeta = \frac{\delta}{\omega_n} = \frac{c}{2m\omega_n}$
- Dimensionless excitation frequency: $\eta = \frac{\omega}{\omega_n}$

Recalling once more equation (18), a better description can be done by means of the natural frequency and the damping ratio as follows:

$$H(j\omega) = \frac{1}{k \left[\left(1 - \frac{\omega^2}{\omega_n^2}\right) + j \frac{2\zeta\omega}{\omega_n} \right]} = \frac{\omega_n^2}{k [(\omega_n^2 - \omega^2) + j2\zeta\omega_n\omega]} \quad (19)$$

And by using non-dimensional frequency magnitude, a finer representation of the transfer function is depicted as below [KOKA10]:

$$H(j\omega) = \frac{1}{k[(1 - \eta^2) + j2\zeta\eta]} \quad (20)$$

The impact of these magnitudes on the amplitude and phase curves shown in [Figure 14](#) can be visualized with a short example:

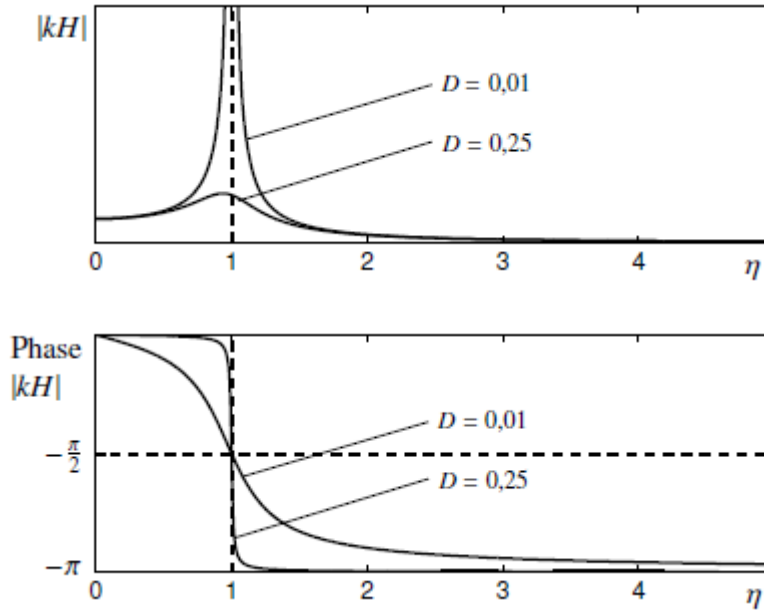


Figure 19. Effect of Lehr's damping factor on the amplitude and phase on a SDOF system

Such angular frequencies can be transferred to the most commonly used frequency domain by considering the trigonometrical angle of displacement within a cycle: 2π . The following definitions are depicted from this transformation:

- Damped natural frequency: $f_d = \frac{\omega_d}{2\pi}$
- Undamped natural frequency: $f_n = \frac{\omega_n}{2\pi}$

Lehr's damping ratio can also be described by the damped and undamped natural frequencies:

$$f_d = f_n \sqrt{1 - \zeta^2} \rightarrow \zeta = \sqrt{1 - \frac{f_d^2}{f_n^2}} \quad (21)$$

Which shows that the frequency of the system when the damping ratio is zero is essentially the undamped natural frequency, f_n .

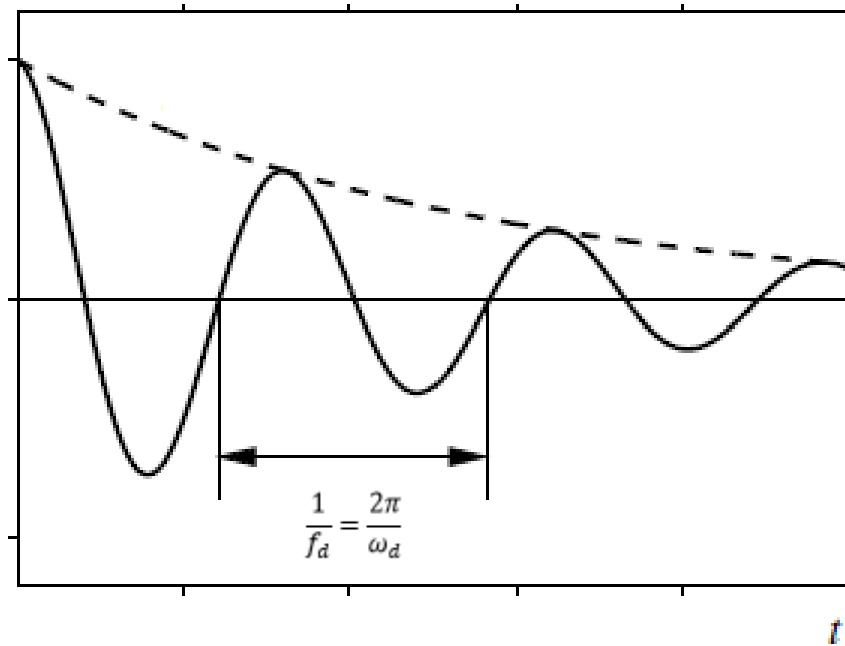


Figure 20. Vibration response of a second-order damped system

2.3.3.2 Multiple Degree of Freedom (MDOF)

The description of a MDOF model of a spring-damper-mass system approaches the same physical concepts elaborated in the SDOF model, but instead of a single element it considers multiple inputs, outputs and elements.

Contrary to the SDOF model, the MDOF is expressed by the use of matrices, which contain the mentioned physical magnitudes of each single element present in the system. The same principles are applied, but the mathematical elaboration adopts a matrix form, instead of single linear relationships.

The equation (1) is now described as follows:

$$\mathbf{f}(t) = \mathbf{M}\ddot{\mathbf{x}}(t) + \mathbf{C}\dot{\mathbf{x}}(t) + \mathbf{K}\mathbf{x}(t) \tag{22}$$

Which in Laplace domain is described as:

$$\mathbf{F}(s) = \mathbf{Z}(s) * \mathbf{X}(s) \tag{23}$$

The bold magnitudes refer to vectors and the capital letters, to matrices. The image below shows an example of a two degree of freedom spring-damper-mass model [GUIL00]:

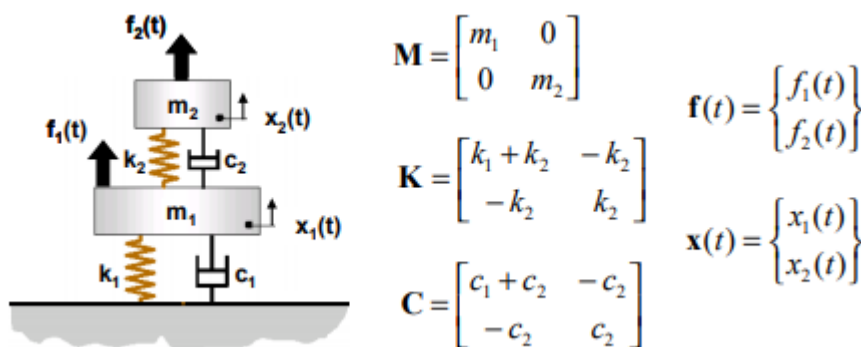


Figure 21. Example of a two-DOF spring-damper-mass system

Most real structures are modelled as MDOF systems. However, these complex configurations are essentially the linear superposition of multiple SDOF systems, as long as the system is LTI.

With that said, and although very few practical structures can be realistically model as an SDOF system, it is its properties that are the basis of the MDOF systems and therefore the focus within this section.

Complex, real MDOF systems are most accurately described by using heavy computation and sophisticated simulation models. Being those not the tools implemented in this experimental project, a more profound analysis on the MDOF model is not discussed here. Nonetheless, a broader mathematical elaboration of the MDOF systems, approaching the matrix representation of properties, can be found in [GUIL00].

2.3.4 Practical approach to EMA

As far as the theory goes, the mathematical foundations that connect structural dynamics and

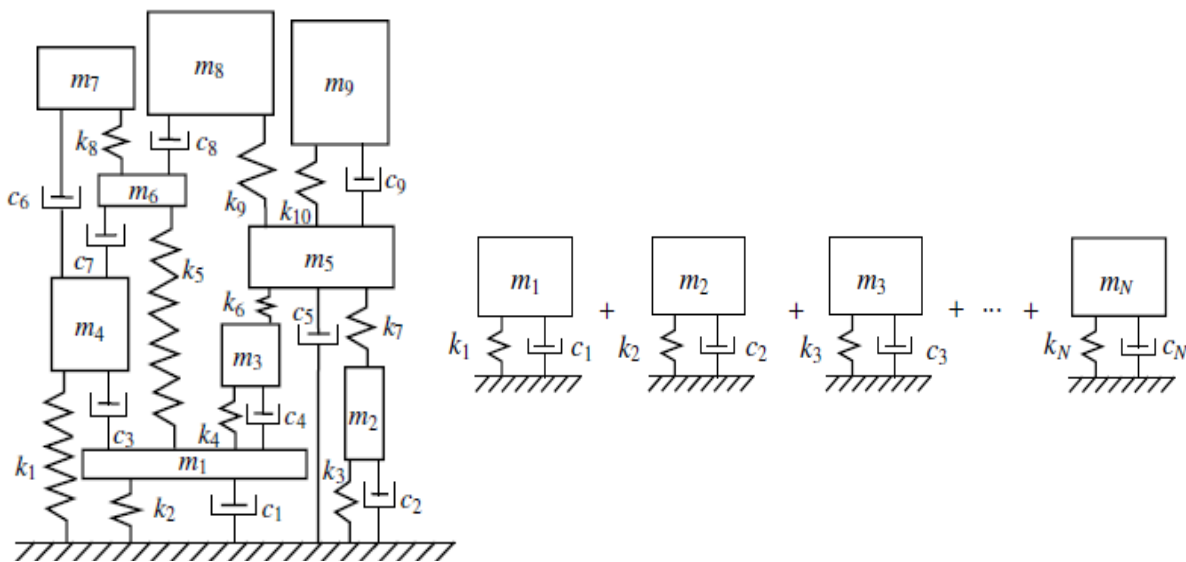


Figure 22. A MDOF system represented as the superposition of multiple SDOF systems

modal analysis are sometimes found excessive and difficult to handle from an experimental point of view. The reality of the vibrational behavior of structures and the “palpable” meaning of the modal parameters cannot be illustrated through the theoretical relationships of the physical parameters described in the modal model. In order to do so, a much more practical approach to modal analysis is needed.

2.3.4.1 Contribution from Avitabile

Prof. Peter Avitabile from the department of Mechanical Engineering in the Francis College of Engineering, and PhD in Mechanical Engineering by the University of Massachusetts Lowell has resolved this situation that he found when teaching undergraduates the foundations of modal analysis. His extensive work on how to describe experimental modal analysis from a non-mathematical perspective is widely acknowledged within the field to have overcome the mentioned problem, as most of the recent work done includes his instructions.

Avitabile’s approach relies on the use of illustrations and multimedia to break down the principles of modal analysis with a very practical purpose. This provides a very visual understanding of the reality of structural behavior and the effects of changes in the modal parameters.

For a better understanding of the practical principles that support the work done in this project, some of the most important descriptions found in his works are addressed in this section [AVIT01].

2.3.4.1.1 The free plate: an illustrative example

Modes of vibration can be simpler explained by the example of a freely supported plate. This is known as the “free-free state”, at which no boundary conditions or external actors can alter the structural vibrating properties of the object of study. As anticipated, the free-free state is an ideal, as the structure would be suspended in the air without any contact to other elements but its own components. Although this might sound very theoretical, there are some ways to approach this behavior to properly study this true modal parameters of certain structures.

A feasible free-free state is achieved by an unrestrained support, with the use of soft springs or foam pads, for instance. The natural frequencies of the bearing method are also present in the response signal, as they play a role in the transmission of the vibration waves through the structure. A correct unrestrained support is accomplished when it allows the object to be freely suspended and exhibit six rigid body modes: three displacements in the x-, y- and z-axis; and three rotations around each of them [HOOP15].

Since this ideal of free-free is based on the assumption that no boundary conditions are present, the reactions between the bearing and the test component would have a natural frequency equal to zero. In reality, the natural frequencies of the supporting method are not zero but necessarily low enough, so they can be distinguished from the ones of the object of study without any prospect of error.

Some studies state the condition to free-free state as the highest natural frequency of the bearing mechanism to be less than the 10% of the lowest natural frequency of the test object or if there is at least a 100Hz gap between them [HOOP15]. This will be further addressed when discussing the results.

By applying a force at one point on the plate, and measuring the response at other point with an accelerometer, most of what modal analysis studies can be described by analyzing the results:

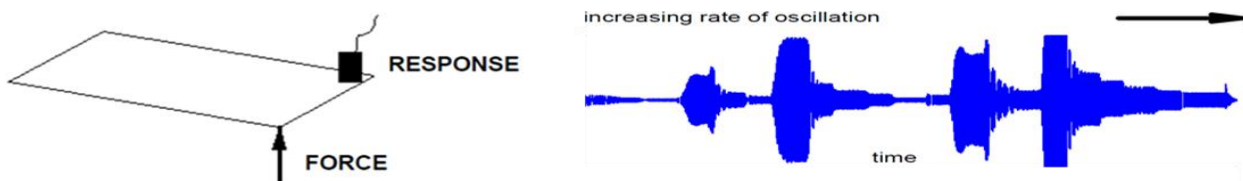


Figure 23. Free-free plate test illustration and output signal representation [AVIT01]

The applied force is yet not a static magnitude like those studied in physics, such as the weight of bodies that cause a permanent deformation on structures. It is a very short-timed input, which varies in a sinusoidal fashion. Even if the magnitude of the force (the peak in the oscillatory curve) is maintained equal when varying the rate of the input force, the output signal will show higher and lower values of the output magnitude (e.g. acceleration). This is because the input energy is most amplified at specific frequencies, the natural frequencies of the plate, and therefore the amplitude of the output signal over time is greater at such frequencies closer to the natural or resonance ones, achieving a maximum at these exact values.

The function in [Figure 19](#) represents the overall time response curve at all different frequencies of the applied oscillation. Although the time domain is still representative of the phenomenon, the frequency domain helps to address more correctly the meaning of the modal parameters.

The input and output curves can be shown in both the time and frequency domain. These two can be understood as the inverse of one another, but their mathematical relationship is much more

complex than that. The Fast Fourier Transform (FFT) is the derived tool from such mathematical elaboration and allows to transform any signal from the time domain to the frequency domain. The inverse process requires the inverse of the FFT.

To put it into simple words, the FFT procedure states that every time signal, independent of how complex it might appear, can be seen as the superposition of multiple singular-frequency sinusoidal functions. All of these sinusoidal functions can be simply transformed to the frequency domain, so the representation of all of these singular frequency signals together into a single frequency chart would be literally the representation of the original, complex time signal in the frequency domain.

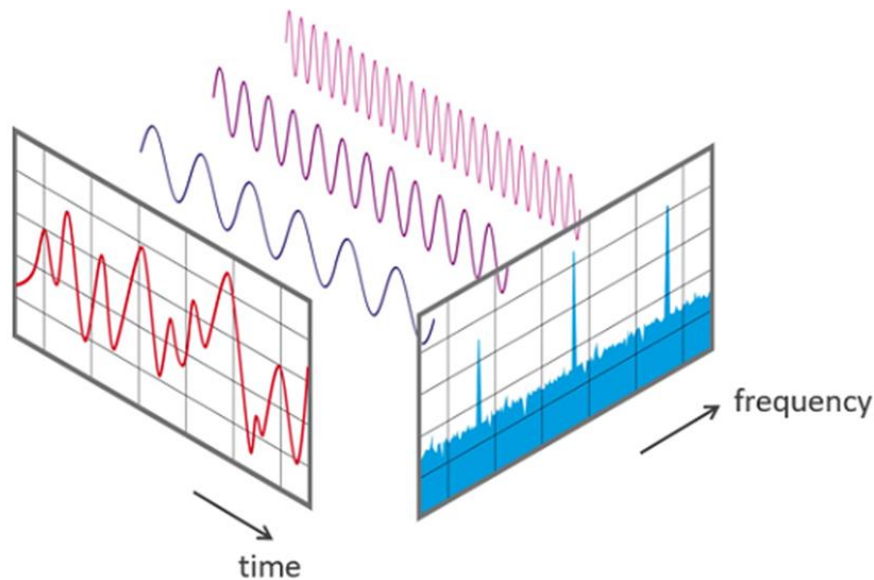


Figure 24. Process of the FFT. Source: NTi Audio

As Avitabile illustrates, the overlay of the time and frequency responses shows the possibility of depicting the natural frequencies of the test object by both curves. That is, the input oscillating frequency at which the time curve reaches a maximum corresponds with a frequency in the frequency response curve at which a maximum is also reached.

Even though both representations of the response function are illustrative of the natural frequencies, the frequency domain is clearly seen as easier to use.

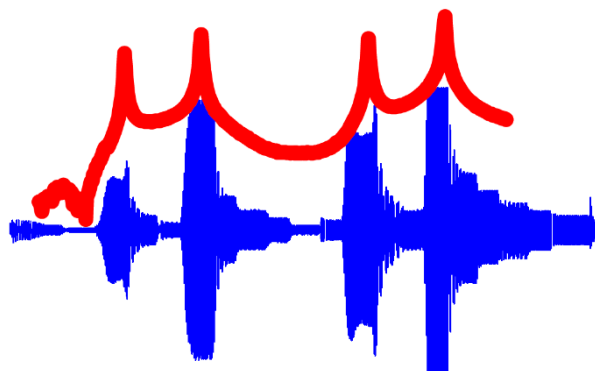


Figure 25. Overlay of the Time and Frequency responses

The following step is to clarify the meaning of mode shapes. As the natural characteristics of a structure allow it to vibrate with more or less amplification depending on the frequency of excitation; the deformation patterns that are taken on at these different frequencies are also different to each other. How a structure is deformed by some kind of oscillating input at a certain rate differs from the way it is deformed at some other input rate, even when the magnitude of the input stays the same.

The form or shape to which the structure is deformed are the so-called mode shapes of the structure, each of them having its own pattern, magnitude of deformation and natural frequency at which they occur.

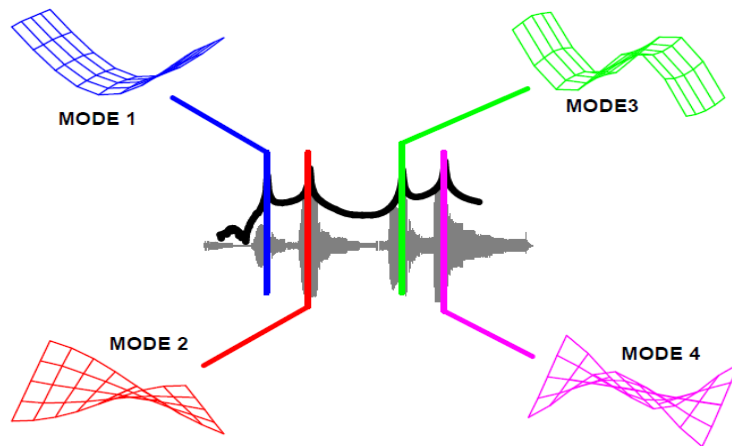


Figure 26. Modes and frequencies of vibration of the free plate

The definition of the mode shapes of vibration should not be confused as the unique vibrating behaviors the structure has. A structure that is subjected to any oscillating vibration input will vibrate. Whatever the frequency of vibration is, the structure will manifest a vibrating response. The vibration occurring at one natural frequency of the structure has the special ability to showcase a clear, highly amplified mode of vibration, for instance a torsion or bending behavior. The vibrating response at those frequencies between two natural frequencies will display a complex mixture of the many vibrating behaviors the structure can exhibit, will be lesser amplified and will be influenced the most by the natural frequency they are closer to.

Defining the mode shapes and modal parameters of a structure is yet the most complete form of analysis of its vibrating behavior, as the most amplified and structurally most important modes are entirely described, which also allow for the description of the in-between vibration behaviors found at the non-resonant frequencies. Design engineers, by means of modal analysis, can identify these mode shapes and understand how they might affect the vibrating behavior of the studied structure; which helps them to work out a better design in terms of its applications.

A compact display of all the relationships between the parameters and concepts explained by modal analysis are represented in a more practical way, just as Avitabile structured it [AVIT01]:

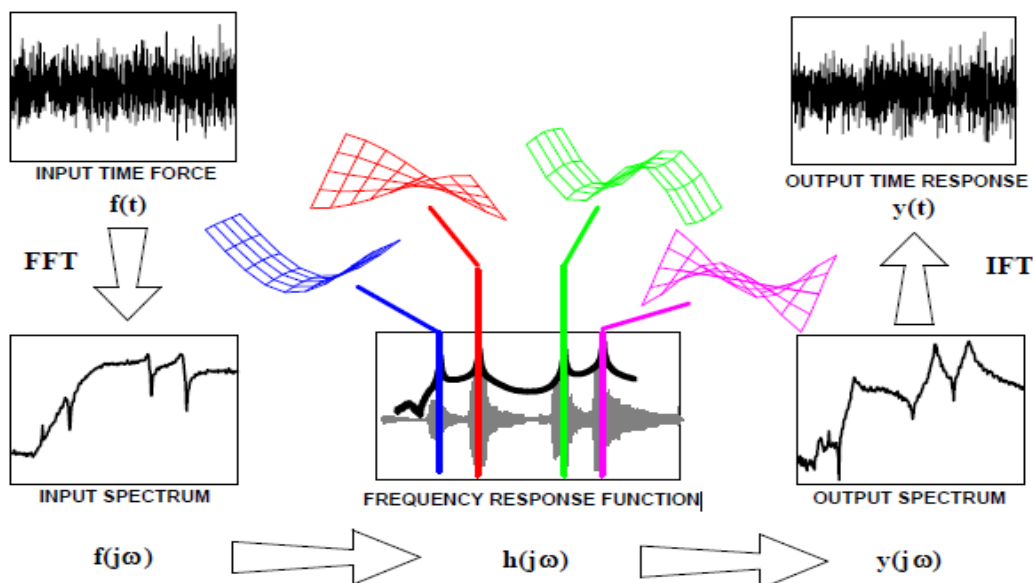


Figure 27. Overview of the modal response analysis process

2.3.4.1.2 Performing EMA

The example of the free plate has been used to describe all of the important concepts in modal analysis into a more visual manner. However, a more extended elaboration of some of the above explained concepts and how to implement them is necessary in order to retrieve the mode shapes of a structure when performing EMA.

The most important feature and main focus in modal analysis is the FRF. At this point, it has been defined as the ratio of the output response to the input excitation force, being it a complex function defined by means of its magnitude and phase. It is important to clarify that the applied force and the response of the structure due to the applied force, both in the time domain, are the two magnitudes that are measured by the use of sensors. The rest of the concepts, magnitudes and functions in modal analysis are depicted as a result of transformations and calculations of these two measured magnitudes.

A signal process analyzer is then used to implement the FFT algorithm that allows to transform the ratio of these two magnitudes in the time domain to the frequency domain. This ends up in the complex FRF previously addressed.

As in the free plate example, the FRF is the relationship between the output signal at one measurement point and the input signal at other (or the same) measurement point. It therefore shows the vibrating behavior of one specific location within the plate when an input is applied at other (or the same) location, along the whole frequency range. This, however, does not explain the vibrating behavior of the plate, but just that of one point of the plate by one specific input location. It is therefore necessary to analyze the behavior at other locations on the plate, that is, to acquire other FRFs within the plate. That is done by changing the position of the output location, the input location, or both simultaneously. Each pair of output-input locations will provide a different FRF within the structure, and the collection of a sufficient assortment of FRFs will end up describing the vibrating behavior of the whole structure.

Due to the symmetry that the dynamic properties (the mass, the damping or viscosity and the stiffness) deliver to a system, the vibrating response related a specific input-output pair is independent of the direction of the path it follows. That is, the structure will equally transmit the vibrating excitation, or in other words, exhibit the same vibrating response by swapping the input and output locations with one another. The path stays the same, and so does the vibrating properties that describe this behavior (the FRF).

With that said, by adding more output locations to the system (e.g.: more accelerometers) and measuring the output response of each of them and the input response of the unique input location, the number of different FRFs obtained correspond with the number of different output locations within the structure. And now, by adding an extra input location and measuring each output-input pair of locations, the number of different FRFs would have doubled.

It therefore makes sense to display the different FRFs within a structure into a matrix, where:

- Each row represents and output/accelerometer location.
- Each column represents an input/impact location.

However, two matrices are needed when describing the system behavior by means of the FRFs: one for the magnitude or gain and one for the phase.

A practical example of a cantilever beam with three different input locations and three different

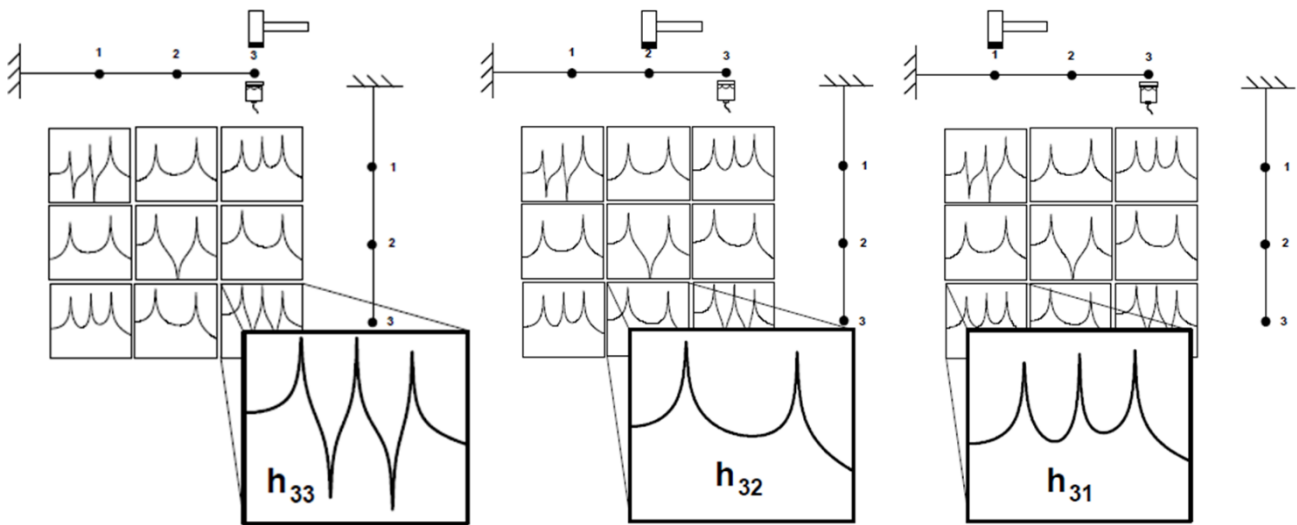


Figure 28. Gain matrix with one indicated drive FRF (left) and two cross FRFs (middle and right)

output locations is shown below [AVIT01]. For size purposes, only the magnitude matrix is included.

When the FRF is the result of the output-input pair of functions of the same measurement point, it is called a drive point or drive FRF. When the locations of the output and the input are different, it is called a cross FRF.

The FRF matrix is symmetric, as depicted from the characteristics of the dynamic parameters. That means that not all elements of the matrix need to be computed to entirely describe the vibrating behavior of the structure. In fact, only a row or a column is sufficient. The crucial aspect here is how large should the column or the row be, in other words, how many outputs related to the same input are necessary, or vice versa. This is directly related to the number of modes that can be detected, as each FRF or output-input pair provides the response at one point within the system. If all measurement points are displayed as a grid, the response of all measurement points at one natural frequency can be simultaneously illustrated and will exhibit the vibrating behavior (mode shape) of the system at that natural frequency.

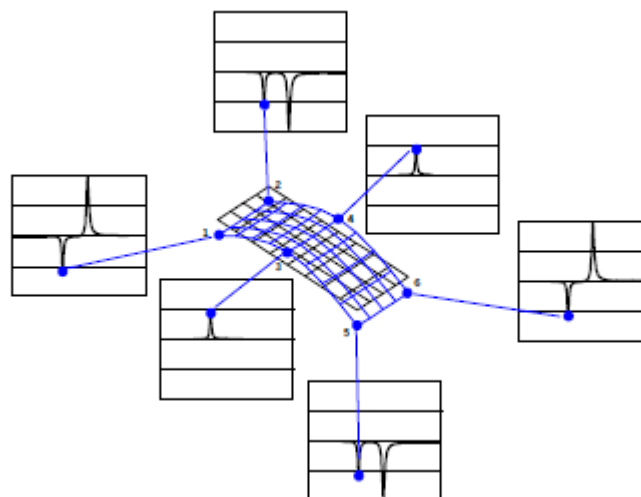


Figure 29. First bending mode shape of the free plate

A more extended explanation of the foundations of this last statement can be found in Avitabile's work [AVIT01].

The choice of a column or a row as the way to define the system is directly linked to the test technique. For such structures, the input force can be implemented with an impact hammer (impact testing) or with a shaker (shaker test). As a full row or a full column both entirely describe the dynamics of the system, it would be theoretically irrelevant which technique to use.

The use of a hammer implies moving the hammer to different input locations and measuring the output at one fixed location with an accelerometer. This is called the roving hammer. On the other hand, a shaker is fixed to a specific input location and the accelerometer is being moved among different measurement points. That is called the roving accelerometer.

When choosing the impact testing with a hammer, two parameters have to be considered: the tip of the hammer and the mass of its head. The hardness of the tip is used to control the frequency range that is excited by the excitation force: the harder the tip is, the wider the frequency range that is excited by the same magnitude of force. However, the power spectral density of harder tips will fall off quicker than that of soft tips [AVIT01]. The correct approach is to identify the frequency range of interest to be excited, and then choose the proper hammer tip for that range: a too soft tip will not reach the higher frequencies within the range, whereas a too hard tip will distribute the energy within a wider range and might therefore not excite the desired ranges sufficiently. On the other hand, the mass of the head of the hammer allows for sufficient energy to come into the system. A very light hammer might not be able to excite the structure at all, whereas a too heavy hammer head would be too difficult to handle and would end up in a very inaccurate excitation technique. A good example to understand the impact of a too light head mass would be to try to excite the mode shapes of a boat with a little hammer the size of a hand, whereas a hammer the size of those used by the reparation industry might be too heavy for pouch-cells, for instance.

When performing experimental modal analysis, there is three key inputs or decision to be made in order to collect the most accurate data available. These three key points are retrieved from all the explanations and important information described above and are summarized as:

Medium	Key Point	Goal
Hammer tip and mass	Defining the frequency range of interest to be thoroughly analyzed	To sufficiently excite all desired mode shapes
Properties of the FRF matrix	Defining the layout of the measurement grid and number of points	Correct display of the desired mode shapes
Anti-aliasing, sampling, quantification and windowing	Compensation	Accurate collection of data

Figure 30. Key decisions on EMA

2.3.4.1.3 Reality of EMA and aspects of interest

When performing an actual experiment, the actual situation and the characteristics of it might differ at a certain point with some of the theoretical affirmations that have been explained. That is, the reality of the EMA as it is to be performed brings up restrictions to which the theory can be applied.

Some of these restrictions are a consequence of the imperfect reality and the applicability of the ideal theoretical groundings, while some others of the testing conditions itself. The majority of these restrictions can be understood prior to the test, but a few others only come with experience. This section describes the sources of all aspects of interest that have been considered for the performance of the EMA experiments done within this work.

Beginning with the input force tool, reality is that there are two main factors that differentiate the execution of an impact test to that of a shaker test, as a contradiction to what the theoretical description of the FRF states: the effect they have on the structure during the test and the feasibility of the test technique they are linked to.

Since the final structure from which the modal data is retrieved is inevitably the object of study plus everything involved in the acquisition of data: bearing mechanism in contact with the structure, mass of mounted transducers, the potential stiffening effects of the shaker attachment, etc., there will be differences between a shaker and an impact test due to their practical aspects when collecting measurement data. Another way to see the effect of the shaker is when experimenting with small structures or test objects. For instance, components like the mentioned pouch-cells could not be tested by means of modal analysis with the use of a shaker [HOOP15, POPP18]. The second aspect to consider when choosing the excitation tool is the measuring technique that goes with it. In some cases, specific measurement points might not be reachable with the roving hammer, either because they are located on inaccessible areas within the structure or because the measurement setup does not provide enough space to reach it correctly during the experiment. On the other hand, the use of a shaker implies a fix impact position and the roving of the accelerometer. This technique would be difficult to implement when there were specific locations of interest within the test structure, to which the accelerometers could not be attached, or it would cost an inappropriate amount of time.

For these reasons, the use of the hammer or the shaker can be in some cases a need and not an option. A thorough understanding of the characteristics of the experiment and its specifications will always help to choose the most adequate excitation technique, which would provide the collection of significantly more accurate measurement data.

The measurement grid, or disposition of the selected measurement points within the test object also finds its limitations when performing EMA. The number of measurement points and their arrangement at first desired for the experiment may not be fully implementable due to, for instance, the geometry of the object. Certain locations within the ideal grid may correspond to parts of the object that will not transfer the vibrational input as a rigid body. These measurement points would no longer be valid for the analysis of the dynamics of the structure by means of modal analysis. Some other measurements locations within the grid might be difficult to reach or in a very improper manner, which could also lead to false data collection due to an inaccurate technique.

When defining the grid, a special consideration must be accounted for: a measurement point located at one of the nodes of a certain mode shape will not exhibit any deformation at the natural frequency at which that mode shape is excited. Care must be taken of, as various measurement points located at nodes location at the same natural frequency will not provide any information on the vibrating behavior of the structure, which would end up in the miss of that mode [AVIT01].

With respect to the FRF, there are some restrictions when performing an experiment that have to be dealt with, prior to retrieving the most important function in EMA. Again, the reality of the measurement needs to be understood and controlled and some points in the form of restrictions need to be described to this end. The process of depicting the FRF begins with the analog signals collected by the measurement devices (e.g.: hammer, accelerometer, etc.). A transducer installed within the sensor, usually a piezoelectric, transforms the physical signal to an electrical one, which is then interpreted by the measurement system. This system consists of a signal acquisition instrument plus the adequate software and is commonly referred to as a FFT analyzer. Reality is that analog signals commonly need an anti-aliasing filter, installed in the front-end of the FFT analyzer, which remove the high frequencies signals that cause the aliasing effect into the analysis frequency range.

The electric signal transmitted from each transducer is then digitalized by an analog to digital converter (ADC). The process of digitalization is the second cause of error by means of the sampling and quantization: the sampling rate controls the resolution of the representation of the

signals in the time and frequency domain, whereas quantization is associated with accuracy of the captured signal's magnitude. As necessary and inevitable as they are, both cause some errors in the measurement data and a flawed representation of the reality of the raw signals.

However, the biggest source of error is the phenomenon called "leakage", which is caused by the transformation from the time to the frequency domain by the use of the FFT. This process entails the sampled data to be a complete representation of the measured data for all duration of the signal, or at least to contain a periodic repetition of it. When this is not satisfied, leakage causes the data to be distorted in the frequency domain. The solution to this undesired effect is the use of weighting functions, called windows, which alter the sampled data and cause it to appear to properly satisfy the periodicity requirement in the FFT process. Their effect of leakage cannot be completely removed, but windows effectively reduce its effect. Depending on the type of signal, there is an adequate window signal for each specific end [AVIT01]:

- Uniform or Rectangular: unity gain applied to all data points and that is used for those cases when the entire signal can be captured or at least the periodicity requirement is satisfied, for instance, input and response signals for impact testing.
- Hanning: cosine function that forces the two ends of the sample interval to be weighted to zero. They are mostly implemented for random excitation and field signals.
- Flat Top: mainly used for calibration purposes, it is useful for those sinusoidal signals that do not satisfy the FFT periodicity requirements.
- Force or Exponential: unity gain that acts only over a portion of interest of the sample interval, for instance, where the impulse excitation occurs. Mostly used for impact excitation input signals, it forces the response signal to die out within the sample interval, so the unnecessary information is rejected and the FFT requirements are satisfied.

Generally speaking, windows cause inaccuracies in the peak amplitude and the damping to be greater than it in reality is. Although they seem undesirable, they end up being far more admissible than the distortion caused by the effect of leakage [AVIT01].

Although the use of these correctional tools worsens the accuracy of the data collected and would be therefore better to not have to use any, they still overcome the problems of signal processing and are in most cases imperative to implement.

The whole structure of the process and its takeaways are below described in a more compact fashion:

EMA Process Step	Source of error
Measurement of the physical output as electrical, analog signals	Sensitivities from transducers
Anti-aliasing filters at the data acquisition device's front-end	Potential removal of valid high frequencies
Conversion to digital signal by means of an ADC	Sampling and quantization
Usage of windows to deal with the effect of leakage	Signal's lost information and leakage residuals

Figure 31. EMA process and sources of error

2.3.5 Impact of vibrations on the industry

One natural condition of structures that is extensively studied by the use of modal analysis is resonance.

Resonance can be described as the physical phenomenon that occurs when a small energy input into a body results into an important deformation within, and that sometimes results in irreversible damage. It is therefore a crucial object of study within the construction field and the main reason to mechanical failure of structures.

A famous resonant accident was the Tacoma Narrows Bridge disaster on November 7, 1940, when the suspension system of the bridge heavily collapsed due to vibration induced by the wind. Even though the bridge had only been open for traffic for a few months, its design failed to have properly considered the wind forces that the structure needed to face, primarily the frequencies of vibration these forces may excite on the structure.

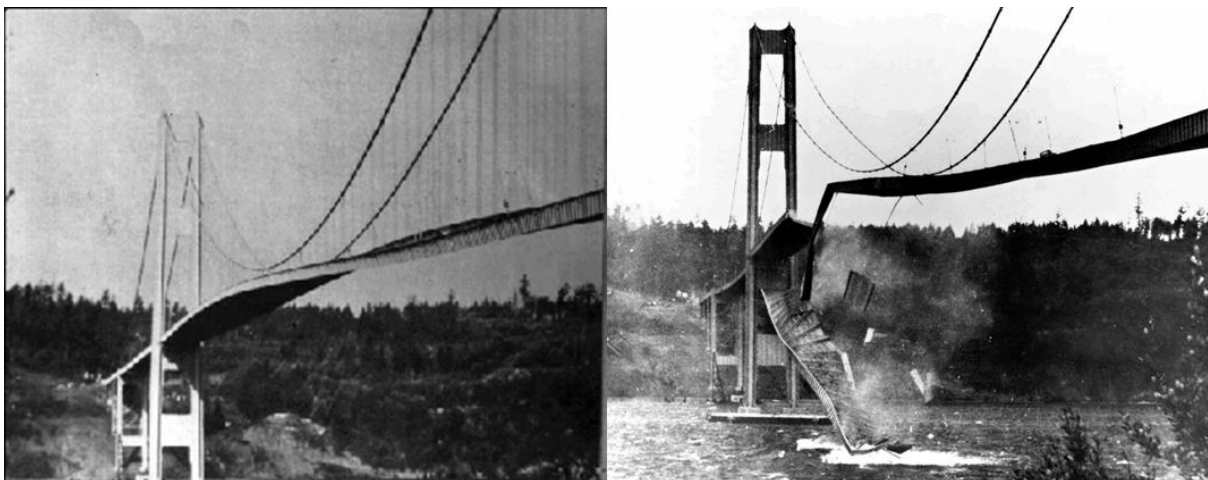


Figure 32. The Tacoma Narrows Bridge disaster, 1940. Source: [GUIL00]

The structural design of the Tacoma Narrows Bridge set certain natural frequencies of the system, as a result of its material properties, weight and dimensions, which were met by the ones from the winds forces present in the area the day the accident happened. The forces of the wind were eventually sufficiently strong, that the effect of resonance ultimately lead to a fatal failure and an unforgettable event in the history of construction.

This is an illustrative example of how relatively small forces can be highly amplified within a structure when its natural frequencies of vibration are matched with those from the input forces, and how importantly is the phenomenon of resonance considered when ensuring the correct performance of structures under the studied operational conditions.

But not only should resonance be considered for structure failure in construction. Most structures resonate at some degree and not necessarily collapse, but only vibrate with an increased oscillatory motion. Resonance is therefore a primary contributing factor to many of the noise and vibration related problems of machinery under operation. This is of severe relevance within, for instance, the automotive industry.

Another important problem of non-catastrophic resonance within the industry is fatigue. As structures are set to long periods of resonating vibrations, the amplification of the undergone oscillating forces causes important stresses within the structure. Even when those stresses do not necessarily go over the mechanical limits of the materials that compose the structure, if they are localized in specific, weaker areas, the long-lasting exposure of these areas to such stress levels can eventually lead to fatigue problems and the breakdown of specific parts or the whole structure. Even if the structure does not ultimately break, irreversible deformations may occur at some point, jeopardizing its serviceable life and functionality, and ending up in unquantifiable costs.

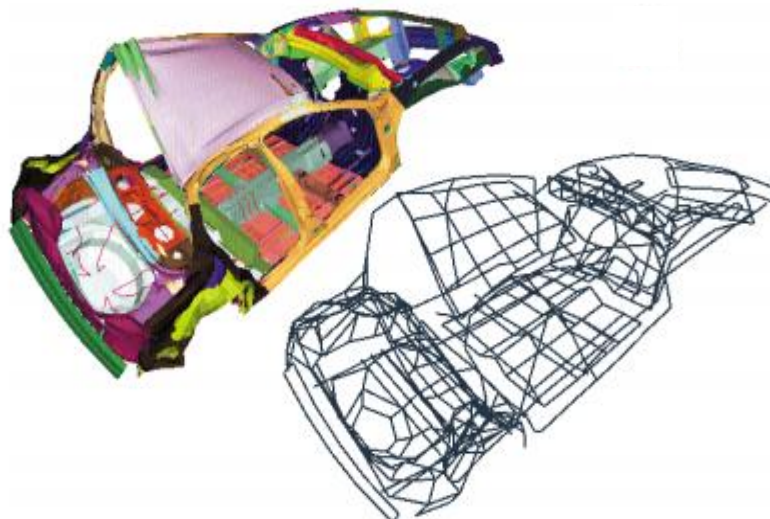


Figure 33. Modal analysis of a car body [GUIL00]

The underpinning theory on the idea of resonance and general amplification of a certain input rate within a structure comes essentially from understanding how energy travels as a wave. Whenever a force is excited into a structure, the energy travels as a wave through the molecules of the materials (or air) within it. How this energy travels back and forth through the structure depends on the structure itself: its geometry, materials and properties. The energy level changes constantly, as some will be elastically transferred between molecules and stay within the system while some other will leave the system through, for instance, heat dissipation. Whenever the following energy input starts to travel through the system, it might add up or counteract the effect of the energy input already present. If the rate of energy input matches the rate at which the energy inside the systems travels through it, the energy level is increased, and so will the amplification seen at the output response.

Resonance and amplified output signals occurring at a certain rate are essentially a perfectly-timed energy flow through the molecules within the system, stimulating the movements between them as the energy level is increasing and therefore causing and amplification of the output response of the system, being it a pressure level, a deformation, an acceleration or a displacement, to name a few.

2.4 DMA

2.4.1 Introduction to DMA

2.4.1.1 First steps into oscillatory experiments

The XXth century was filled of material experimentation and the first attempts found for measuring the elasticity of the material through oscillatory measurements were done by Poynting on 1909 [POYN09]. By the time, there was no sufficient development of commercial instrumentation and the earlier work done was mainly focused on the study of metals. After the introduction of the Weissenberg Rheogoniometer in 1955 and its more than 20 years domination in the market [DEAL83], Ferry was able to give the most accurate development of the theory available at the moment with his “Viscoelastic Properties of Polymers (1961)” [FERR80] which came by a time in which the polymer science had already started to settle within the industry.

Beginning in the late 60s, commercial instruments became more user friendly and the modern period of the Dynamic Mechanical Analysis (from now on: DMA) was started. As a natural transition, a few institutions, such as the Rheometrics Corporation and Bohlin Rheologia were born in the 70s. During the following years, many vendors like Polymer Labs, Du Pont and Perkin-Elmer competed against each other to offering the best material characterization machinery, which led to easier to use, faster and less expensive instruments. This, together with the revolution of computer technology and evolution of software development, changed the industry drastically as all DMA types became more user-friendly.

2.4.1.2 Contribution from Menard

The most current foundations of the DMA date back to the recent end of the last century and are attributed to the, by many considered, “Father of the DMA”: Dr. Kevin Peter Menard. His book “Dynamic Mechanical Analysis, A Practical Introduction (1999)” [MENA08] constitutes the main source of most works done in the field within the following years, and it is no exception for the explanations here present.

Along with the extensive knowledge provided, the way Menard approaches the basics of DMA and the theory behind it is well considered within the industry to stand out for its clarity and practical end. This is found to be extremely convenient for the goals established for this work and is the main reason why he deserves his accreditation.

His book from 2008 collects all necessary guidelines with a very practical focus to performing each type of DMA, but it also presents its theoretical foundations in a very comprehensive way for anyone within the engineering, with no demand for prior knowledge on the subject. This was the main concern that his fellow colleague and friend Witold Brostow had as an educator at the University of North Texas [MENA08] as he experienced that most practitioners stayed away from DMA, possibly due to the use of complex and imaginary numbers. For these reasons, Menard approached his explanations by minimizing the mathematics within and avoiding an unnecessarily rigorous address to the topic.

The theoretical foundations of DMA found in the section below also follow this approach that he made.

2.4.2 Foundations and basic principles

In order to get the whole picture on the theoretical groundings to be depicted in this section, a minimum foundation on the elemental rheological concepts is required. Since incorporating the very basics of Materials Engineering in this document would be very inadequate for the extension of this section, which would also end up being excessively theoretical (the exact opposite intention

of this work), and considering that the reader is meant to have a prior knowledge on the matter, the very basic groundings on the mechanical properties of materials are therefore not disclosed within the following explanations.

However, as some hesitation on the exact meaning of specific engineering concepts may arise, a fantastic source on the basics on rheology can be found in Menard's Book, referenced at the end of this document [MENA08].

From his own words, DMA can be described as “applying an oscillating force to a sample and analyzing the material's response to that force”. This analysis of the response of the material is done by calculating certain mechanical properties of interest such the stress, strain, stiffness and the so-called viscosity of a material or its “tendency to flow”.

As a result of an oscillating force, the amplitude of the sinusoidal functions and the phase lag between the input and the output are of capital relevance. This is the point at which the science behind DMA gets trickier, but it will be explained with sufficient detail and comprehensibility.

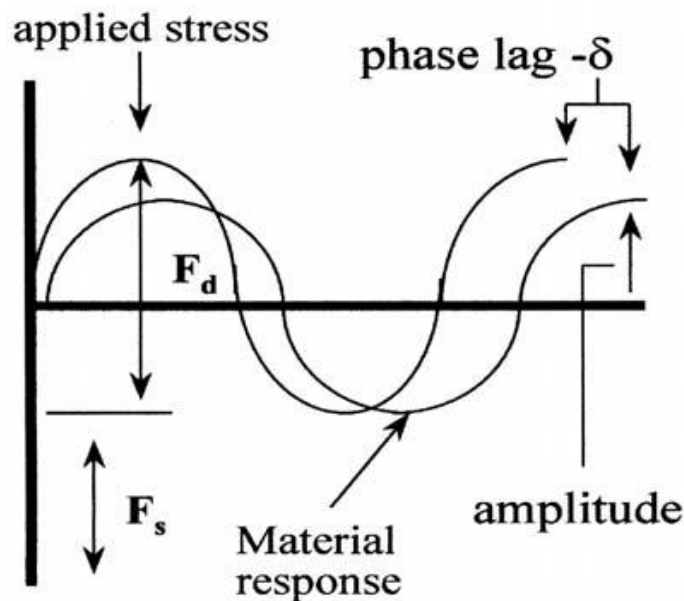


Figure 34. Relationship between input and output on DMA

With that said, the DMA works by supplying an oscillatory force, which causes a sinusoidal stress to be applied to the sample. As a result, a sinusoidal strain is generated as a response of the material to this varying stress, due to its elastic behavior.

The amplitudes at the peaks of these sinusoidal curves, as well as the phase lag between stress and strain are then measured. This allows for the further calculation of the desired mechanical quantities, that is: the stiffness (modulus), the viscosity and the damping. The F_d and F_s tagged in the figure are the corresponding dynamic (oscillatory) force and the static force, which is also known as the clamping force.

The modulus measured in DMA is a complex one in contradiction to the Young's Modulus of the classic stress-strain curves, which is the slope of the curve in the initial linear region:

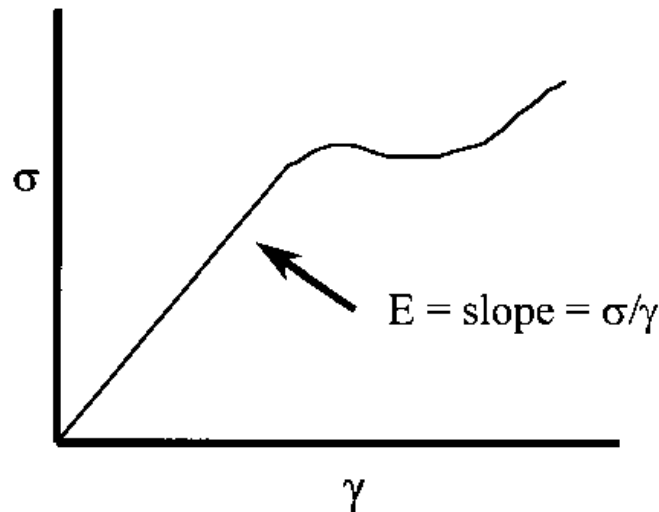


Figure 35. Stress-Strain curve and Young's Modulus for elastic behavior

The **Complex Modulus** in DMA (E^*) is then made up of a real and an imaginary part, which are described as follows:

- **Elastic or Storage Modulus (E')**: ability of the material to elastically return or store energy. It is the real part of the Complex Modulus.
- **Loss Modulus (E'')**: ability of the material to lose or dampen the energy intake. It establishes the counter imaginary part of the Complex Modulus.

Being **delta (δ)** the phase angle or lag between input (sinusoidal stress) and output (sinusoidal strain), its tangent value corresponds to the ratio of the Loss to the Storage Modulus, also called the **damping**. As the material becomes more elastic, relative to its counterpart the viscous behavior, the phase angle becomes smaller and the Storage Modulus approaches the Complex Modulus.

Ultimately, even thought-to-be rigid materials also exhibit some kind of flow behavior, which is, like previously mentioned, the so-called viscosity and described as the tendency to flow. It is scaled so that it increases with resistance to flow and is calculated in DMA as a **complex viscosity (η^*)**. This particular property is not of much interest of analysis within this work, but is however important to mention.

All mentioned dynamical mechanical quantities of materials are sorted in the following sketch for a more visual understanding of the complex relationships between them:

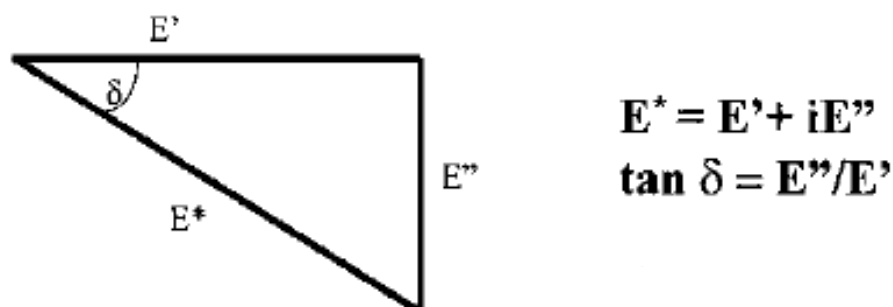


Figure 36. Triangular relationship of the complex Moduli

The concepts of Storage and Loss Moduli can be properly described by the example of a bouncing tennis ball. The elastic-part of the response is the energy storage by the bounce, which is seen as how high the ball can get after it has bounced on the floor. On the other hand, the Loss Modulus (Loss Energy) would be the difference between the initial and the final height from which

the ball was released and to which the ball bounced back, respectively. This difference of height is the energy dissipated by the ball during the whole bouncing process, as illustrated in the following image:

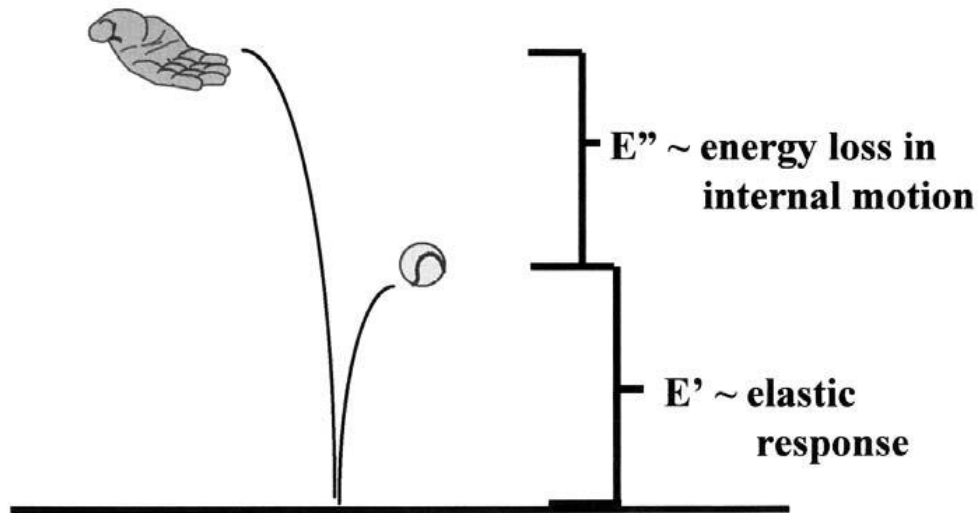


Figure 37. Energy diagram of the bounce of a tennis ball

2.4.3 Theory and governing equations

As Menard clearly explained [MENA08], the properties of materials find themselves between two opposing behaviors and their limits.

First of all, the limits of the Elastic or **Hookean behavior** that dictate the elastic response of the material. The elastic model, attributed to Robert Hooke, is described as a spring and relates the stress to the strain by its constant, k . Hooke's law states that the spring's deformation (strain) is directly and linearly related to the stress applied (from a force) by the spring's specific constant. The higher the constant, the larger stress is demanded for the same deformation or strain, the stiffer the material is and the steeper the slope gets in the stress-strain curve.

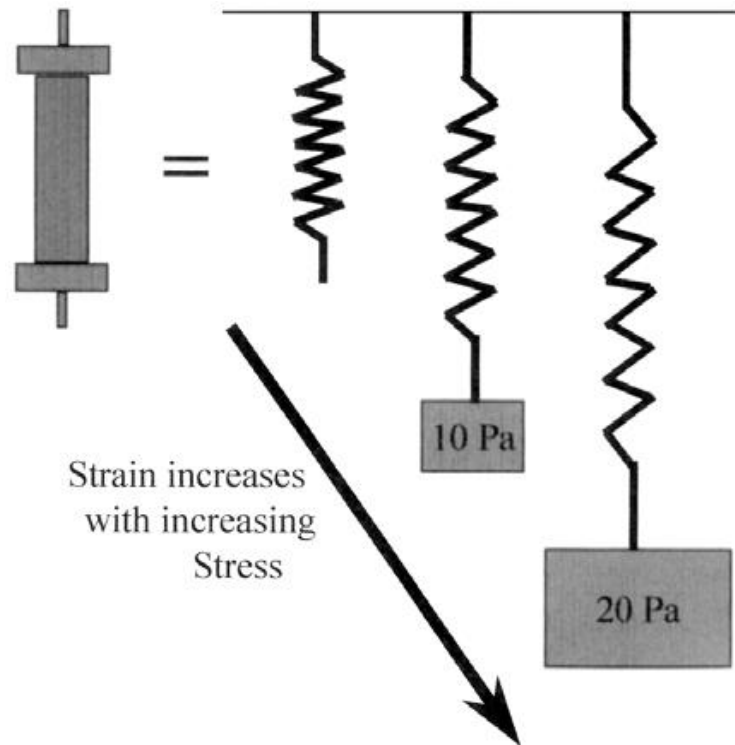


Figure 38. Mass-spring system

As seen in [Figure 7](#), the initial slope of the stress-strain curve is also Young's Modulus, E . Therefore, the steeper the slope, the higher the Modulus; being the Modulus defined as the ratio of stress (σ) to strain (ϵ) within the elastic range and a measure of the material's stiffness.

$$E = \frac{d\sigma}{d\epsilon} \quad (24)$$

There are some other parameters of interest in rheology that can be retrieved from the stress-strain curves. They will be however left out from the descriptions within the section, as they belong to a field of study outside the purposes of depicting DMA. Further knowledge can be found in the Bibliography [MENA08].

An example of materials with noticeable elastic behaviors are steels, aluminum and metallic materials in general.

Secondly, the other end of material behavior belongs to the limits of the flowing or viscous behavior, as described by the **Newtonian Model**. This model is presented as so it mimics the behavior of a dashpot, in which a header pierced with holes allows for a liquid to forcedly go through them. The energy that the header carries is then dissipated by the shear forces as the liquid goes through the holes. As the rate of the shear is increased, the rate of flow of the material is also increased.

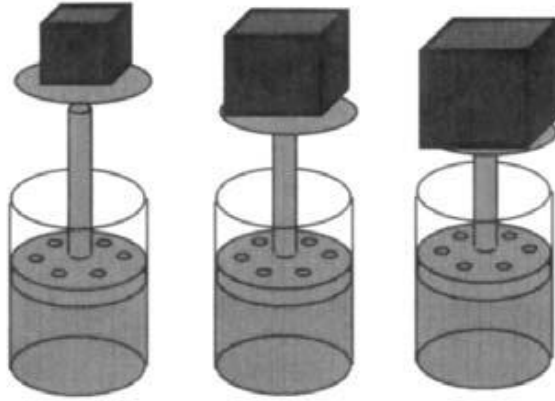


Figure 39. Dashpot

Without going into further, more complex detail, the equation governing the Newtonian Model is the linear relationship between stress and strain-rate, where stress is related to shear rate by the viscosity as shown in equation (2):

$$\eta = \frac{\sigma}{\frac{d\gamma}{dt}} = \frac{\sigma}{\dot{\gamma}} \quad (25)$$

The viscosity being is in this case the slope of the stress-strain rate curve. Examples of Newtonian materials (most commonly called, Newtonian fluids) are mainly oils.

It so happens that all materials exhibit a combination of the spring-like behavior described by the Hookean Model and the dashpot-like behavior described by the Newtonian Model: they are viscoelastic.

With that said, if a sinusoidally oscillating stress (dynamic force) is applied to a material sample, it will deform also sinusoidally, as long as it works within its viscoelastic region.

The stress and strain applied at any point on the curves while only considering the elastic limits of behavior are determined by the following equations:

$$\sigma(t) = \sigma_0 \sin(\omega t) \quad (26)$$

$$\varepsilon(t) = \varepsilon_0 \sin(\omega t) = E\sigma_0 \sin(\omega t) \quad (27)$$

As it can be seen, there is still no phase lag considered at this point, as the material behaves perfectly elastic.

However, by approaching the viscous limits of the material, the equations explain the behavior of the material as follows:

$$\varepsilon(t) = \eta \frac{d\sigma_0}{dt} = \eta\omega\sigma_0 \cos(\omega t) \quad (28)$$

or:

$$\varepsilon(t) = \eta\omega\sigma_0 \sin\left(\omega t + \frac{\pi}{2}\right) \quad (29)$$

And by substituting the relationship between viscosity, stress and strain rate, the equation ends up as follows:

$$\varepsilon(t) = \omega\varepsilon_0 \cos(\omega t) = \omega\varepsilon_0 \sin\left(\omega t + \frac{\pi}{2}\right) \quad (30)$$

A material that lies between these two limits stated by equations (29) and (32) will therefore present a phase delay at the strain curve in relation to the stress between the perfectly elastic behavior (zero delay) and the perfectly viscous behavior ($\pi/2$ delay). As it can be predicted, this delay is described as δ , and the viscoelastic response of the material at any point in the curve under an applied oscillating stress is defined as:

$$\varepsilon(t) = \varepsilon_0 \sin(\omega t + \delta) \quad (31)$$

Going through some trigonometry, this winds up as the following equation:

$$\varepsilon(t) = \varepsilon_0 [\sin(\omega t) \cos \delta + \cos(\omega t) \sin \delta] \quad (32)$$

The equation can be then broken down into the in-phase and out-of-phase strain terms as follows:

$$\varepsilon' = \varepsilon_0 \sin(\delta) \quad (33)$$

$$\varepsilon'' = \varepsilon_0 \cos(\delta) \quad (34)$$

Which allow to rewrite equation (32), by simplifying it into:

$$\varepsilon(t) = \varepsilon' \cos(\omega t) + \varepsilon'' \sin(\omega t) \quad (35)$$

The vector sum of the two obtained components ends up giving the complex or overall strain of the material sample:

$$\varepsilon^* = \varepsilon' + i\varepsilon'' \quad (36)$$

This complex number relationship is the key to understanding the triangle layout shown before for the Storage, Loss and Complex Moduli. How this relationship is depicted from the strains equation (36) is the last step to explaining the theory behind DMA that is necessary for the scope of this work.

The approach on using this complex numbers formulation allows to break down a single modulus into two terms: the one related to the ability of the material to storage the energy intake (or how elastic it is) and the one related to the ability to losing, damping or dissipating that energy (or how viscous the material is). The example of the tennis ball is the perfect support to understanding this idea and might need a second look at this point.

At the end, as the here studied idea is the effect of an oscillating force, this approach is the better strategy to getting this information by the use of DMA.

Beginning with the Storage Modulus (E'), there is an equivalent relationship linked to the Young's Modulus, as they both relate to the elastic behavior of the material. However, they are not and should never be considered the same concept. Young's Modulus is retrieved over a range of strains and stresses as the slope of the curve and its test relies on a constant stretch of the material, whereas the E' comes from a single point at the curves (the peak) and its origin is a dynamic test with an oscillating force applied on the material. They have some similarities in regard with the property of the material studied and what they represent, but they are definitely not the same.

Going back to the tennis ball, the Storage Modulus, E' , or as it is sometimes called, the elastic modulus, the in-phase modulus or the real modulus, can be seen as a magnitude of the amount of energy the ball gives back after the bounce. It is calculated as follows:

$$E' = \frac{\sigma_0}{\varepsilon_0} \cos(\delta) \quad (37)$$

On the other hand, the Loss Modulus, E'' , also called the viscous modulus, the out-of-phase modulus or the imaginary modulus, is described as the amount the ball does not recover as this energy is lost to friction and internal motions inside the ball. Its magnitude is computed as:

$$E'' = \frac{\sigma_0}{\varepsilon_0} \sin(\delta) \quad (38)$$

Ultimately, the previously mentioned tan delta, $\tan(\delta)$, is essentially the tangent of the phase angle between the stress and strain curves. It is one of the most important magnitudes, as it indicates how efficiently the material dissipates energy to internal friction and rearrangement of molecules. It is often called damping and its magnitude is measured as the ratio of the Loss Modulus to the Storage Modulus, as it can be depicted from the triangle sketch:

$$\tan(\delta) = \frac{E''}{E'} = \frac{\varepsilon''}{\varepsilon'} \quad (39)$$

It is independent of any geometry effects, which makes it a very interesting property.

In order to recap all information so far explained, an anew focus on the initial idea of an oscillating force and dynamic response is extremely helpful at this point.

With that said, the sketch below provides an overview of the relationships described in equations (28) and (33), that needs to be profoundly comprehended prior to performing any kind of DMA, and that is, the relationship between and oscillating force applied to a material and its resulting oscillating strain. All material properties studied within DMA are calculated from the defining components of the sinusoidal stress and strain curves. Therefore, a final revisit to these curves is the best way to finishing the discussion:

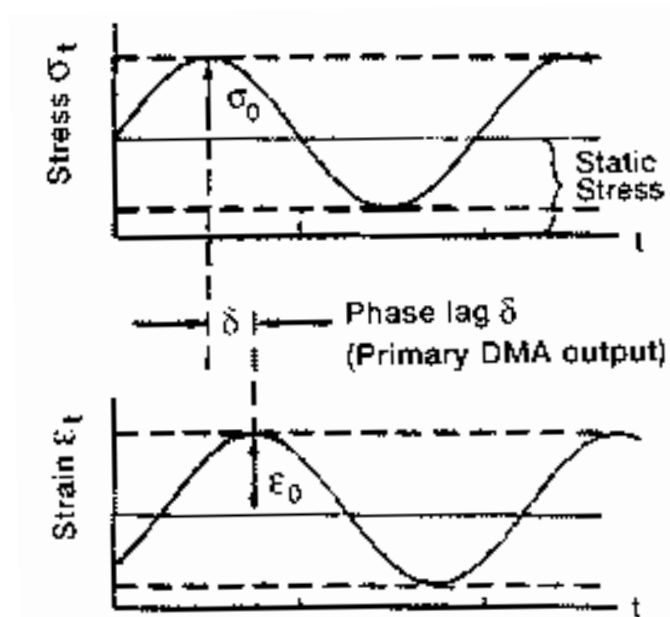


Figure 40. Stress and strain curves as a function of temperature

In case needed, a more profound discussion on the concepts of DMA and a deeper dive into the mathematical foundations behind it can be found in Ferry's work [FERR80].

2.4.4 Instrumentation

The instrumentation for the performance of DMA experiments has been already developed for over 50 years. The commercial machinery currently available in the market has therefore experienced a significant technological growth since the first tools were developed in the 1960s for dynamic measurement of materials properties.

The sketch below shows the inside structure of a modern Dynamic Mechanical Analyzer (also called DMA, as the technique itself) and labels the components of relevance.

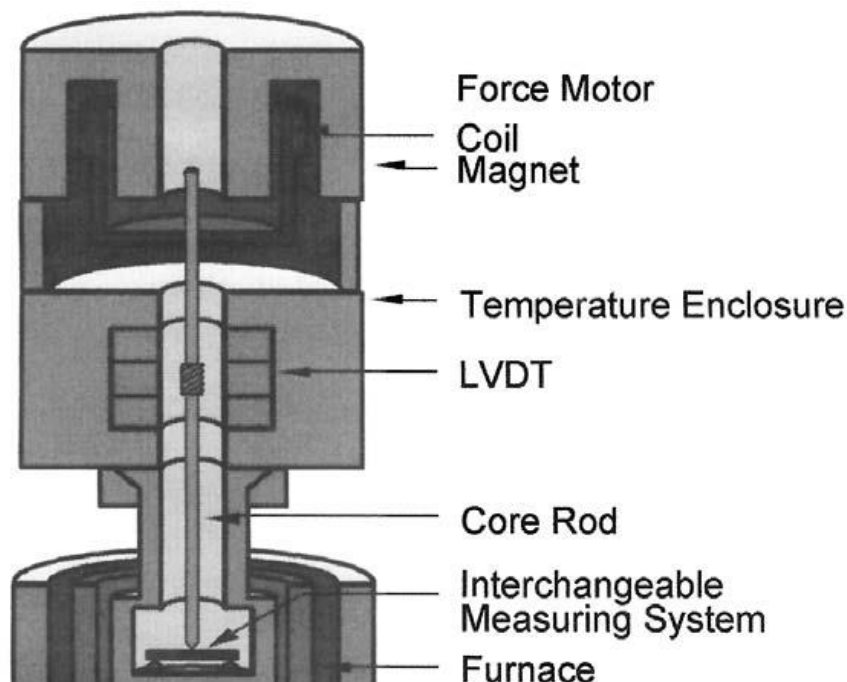


Figure 41. Sectional view of a DMA and its parts

n

The instrument is made up of 4 distinguishable parts that control the deformation, temperature, sample geometry and sample environment. The Motor is at the top, followed by all components that conform the Detector, where the Linear Variation Detector Transformer (LVDT) is found. At the bottom, all elements conforming the Environmental System are responsible for the capability to simulate very different temperature scenarios. The Measuring System is also found within this part and allows for different measurement arts, such as tension, compression and 3- or 4-point bending; being the first two the most common ones.

The recent models with a bigger presence within the market are almost entirely supplied by companies of two very different origins. On the American side, the companies METTLER TOLEDO, TA Instruments, Inc. and Perkin-Elmer, Inc. are responsible for the American domination of the sector; while in Europe, the England-based Prescott Instruments Ltd. and the German company NETZSCH GABO Instruments GmbH are well established within the smaller continent.

2.4.5 Working principles

As previously and shortly explained, DMA works by applying an oscillating force on a sample of a certain material and calculating the stress and the strain that the sample experiences, being both, consequently, a function of time.

Recalling the theoretical breakdown of the sinusoidal stress and strain functions, the magnitudes interpreted by the measuring system are the amplitude at the peaks of both functions, that is, σ_0 and ϵ_0 , as well as the phase lag, δ , which is retrieved as the time between peaks and then transferred to the angle domain.

The magnitudes that the DMA actually measures are the time function of the applied force through a force transducer located between the motor and the sample, and the elongation that the material experiences, also a function of time, with the help of the LVDT. The known geometry of the sample allows for the translation from the measured magnitudes to the three main magnitudes above indicated. And from these three main magnitudes, the rest of the previously referenced mechanical dimensions are depicted.

An overview of the whole process a DMA follows is sketched below to provide a more structured overview of the steps described within this section:

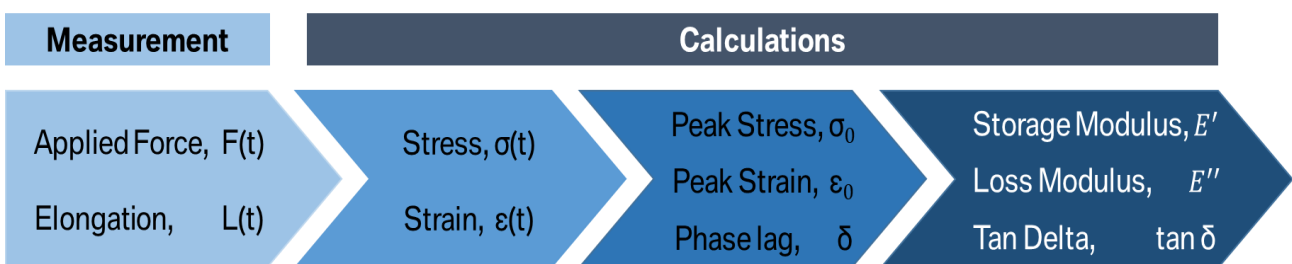


Figure 42. Physical magnitudes present within a DMA and their process

2.4.6 Material Experimentation: Why DMA

The addition of this technique as one of the main blocks conforming the structure of this work came as an urge to clarify what happens at the cell module level by performing experiments on specific components of the mentioned modules.

These kind of tests were initially referred to as experiments, or essentially tests, at material level. They have the goal of finding a clarifying change of certain chosen mechanical properties of these module components, which could, potentially, be related to the altering behavior at the module level that is initially seen by the use of Modal Analysis.

However, the choice of this technique was not set from the very beginning of the project. Contrary to Modal Analysis, DMA came as an idea to complement the results and to try to illustrate the findings of the MA-tests at a more understandable level. The use of this technique was not predetermined and the decision of its usage came after profound deliberation and comparisons of different techniques that may be able to perform revealing material-level tests.

The decision-making process of which technique to choose for this matter was approached as the search for convenience and exactitude simultaneously. In other words, the material-level test technique was demanded to be feasible within the time and equipment available, but also precise and addressed in the direction of the work expectations. It also needed to be widely established within the engineering field, as new emerging techniques may have been more prone to doubts, open-questions and general uncertainty about the results at the end found. A new technique would not help to building a standardized, structured method either, in order to being able to establish a procedure robust enough to be used with future projects and designs.

Among the techniques considered after some research was done, old and well-known approaches, such as Tensile Test or even some sort of Finite Element Analysis (FEA), emerged. These techniques are sufficiently established and very well known within the engineering industry, so they initially seemed as a very doable approach to choose from. New in-development techniques, such as the Small Punch Test were also found to be interesting at a first consideration.

The reason why a simple tensile test and its other versions (compression, 3-point bending, etc.) were ultimately discarded is because of the need of simulating various temperature scenarios and comparing them to each other under the same circumstances. Being those static techniques, tensile or compression tests would wind up demanding a lot of test time as every temperature scenario would require its single test to be performed. Even though a large amount of different temperature scenarios was not really needed for the purposes of this work, the potential need of further scenarios to be tested in the future and the likely rise of test requests and materials to be analyzed made these simple techniques very inadequate for the building of a robust method.

Additionally, the purpose of these old-school kind of tests is to study the behavior of a material at its whole operating range but at stable operating conditions. This is essentially contrary to the way the desired analysis was required to be performed and to which properties were needed to be retrieved from the material-level experiments. Moreover, the obstacles of performing static analyses is the high likelihood of not simulating the exact same conditions at each test, besides the temperature change between them. This problem would be entirely overcome by looking for a more dynamic technique.

Whether the simple test machinery available for the tests was or not capable of simulating different temperature scenarios, or there was or not a solution to it by including the machinery inside a climatic chamber, which sounds a bit optimistic due to its static structure and weight, was also an open question that ended up declining the possible usage of tensile testing as the material level approach selected for the scope of this work.

On the other hand, the decision to not to undertake Finite Element Analysis came from different reasons. The scope of this work was determined to experiment with “Hardware” matters. A parallel “Software” analysis would fit perfectly as a complement to the findings within this work,

but a fusion of the two approaches into one project work was not considered to be a feasible idea, mainly because of time effort and the different abilities and student profiles that are needed for it. It did not make much sense either to merge both opposite directions, as the scope of this work was substantially thought for experimental, hardware matters. In other words, this work was intended to collect as much as experimental experience as possible in regard to module and material testing within the electric storage industry and the mechanical engineering field, and therefore thought to be entirely built up of experimental, laboratory methods. As included in the last section of this document at the summary of the conclusions, a fine element model analysis would be a very attractive complement to the experimental method developed within work, and a further study of the correlations between the two approaches would be of much interest.

With regard to new techniques yet in development, and as briefly explained above, the problems with them are fundamentally the uncertainty of achieving a precise technique that allows for the collection of valid data, due to the lack of experience and expertise in the field, along with the amount of time and effort to properly learning the technique, which takes most time whenever there might be difficulties and gaps of information and documentation about it. By choosing a technique that is still in development, the problem of convincing about the validity of the results may also emerge and can put the grounds of the whole work into danger. A robust, strong material analysis method along with a refined and gentle testing technique that comes with it are essential for the collection of precise and illustrative data, which at the end of the day are the basis for the whole project boundaries, perspectives and horizons.

Specifically about the Small Punch Test, although it may have many similarities with other established engineering techniques for material testing, it is necessary to also account for that the purpose of this technique is to study material failure, and not material behavior under a controlled regime or operational range. The Small Punch Test is employed in the analysis of the yield strength, the determination of the ultimate tensile strength and also in the modelling of fracture, as found in the literature [JANC16] This differs widely from the approach to be undertaken here and is the reason of the reject of this technique for the purposes of this work.

As a result of the investigation undertaken and the decision-making approached for the material testing technique selection, it was concluded that the Dynamic Mechanical Analysis does not simply cover all demands requested for this block of work, but also does it in a very efficient way.

3. WORK METHODOLOGY

3.1 CELL MODULES

3.1.1 Components of interest for the analysis of the influence of temperature

Although most elements within a module are in constant development in the industry and therefore subjected to being replaced sooner or later by the upcoming designs, a general look at how the modules are designed and which functions their components have stands for a favorable approach to find out the main elements of focus.

A similar architecture of the above depicted module ([Figure 11](#)) is provided below in explosion-mode for a closer look into all its components:

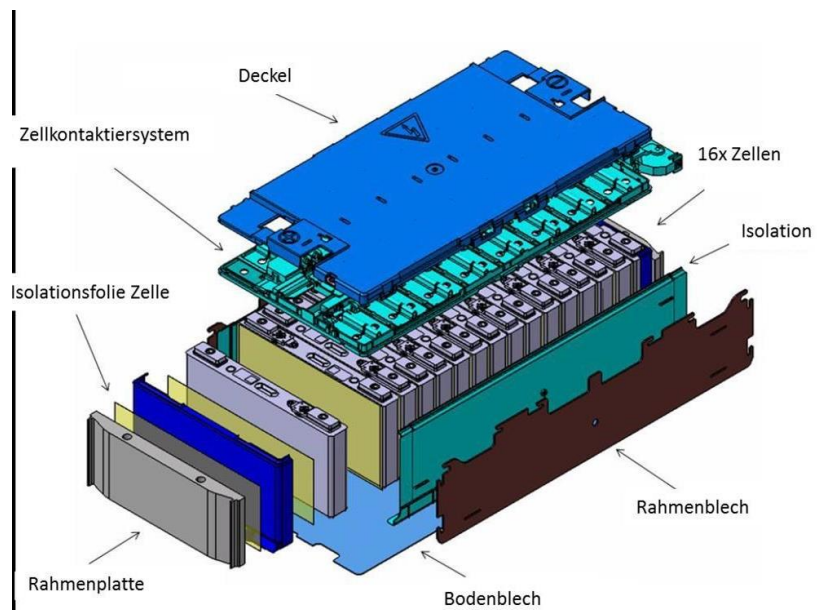


Figure 43. Explosion view of a cell module architecture

Modules can be seen as a rigid frame structure made mostly of some kind of aluminum alloy with symmetry along its longitudinal axis, perpendicular to the cells layout. The pointed German words “Rahmenblech” and “Rahmenplatte” refer to the metallic plates and sheets at the four sides of the module, plus another aluminum plate at the bottom to isolate and enclose the system from this side.

Most of the material present in a module is metal, and this allegation is further justified when considering a “dummy-module” with cells made of aluminum, without any kind of active material inside them. The crystalline structure of aluminum is the basis for its very high melting point (>600°C) and its stable performance at a remarkably wide temperature range [ENGI19]. Many of its mechanical properties, including the stiffness, are only truly altered when reaching temperatures on a much higher order than those found in the living environment. It is therefore not expected that such elements within the cell module are responsible for the changing vibrating behavior when subjecting it to varying temperature conditions during service.

On a second group of elements, the cell-contacting system is located on the upper face, at the top of the cells, and is protected by a cover made up of some kind of plastic material. The very low weight and also the purpose of these two components do not have much to do with the structural functionality of the other elements, because they are not intended to help holding the system together. They have been designed as add-on parts to the architecture of the module, and

as they do not play an important role on the vibration transmission throughout the module, will therefore not be a subject of interest for the analysis done within this work.

However, there is a third cluster of materials, which can be referred to as the polymeric materials within a module. This group is composed of all adhesives that attach the inside and outside parts of two elements together, as well as the isolation films between them. These isolation foils are very light and thin and do not have any structural purpose, but to impede from moisture, dust and other particles to come into delicate areas within the module. However, the adhesives that hold the frame together with the cells play a decisive role on the vibration transmission during operation. In addition, a structural foam found inside the module acts as a tolerance compensator, also playing an important role in the structural behavior of the module.

After this thorough description, the three elements of interest found within a module and their given names for their analysis present in this work are the following:

- TCE: Tolerance Compensator Element
- SA: Structural Adhesive
- HCA: Heat-Conducting Adhesive

These three elements will be further addressed by this terminology and constitute the target of the material experimentation, designed to complement the analysis undertaken at the cell module-level.

3.2 MODAL ANALYSIS

3.2.1 Equipment

a) Input tool: Impact Hammer (tip)

The impulse hammer used within this work is the Model 086C03 by PCB Piezotronics Inc. It consists of an integral, ICP® quartz force sensor mounted on the striking end of the hammer head. The sensing element functions to transfer impact force into electrical signal for display and analysis and is classified as ICP® (Integrated Circuit Piezoelectric), low impedance, voltage sensor. It is structured with rigid quartz crystals and a built-in, microelectronic, unity gain amplifier. The cable is connected to the end of the end of the handle for convenience, and to avoid damage in the event of a “miss-hit”.

The ICP® sensor operates over a standard two-wire cable from a PCB® power unit. The ICP® signal conditioner supplies constant current excitation to the sensor over the signal lead and AC couples the output signal.

The hammer is a single, integral unit. Laser-welded construction of the sensor element ensures reliable operation, even in adverse environments. The mechanical assembly is locked together with a structural epoxy adhesive so it would not be taken apart.

The striking end of the hammer has a threaded hole for the installation of a variety of impact tips. The tip functions to transfer the force of impact to the sensor, simultaneously protecting the sensor face from damage. Tips of different stiffness allow to vary the pulse width and frequency content of the force. An extended mass allows for further tuning by concentrating more energy at lower frequencies.

Figure 44 shows the Power Spectral Density (PSD) of the tip assortment that the hammer model provides. Based on the frequency range of interest, the tip choice was the plastic one, referred to as “Medium” in the image.

b) Output tool: Accelerometer

A triaxial accelerometer Model 356A02 by Piezotronics PCB was used to collect the response of the module to the excitation impulse.

The data sheet shows a sensitivity of 10mV/g (+-10%). However, the actual value for each of the axes was measured by a calibrator by Brüel & Kjaer.

c) MKII – Signal acquisition system

The signal acquisition device (FRF front-end analyzer) used to process the data collected by the sensor was the MKII by Müller-BBM.

It is composed of two slots, four subslots each. Allows for ICP and Tachometer connecting devices. The MKII stayed outside the climatic chamber during the measurements for safety reasons.

d) Measurement Software PAK

The software (back-end FFT analyzer) as the complement to the signal acquisition instrument is the PAK 5.9 developed by Müller-BBM.

To become an advanced user of the software, a few trainings sessions with the help of an expert are needed.

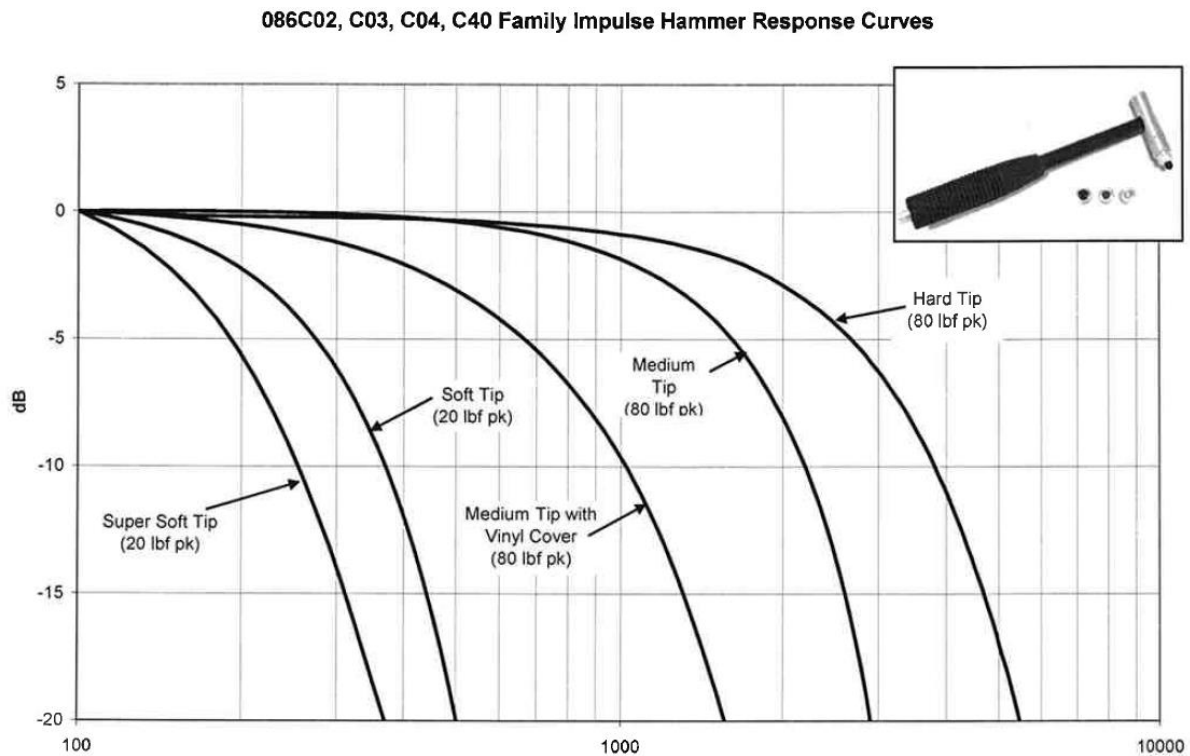


Figure 44. Piezotronics 086C03 Impulse Hammer: tips assortment response curves

3.2.3.4 Design of the test frame and bearing mechanism

A) Test frame design

The design of the test frame is not as crucial as the bearing technique employed to hold the test specimen into a stable, secure position, but needs to ensure that it is capable of holding the whole weight of the specimen, and that also can be correctly placed on a flat surface into a very stable position.

It is also in some cases very convenient that the test frame can be easily transported. That means that the test frame should not be too heavy, so it can be handled smoothly and conveniently for the purposes needed. It is however true, that the test frame must be capable of bearing with the weight of the test object and that must be the prior design factor. This may be in some cases restrictive to having a light test frame, but having this idea in mind can help tremendously with the handling and transporting of the test frame – test specimen set.

As clarified above, the design of the test frame will depend upon the dimensions and weight of the test object. Therefore, and whenever it is possible to design and build an own test frame for the desired test to be performed, it should be done in a way that it complies with all specifications of both the test specimen and the climatic chamber, but also that it remains as light as possible. Both simplicity and functionality are key here.

For the case of the test frame used during the experiments within this work, an already-built test frame available at the Laboratories in Munich was employed. It is mainly made of aluminum rods, with a simple, light-weight design, very convenient for the purposes of the kinds of

experiments wanted to be undertaken. Its dimensions made it also possible to fit it inside the climatic chamber, needless to say how important that is.

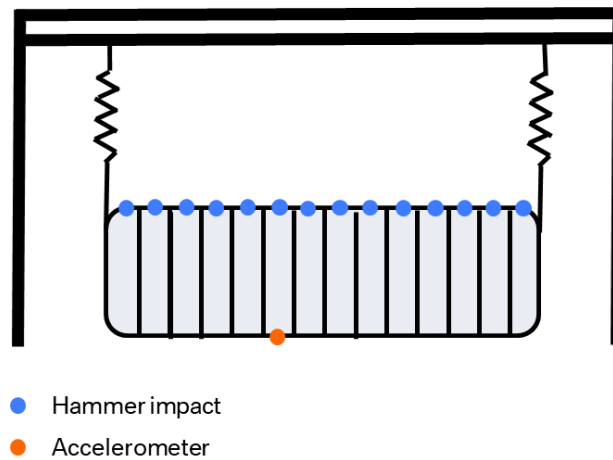


Figure 45. Taste frame and module setup

B) Bearing mechanism

As important as the correct bearing of the test specimen is, the restrictions that may appear when choosing the best bearing method must be acknowledged the first restriction being the test frame itself.

When having a correct design, the test frame should allow for the placement of strings, extensible rubber bands or any other bearing object with a certain degree of elasticity. These can be achieved by the installation of metal grommets or eyelets at the top part of the test frame.

The second restriction to the bearing equipment used is no other than the test specimen itself. Once we are capable of hanging it by some kind of spring or bands, where exactly to connect the mountings to the test object can be an unexpected challenge. There is the option of also placing some grommets to the locations of the test specimen where it is expected to have a better support. However, this can sometimes not be an option due to very small dimensions of the object. Theoretically, no extra accessories that can alter the real vibrating behavior should be added to the test object. This has even more impact the smaller the test object is.

For this reason, time was invested to come across the best location where the test object could be connected to the bearing mountings without adding any extra accessories, as well as what would be the best mounting to do so. It can be common that a test object such as a cell module may have some holes and certain spaces as part of its design. These are usually found in order to decrease the amount of material used to build these modules, as well as to lower their weight for better performance. The exact locations where the bearings were placed on the module without any use of extra grommets or other accessories is illustrated in the image below

For the particular case of the module tested in all four temperature experiments undertaken within this work, the test object was not entirely symmetric. Indeed, the initial idea of bearing the cell module by its upper surface, which seemed very convenient at the first place, was not really possible due to the lack of the small holes on one side of it, as a result of its not-symmetric design.

An initial approach was considered in order to overcome the problem of non-symmetry. The cell module was rotated 90° over its longitudinal axis, so the small holes on the right side, symmetric to each other through the lateral axis, were chosen to be the locations to meet the bearings and how the module was then be suspended.

However, the complexity of this idea relies when executing the measurements. As the longitudinal axis is the one at which the vibrating response of the cell module is desired to be studied, it would be more convenient to have the surface where the measurement grid is set up straight and parallel to the floor. Otherwise, the hitting technique when performing the impulse hammer measurements was compromised by gravity, and the situation made it altogether very uncomfortable to perform a proper measurement. Additionally, the extra bands needed to straighten up the module parallel to the floor played a damping role, which was a little over of what was needed, which ended up not providing a proper bearing mounting that complies with the prerequisites when performing modal analysis.

The final idea and the bearing technique used for the tests in this work got rid of the expandable bands and also got back to the initial premise of having the module relocated, such as its longitudinal and lateral axes are both parallel to the floor. With this layout, the direction of the hammer hits are the same as that of gravity, which makes it much simpler and more convenient for both the operator and to get more precise results. The standalone factor to account for was the stiffness of the springs used. Since the new layout provided a symmetrical arrangement of the four springs along both axes in the measurement grid plane, the use of four equal springs would make the test specimen be arranged completely straight and parallel to the floor, with the measurement grid facing up to the operator approaching it with the hammer during the measurements.

Following the theoretical guidelines described in the State of the Art, there was an initial attempt to calculate the exact stiffness of the springs to be used by fixing a desired natural frequency of the bearing system. This guidelines consider the whole system as a first-order spring-mass system, in which the mass of the test specimen (m), the stiffness of the springs (k) and the natural frequency of vibration are all correlated by the following equation:

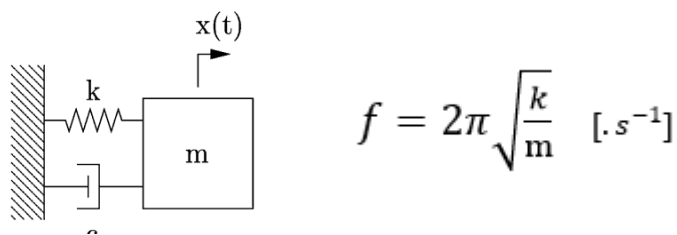


Figure 46. Spring-mass relationship for frequency estimation of the springs

With this relationship in mind, the process of calculating the needed stiffness for a desired vibrating state (natural frequency) was set to be the following:

1. By knowing the mass of the test specimen, the stiffness of the springs can be retrieved by substituting the values of the mass and the desired natural frequency of this spring-mass system. Regarding the stiffness, it needs to be clear how the arrangement of the different springs affect what is considered as the k of the system. With a parallel layout of springs, the stiffness of each spring is to be summed up, as they work together holding the mass. That is, when all springs are set to be equal, the real stiffness of each spring is the result of the value for k calculated from the equation divided by the number of springs.
2. Once the stiffness of a single spring is known, the search of a spring type with a stiffness of this magnitude needs to be found. What's usual is that the value retrieved from the calculations is not an exact value of a stiffness that can be found in the market. That means that the closest value available needs to be taken. In case of doubt, it is better to go for a slightly greater value instead of for a one lower than the theoretical one, as a resulting higher frequency could be problematic.
3. As last step, the new real natural frequency of such resulting mass-spring system needs to be recalculated by returning to the equation above.

The above calculations were undertaken for the case of the particular cell module studied within this work. Below is a table that collects the values for each parameter of the studied case, along with a figure of the actual layout employed for the calculations.

However, these prior calculations were found to be very inconvenient for two simple reasons. The first one coming from experience and from the lessons learned from experts in the matter in regard to the “feeling” that is needed when deciding the bearing concept in modal analysis. What really is important is to set up a bearing layout that allows the test specimen to vibrate freely under a controlled rhythm or frequency. This requires very little time to be understood and just one or two real exercises to understand what appropriate and inappropriate mean. Generally speaking, a vibrating state of 1 or 2 Hz is very easy to understand and determinate with own eyes by simply exciting the system with one hand and leaving it to vibrate freely for a short period of time. Due to the inverse relationship of time period and frequency, a vibrating system at a frequency of 1 Hz can be seen by accounting for one second per cycle. As in most cases the natural frequencies to be retrieved from the test specimens are way above this order, a simple hand-impulse evaluation is sufficient to see if the natural frequencies of the bearing system are within the desired order, complying with the theoretical concepts previously introduced in the State of the Art section. With that said, too stiff springs will set a vibration behavior where the test specimen is moving very quickly and with little amplitude. The operator will also find it very difficult to excite the system with a simple hand impulse. On the other hand, too little stiffness will result on a very loose vibrating behavior, where a single hand impulse may end up inducing an uncontrolled, overexcited system, which could also disrupt the bearing system and make the whole setup fail.

For this matter, many different springs available at the Vibroacoustic Laboratories were evaluated. Some of them being too stiff and some others being not capable enough to hold the module into place without an enormous extension. After a few evaluations, a certain size of spring was found to be very appropriate for the particular module and layout studied within this work. A total of four equal springs were set up symmetrically along the longitudinal and lateral axes in the four corners of the module. Eight carabiners were used at each end of the four springs for better support of the module and to being able to reach the little holes at the lower corners of the module with the selected springs. The dimensions of the carabiners have no direct impact on the bearing system properties unless they are extremely big and can influence the vibrating behavior of the test object. It is only necessary that they fit the holes or specific locations where they are connected to the object. The ones chosen for the tests within this work were all equal size and very light. However, it is interesting to specify the dimensions of the springs used.

With the experience collected, it is the desire of the author to make it very clear how important it is to develop a good feeling of what to expect for a spring layout to be good or not for the particular purposes and object to be tested. As explained above, the theoretical guidelines on how to choose the perfect spring for the desired layout end up being not appropriate at all for most cases. Therefore, the author strived to get a good feeling from all tested springs and layouts on what would be the influence on the vibrating response of the test object coming from the test frame. This would be the only recommendation for the topic of bearing method selection provided from the experience collected by the author within this work, along with the remark on not considering of much importance the theoretical guidelines that can be found about this matter.

After the bearing system has been selected and set up, a quick test to check whether the system response is found to be convenient and whether the bearing supports function correctly is mandatory. This needs to be checked prior to beginning with the real tests and is recommended to be done with certain frequency in order to make sure that the system setup is fine and ready to be tested.

3.2.3 Measurement Technique and Strategies

After gathering sufficient experience with hammer measurements in the Vibroacoustics Laboratory, as well as having correctly understood the direct influences of the impulse hammer

specifications and having chosen and tested the final parameters of mass and tip, the final step is to carry out the tests in a climatic chamber that allows us to adjust the desired temperature of the corresponding test.

In addition to good planning, tests in the climate chamber also require deep concentration during measurements. It is especially important to feel comfortable and to perform a measurement with confidence and precision, which can be repeated many times. The higher the precision during the test and thus the reciprocity capability, the lower the probability of making a human error and not having to repeat the invalidity test, once the measurement results have been checked and the input-output correlation has been evaluated. At this point it seems important to emphasize again that the major source of inaccuracies and inaccuracies in measurements is human error in carrying out the modal test technique. Unlike the WFD, the modal analysis through impulse hammer consists not only of the variability of the parameters, but mainly of the randomness of the human measurements as a potential factor of alteration of the results. For this reason, it is imperative to make a reflection prior to the test on how to carry out the measurement, what are the critical steps to take into account and what to look specifically to perceive if the impulses are good enough. All this requires extensive experience with numerous measurements prior to the climatic chamber test, as well as the awareness of having a good "feeling" when carrying out the impulse hammer technique. The keys are the ability to reciprocate and awareness during performance.

In order to know the true temperature at which the module is found during the test, it was decided to install a series of thermocouples that record the temperature at different points on the module. A total of 8 thermocouples were placed, trying to cover all the different zones that compose the surface of the module, as well as looking for symmetry between the longitudinal and transversal sides. Due to the design of the module, it was not possible to place any sensor inside the internal structure, as these zones are not reachable from the surface. This aspect will be taken into account during the tempering times of the chamber, giving extra time to accommodate the conductivity of the temperature to the most internal areas of the module, especially those more extreme.

Below is a table with the specifications of the type K thermocouples used for recording the temperature during the course of the measurements. This type of thermocouple is used continuously by the workers of the climatic chambers for the recording of temperatures. In spite of not having several options to choose from, the experience of the workers with these thermocouples and their universal distribution in the market (they can be found very easily) make them in any case a more than sufficient option for the task entrusted.

Below is an image of the thermocouple arrangement chosen for recording the temperature in the module. It is important to point out that this distribution remained unchanged during all the tests carried out in the climatic chamber in all the study temperature scenarios. This is of great importance to isolate a possible temperature logging difference between tests that may affect the reliability of these tests.

The physical temperature signal interpreted by the thermocouples is transformed into an electrical signal, which is finally interpreted by a sampling software. The software used to record the temperatures read by the 8 thermocouples, as well as their subsequent evaluation was the TurboLab 7.0 program.

Due to their continuous occupation for different test modalities and experiments, the availability of climatic chambers was the limiting factor for carrying out the tests. The climatic chamber tests were therefore concentrated in one week on the test benches of the BMW Group in Munich. This restriction made it necessary to plan each test carefully, paying particular attention to the chamber tempering times between one test and the other.

As mentioned above, ensuring perfect conditions and a robust test performance strategy that minimizes human error and the influence of other external factors is of crucial importance for good data collection. This is all the more important in view of the close availability of climatic chamber usage times and the long periods of tempering between tests.

The following section describes the strategy adopted to carry out each test, as well as the method of ensuring correct data collection.

3.2.3.1 Climatic chamber testing strategy

Before designing a correct execution strategy, it is crucial to gather experience and know well the particularities of the climatic chamber to be used. Several tests, at a slower pace and in order to test different strategy ideas, were carried out in the climatic chamber in the days prior to the final tests. It is crucial to feel capable enough to carry out a test lasting more than two hours with the confidence of being able to carry it out with sufficient and constant precision throughout the entire test. Worse data collection at certain points of the test that are more prone to this, especially in the final parts of the test, and that compromises the overall results of an entire test of this duration, should be avoided at all costs. Again, the basis for solving this problem is none other than sound technique, comfortable measurement conditions and the most accurate signal collection possible. It is very important to design the test times according to the specifications of the climatic chamber, respecting the necessary tempering times and the different forms of heat loss.

Different strategies were initially designed for correct data, but only one was finally applied to all trials equally. Each of them is described below, explaining advantages and disadvantages and the specific characteristic that explains their possible application or, on the contrary, their irremediable discard.

3.2.3.1.1 Designed measurement strategies in the climatic chamber

A) Test method with closed chamber

This strategy was initially considered for its logical application: with closed door, theoretically there is no heat exchange between inside and outside, which ensures a stability of the temperature present in the module throughout the course of the test, no matter how long it may be. The advantage is clear, since the chamber is designed in such a way that it assures a very good insulation of the external heat or cold to the chamber, maintaining its isothermal interior. In any case, the chamber would not stop working during the test, thus requiring very little capacity to maintain the temperature of the interior constant. In this aspect, the only external heat agent would be the author of the test and the short time it would take to open the chamber when it enters it. In fact, a first test at +40°C in closed door was successfully carried out in a period of less than two hours, which served as a first experience to test the reliability of this method. On the other hand, the great disadvantage, and the reason why this method was finally discarded is nothing more than the safety of the author of the essay. Due to the long test times and potentially extreme conditions, this strategy is no longer suitable mainly for safety reasons. On the other hand, and this is another big reason why this closed-door measurement method is discarded, such a test can become feasible when the internal conditions of the chamber are not too external. Even with the right equipment, a test can be carried out in very cold conditions, such as -20°C. The problem is not the entire temperature range studied in this paper, but the extrapolation to even more extreme temperatures in future tests. If this work is to serve as a guide for future analysis and testing under a different and potentially more extreme range of conditions, the test method must ensure the viability of performing the experiments under any desired test condition, always limited by the scope of the climatic chamber.

In addition to this, a closed-door test jeopardizes the amount of air available to the author during the test. It was proved during the closed-door test at 40°C that the test is viable for a period of up to two hours. In no case can the viability of this test method be assured under longer periods or even more extreme conditions for the author. Since it is not possible to ensure the complete safety and viability of the test under more complex conditions derived from those carried out in this work, this closed-door test method was completely discarded as a possibility for future replication of the same.

It is important to note that, despite the non-negative experience of a single complete closed-door test at 40°C carried out by the author himself in a period of two hours, the experience and subsequent awareness gathered in this work aims to make clear the discard of any possibility of closed-door test technique in a climatic chamber. In no case should the closed-door testing strategy be considered as a valid method.

B) Test methods with door opening

Once the option of testing in closed-door insulation had been completely ruled out, the alternative was to look for an open-door test method, at least for a period of time, in which a heat exchange between the chamber and the environment inevitably occurs and, in turn, a variation in the humidity level inside the chamber due to the entry of air with a certain concentration of water in its composition.

The idea is clear: the shorter the time in which the chamber is exposed to a thermodynamic exchange with the outside, the less the destabilization of the temperature during the short period of measurement between the successive hits and the shorter the subsequent time of re-tempering to the desired initial temperature value. In this respect, the data collected by type K thermocouples play a crucial role in the feasibility of an open door test method.

After a brief test and collection of data on the behavior of the temperature in the successive locations of the thermocouples on the module inside the climatic chamber, it is verified that short periods of measurement, of the order of one minute, are easily recoverable in a considerable order of time. A small experiment at an extreme temperature of -20°C, whose difference with the ambient temperature outside the chamber is the greatest of the four scenarios studied, shows that after one minute of door opening, the temperature rise inside the chamber during that time is easily recoverable after an order of three to four minutes of re-tempering behind closed doors. This data is the key to validating the viability of an open door test with the appropriate strategy and the definitive confirmation of its choice as a definitive and standardized test method. The real factor of interest is the need to carry out the test as quickly as possible during this period of door opening, so that small temperature differences between successive hits have a negligible impact on the results and the temperature dispersion interval is therefore considered negligible. Again, the data collected by the eight thermocouples play a crucial role in the confirmation of this hypothesis and in the validity of the tests performed under this method.

Thus, the logical initial problem of an open-door test with heat loss or natural heat gain has been shown to be solved with adequate measurement and re-tempering times. Below are the two open door techniques designed, whose implementation was studied and finally carried out in one of them.

B1) Sequential test with door opening

This method is attributed to my supervisor at the BMW Group, Dr. Maximilian Altmann, and its essence is the need to combat the dynamic temperature variation between successive points. The idea to solve this unwanted drop or rise of the temperature between successive points is the change of sequence to follow between each stroke. The method consists of following a specific sequence of points and, once the sequence is over, repeating it in the opposite direction. Considering that the temperature drop or rise occurs linearly during the test time, the sequence strives to stabilize these temperature differences during the process, so that the temperature gains or losses are similar during the test time for all points equally.

B2) Point-by-point (PbP) Test with door opening

The third and final test method is simply to perform a series of strikes at the same measuring point over a short period of time in which the climatic chamber door remains open. During this short time all the hits that are considered necessary for the same point must be carried out with the greatest precision and in the shortest possible time. This will avoid large temperature differences between successive hits and generally good test results. Once the desired stroke sequence for a

particular measurement point has been completed, the door is closed and the transfer functions, which are the main focus of study in this type of test, are evaluated.

The great advantage of this method is the fact that virtually the entire overall test time is profitable. During the time in which the door is closed and the quality of the numerous hits made is evaluated until it is decided to continue with the next measurement point, the climatic chamber will remain active, with the door closed, and will then be able to re-temper to the test temperature and combat the small loss or gain of heat present during the short measurement period.

If the times have been well studied previously, a very convenient time/measurement ratio can be achieved with a total efficiency close to 100%. For the specific case of the tests carried out within this work, it was intended to collect all the hits in an interval of one minute or slightly more, but in no case more than two minutes. Simply for convenience, a measurement rhythm of five minutes was established between point and point, which would give a remaining time of between three and four minutes. This would allow for accurate detection of the TurboLab times for temperatures read by thermocouples throughout the measurement process, and is, in general, a very adequate number to establish as a standard tempo for future tests. Before definitively establishing this measurement rhythm, its validity was checked for the most extreme temperature case, -20°C . It could be observed that with a measurement time of no more than two minutes, the remaining re-temperature time was necessary both to re-establish the desired temperature within the climatic chamber and to carry out a thorough evaluation of the selection of the best hits on which the average value is calculated.

Either case, it is strictly necessary to understand the functioning of the particular climatic chamber being used, as well as the temperature flow experienced by the test object in question through the data collected by the temperature sensors, in order to be able to determine the appropriate point-to-point test tempo for the particular conditions of the experiment to be performed using this open door point-to-point test method.

Below is a brief schematic explanation of a complete open-door point-to-point measurement sequence, as carried out in the climatic chamber of the BMW Group's laboratories in Munich for the temperature tests collected in this work. In this example, the 20 measuring points are shown and the test times between points and the temperature present in the different points of the module are collected. The example is the real case study at -20°C , in which between 20 and 35 hits per point were achieved, depending on the particular location and the feeling at the time of measurement during a period never exceeding two minutes.

In order to pack all advantages and disadvantages of the three methods altogether into a more visual structure, the matrix below was designed for a better understanding of the previously described methods.

The matrix layout helps for a better decision-making on which method to use, depending on the work conditions and the purpose of the test. The scores of each method belong to the particular case studied here and allowed to choose the measurement strategy that better fitted the scope of this work.

The way the matrix is designed is described as follows:

- The rows contain the measurement features that may be taken into consideration for a complete description of the demands required to each proposed method.
- The columns incorporate the different measurement strategies to choose from.
- An initial column includes the weights of each feature, which allow for a proper differentiation of how important each feature is relative to the others. The features can be classified within 8 values, with an increase of 0.25 each going the weighting from 0.25 to 2. A lower weight does not necessarily mean that the feature is not relevant, as all features have an impact on the strategy choice and must therefore be taken into account as long as they are included in the matrix. The values selected for the weights help to understand how important some features might be relative to others in terms

of the peculiarities of the experiments to be carried out. Some of them may be equal, whenever the features are considered to have the same impact on the decision making and should therefore be accounted equivalently.

- The scores inside the matrix are distributed from 1 to 5. A larger number means that the specific feature is better fulfilled. Special attention needs to be put on those characteristics that can be defined in a non-positive way, for instance: “time consumed”. The approach to avoid a false evaluation is to always think on how well the method meets the problematics of the feature.
- The overall score of each measurement strategy is calculated at the bottom row as the weighted addition of the scores on each feature.

	Weight	Closed Chamber	Sequential test with door opening	Point-by-Point with door opening
Temperature decay	1	5	0	4
Time consumed	0,5	5	5	3
Accuracy of results	1,5	5	2	4
Need for retempering	0,75	5	2	4
Safety	2	1	5	4
Long-lasting testing	1,75	0	3	5
Applicable to further tests	1,5	1	5	5
OVERALL		22,25	30,25	38,75

Table 1. Testing strategy matrix

Prior to the conclusions withdrawn from the matrix, some of the mentioned features may need some explanation:

- The concept of “Safety” is of crucial importance here due to the safety concerns resulting from the performance of such tests under the extreme temperature conditions. The wellness of the operator must be ensured at all times. A performance inside the climatic chamber can put the operator under severe risk.
- “Long-lasting testing” refers to the possibility of performing tests with a larger measurement grid with many measurement points. Although this does not come into the specifications of the tested cell module, it plays an important role on the development of a method that also meets stricter testing specifications. It goes a bit in hand with the applicability to further tests for the case studied here, but also demands a special mention.
- The matrix overall scores show that the Point-by Point with door opening strategy is the best pick for the purposes and the characteristics of the experiments. It can also be seen that both strategies following the door opening idea really stand out from their counterpart, the closed chamber option. This is due to the high impact that the safety

and the allowance for long-lasting tests have on the specifications of the experiments studied in this work.

3.2.3.2 Positioning and fastening of the test object inside the climatic chamber

Two crucial characteristics to obtain good interpretable results during the modal analysis are the correct positioning of the test object in the climatic chamber and its adequate subjection with respect to the test frame. The first is simply necessary to provide a comfortable measurement position that allows the execution of a robust measurement method, accurate throughout the test and seeking to minimize human error. The second is really important to ensure compliance with the theoretical and empirical guidelines for a modal analysis test with impulse hammer, so that the natural peaks and frequencies of the test frame, undesirable, are easily recognizable and distinguishable from those of the object of study.

In the following two sections each of these characteristics is explained in detail, relying on the case of the test frame in the theoretical base relative to modal analysis, but in any case for practical purposes, so that what is described here can be extrapolated and applied to cases slightly different from the one implemented within this work.

3.2.3.3 Placement of the test frame and the test object inside the climatic chamber

This concept has no theoretical purpose other than to ensure the following three vitally important aspects:

Firstly, a complete immersion of the test frame together with the specimen test inside the climatic chamber. In this way, the specimen test will take advantage of the power of the climatic chamber in its entirety, consequently reducing the time of tempering and re-tempering between measurements.

Secondly, the assembly must be completely stable inside the chamber so that under no circumstances is there a risk of the assembly falling or becoming destabilized. This should not occur either during the test or between tests, as any change in the placement of the assembly could influence the readings of the acceleration and temperature sensors (thermocouples), which would jeopardize the comparability of the results between tests and, in general, the validity of the measurement method.

This aspect is particularly important since measurement periods can be extended by days or even weeks, depending on the capacities of the climatic chamber and its availability for use. It is important to try to carry out all the desired tests within a time interval in which the test frame and specimen set is always controlled and untouched, remaining in the same position throughout the process. Under no circumstances should the whole unit be removed from the climatic chamber, unless this is strictly necessary for logistical reasons. Any variation that can be avoided will be avoided, since the impact of these on the results is not really calculable and threatens the feasibility of the method.

Due to the experience acquired during the tests gathered in this work, it is advisable to use some type of commercial foam, such as polyethylene (PE) used commercially for packaging and packaging, which can be placed between the floor of the climatic chamber and the test frame supports as insulation. With a certain thickness, it is possible to obtain a structure rigid enough to support the weight of the test frame and test specimen together, at the same time that it isolates the potential vibrations coming from the electric motor that feeds the climatic chamber. At this point it is important to ensure an eventual distribution of the thickness of the holding foam used along the entire surface of the test frame and specimen set, respecting its natural orientation with respect to the flat floor. A holding foam with considerable thickness variations on its surface could

destabilize the whole and cause a repositioning of it due to the force of gravity, which might not be reproducible in successive tests. In addition, a non-homogeneous foam could cause the test specimen to fall, unsteadily positioned, endangering the safety of the test operator.

Finally, the positioning of the unit inside the climatic chamber must be such that the operator is at all times comfortable during the measurement periods and can reach all the measurement points on the measurement grid with relative ease.

Although it does not seem to be a limiting factor for the quality of the test at first, it should not be forgotten that the tests can last for hours, depending on the number of measurement points present in the measurement grid. If several tests are to be carried out on the same day, the fatigue accumulated by poor measuring conditions can seriously deteriorate the quality of the induced hits, especially in the final parts of the test.

Along with the comfort and correct conditions of the operator, how reachable all are points within the measurement grid when the tests are going to be executed also becomes important. Although this should be considered in steps prior to the tests when designing the grid, there may be some cases in which the grid should be modified after a bad experience during the tests, so that a more convenient one is designed, which fits better with the test conditions. It seems a little difficult to know in advance whether the grid design will or not comply with the restrictions found when undertaking the tests, but this idea should at all times be in mind when designing which will be the best grid design for the purposes of the tests and the results desired. In any case, it is necessary to ensure at the end of the day a measurement grid whose points are entirely correctly reachable and executable from a given measurement position. Normally, this idea should not compromise the availability of a valid measurement grid design for the intended modal analysis results. It is the author's task to manage this commitment that creates the design of the grid and to find the best solution for the specific case study. However, this should not be a big problem considering the indications explained here.

3.3 DMA

3.3.1 Measurement equipment

3.3.1.1 Instrumentation

The measurement equipment consists simply of the DMA GABO EPLEXOR from company NETZSCH GABO Instruments GmbH. This machine combines the dynamic mechanical thermal analysis with dynamic material testing. The testing instruments of the DMA/DMTA GABO EPLEXOR 500N series goes up to $\pm 500\text{N}$ and enables the dynamic mechanical (or static) characterization of a wide range of different materials including polymers, composites, metals, glasses, ceramics, biomaterials and even liquids.

The modular design of the high-force DMA systems allows for measurements in the tension, compression, bending and shear modes. The testing machines in this series differ from each other mainly in terms of their maximum dynamic force ranges of $\pm 25\text{N}$, $\pm 100\text{N}$, $\pm 150\text{N}$ and $\pm 500\text{N}$. For the case of the EPLEXOR 500N, these ranges are changed by choosing from one of the different heads, whenever it is more convenient, depending on the material that is subjected to test. A small force may not be sufficient to induce elongation on very stiff materials, but a very high force can be inconvenient as well by causing the material to fail. A good understanding of what to expect from the material's behavior before it is subjected to test helps to choose the correct head.

All testing machines in this series are compliant with the standards DIN 53513, ISO 6721/1, ISO 6721/4, ISO 6721/5, ISO 6721/6, ISO 4664, ASTM D4065, and ASTM D4473.



Figure 47. DMA GABO EPLEXOR 500N

DMA GABO EPLEXOR 500N Key Technical Data	
Temperature range	-160°C to 1500°C
Frequency range	0.01Hz to 100Hz
Static force range	500N
Dynamic force range	$\pm 25\text{N}$, $\pm 150\text{N}$, $\pm 500\text{N}$
Static displacement	Up to 60mm
Dynamic strain	$\pm 1.5\text{mm}$ (3mm)

Table 2. Technical data of the DMA GABO EPLEXOR 500N

It has been noticed that the name of the instrument has recently been changed by the company. This is due to the acquisition of GABO by the German company NETZSCH on July 9, 2015. There is no information of the old GABO Instruments available anymore, as the website redirects to the new one generated by NETZSCH. Further information on the accessories available for the instrument can be found in the website [GABO19]

3.3.1.2 Software

For data acquisition and curve analysis, the DMA GABO EXPLEXOR® 8 software is the excellent solution provided by company NETZSCH GABO to operate together with the DMA test setup from the DMA GABO EXPLESOR 500N measurement instrument.

The software is perfectly integrated into the hardware system and allows for a comprehensive operation of the experiments. It is sufficiently sophisticated to provide all technological features required for a fine dynamic mechanical analysis of materials and, at the same time, understandable enough, so anyone can work with it comfortably after a small training and time invested.

The following chart contains the technical data provided by the manufacturer on its website [GABO19]:

Feature	Range
Frequency sweep	0.01Hz to 100Hz
Time sweep	1s to 10 ⁷ s
Temperature sweep (controlled temperature variation at fixed frequency)	
Static and dynamic stress or strain sweep	
Temperature and frequency sweep - Isothermal frequency changes (temperature steps)	
Constant stress amplitude mode per ASTM D623 (heat build-up test with static load and dynamic deformation – optional)	
Universal test driven by the servo motor (optional) or by the shaker (optional)	
Time-temperature superposition – TTS (WLF, Arrhenius, numeric – optional)	
Evaluation of complex modulus (E*, G*), storage modulus (E', G'), loss modulus (E'', G'') damping factor (tan δ), glass transition temperature and optional creep, relaxation and retardation, fatigue, energy loss, Payne/Mullins effect analysis and crack growth testing	
Hysteresis presentation of results (optional)	
Determination of the thermal expansion for tension mode (optional)	
Prediction of the rolling resistance of tires (optional)	

Table 3. DMA GABO EPLEXOR® 8 Software features

3.3.2 Test conditions and settings

As mentioned in prior sections relating to the technique of DMA and its theoretical foundations, the Dynamic Mechanical Analysis can be performed by continuously varying the temperature of the chamber where the specimen sits, the frequency of oscillation at which the specimen is subjected, or both of them simultaneously.

The specific technique or test method employed for the respective DMA experiments performed within this work is the so called “Temperature Sweep” in tension fashion, at which the dynamic elastic properties of the material are tested under a varying temperature range, and with a constant frequency. The idea behind the choice of this experimental type of DMA-procedure is because the temperature and its influence is the only physical property that is desired to be analyzed. By a “Temperature-Frequency Sweep” type of procedure, the change of both the temperature and frequency would induce variations in the mechanical properties of the materials under study, so no unique factor but a mixture between the two would be the cause of these fluctuations in the properties’ values. A Temperature-Frequency Sweep would be interesting for a more practical application, in which a certain, real dynamic scenario would be desired for the simulation.

Even though a much wider range is within the capabilities of the machinery (Table 2), just the desired temperature range for this work was set for testing. By testing a wider range, a greater amount of measurement time will be naturally demanded, jeopardizing the initial planning of the tests. Longer lasting tests may also be more prone to suffer from failures and inaccuracies. And most importantly, the focus of the results might get lost by the greater amount of data found in the test results, losing perspective of what it is really meaningful here and misleading the reader off the crucial information that needs to be understood at this point.

The idea behind the temperature analysis is to simulate the whole operational temperature range that the module might be subjected to. Based on the standards by the European norm for transportation of goods [UN38] and the specifications of Lithium-ion batteries [KORT13], such components are set to work within the temperature range of -40°C to $+50^{\circ}\text{C}$. As the purpose of the DMA experiments is to retrieve valuable information from the three polymeric elements under operation, the temperature range of interest was the exact range specified by the norm.

As indicated by the experience co-workers at the Materials Laboratories in Munich, a transient testing phase may appear at the beginning and at the end of the measurement. This is a response of the machine trying to stabilize itself at the limits of the measurement range indicated. As a cause of this transition process, even though it might seem to be short, some irregularities in the vicinity of the lower and upper limits can occur, compromising the validity of the results in these two areas. The recommendation to overcome this problem is to simply widen up the temperature range at both limits, in order to make sure that the transient phase only exists outside the range of interest, so no single measurement point to be tested is affected by it. Just for simple convenience, an extra 10°C was added to each limit temperature, making it from -50°C to $+60^{\circ}\text{C}$. For final clarification, the exact same temperature range was set for each of the three materials to be tested, as well as a constant 10Hz oscillating frequency for the whole and each of the measurements. The following table collects all important parameters that were set equal for the three valid experiments.

Sampling frequency	Sample temperature range	Temperature range of interest
10Hz	-50°C to $+60^{\circ}\text{C}$	-40°C to $+50^{\circ}\text{C}$

Table 4. Temperature-Sweep experimental settings

By further analyses of the results, it was found that this addition to the desired range was sufficient for the experiment to be run under correct conditions within the desired temperature range for this work.

All configuration parameters implemented for each of the experiments are included with detail in the Appendix.

3.3.3 Preparation of test specimens

The elements of interest within the cell module cannot be directly tested as structural components. Experimental material testing involves the use of specimens, also called samples, which are designed with a specific geometry and shape that complies with the characteristics of the instrumentation and the technique itself.

For the case of the two adhesives (the SA and the HCA), an experimental process for the construction of the samples was implemented. This process begins with the collection of the materials in its most elementary form. Both the SA and the HCA are a two-component (2K) adhesive, and both the SA and the HCA are made out of two different materials that are mixed together. This could be considered the starting point to this process.

The steps to this experimental process are collected in the form of guidelines, including images and remarks on important aspects to account for during the process of sample preparation. These guidelines were thoroughly followed for the preparation of the SA and HCA and the process resulted in the construction of valid samples for both materials, which were further tested by means of DMA.

3.3.3.1 Experimental guidelines

a) Purpose

This test specification is intended to ensure uniform performance in the manufacture of adhesive samples, so that they can be used to a material testing end.

b) Process steps

1. Injection of material

The material is injected from its original storage conditions on a Teflon-coated round plate. A similar second plate is then placed over the material, acting as a press.

The Teflon foil allows the material to be released once the layer is ready. The ideal size of the plates is 20 - 25 cm and it is important that they are made of aluminum or steel and are thick enough (approx. 1 cm) to have the necessary bending stiffness during pressing.

The Teflon foil on each plate should be treated with extreme care. As its surface is the one in direct contact with the mass of raw material to be shaped, any scratch, hole or other irregularity will be mimicked to the surface of the end sample, making it inadequate for a DMA experiment.

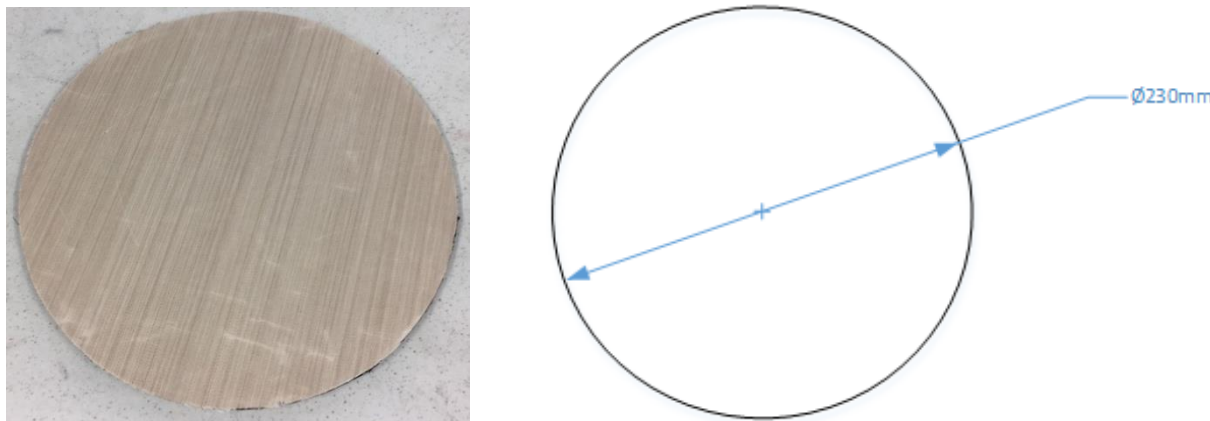


Figure 48. Image (left) and sketch (right) of the Teflon-coated plates

2. Production of adhesive layer

The top plate is then placed over the material. The surface of each plate that contains the Teflon-foil must be in contact with the material. It will then be evenly distributed over the surface of the plates, forming a layer of adhesive with constant thickness.

The correct approach is to take two separators (also called spacers), which have the exact same thickness as the one desired for the specimens. They are used to adjust the adhesive thickness by creating a gap between the plates. For the tests performed in this work, the separators used for the preparation of both the SA and the HCA samples were 4mm thick.

Either 4 small spacers or 2 large ones can be used. It is important that the spacers remain in their place during pressing and are not washed out by the adhesive. It must be ensured that tilting and thus the loss of plate parallelism is prevented.

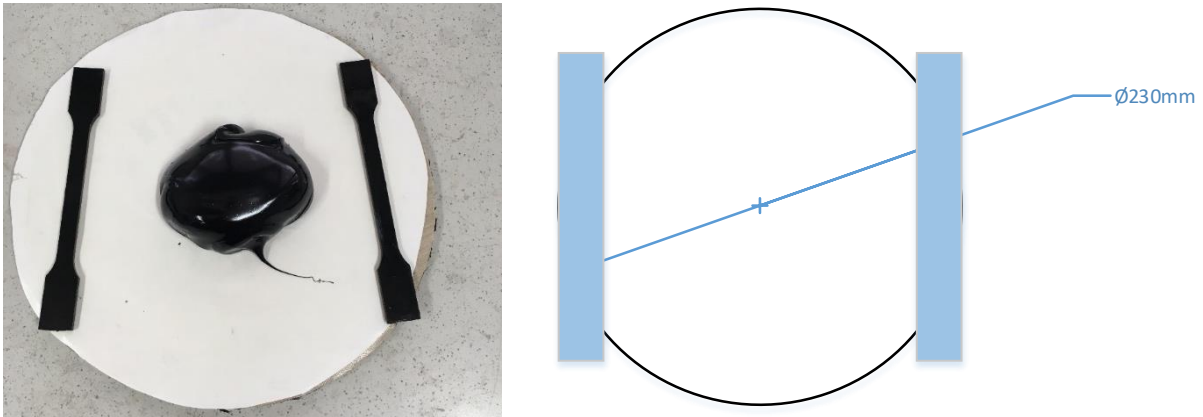


Figure 49. Image (left) and sketch (right) of round plate with spacers

After the adhesive has been applied and the spacers have been inserted, the plates are brought to the desired distance using screw clamps or a press. Again, it is imperative that the separators remain in their intended position.

This action can also be done by hand. By placing one of the plates on a flat surface, the second plate can be handled from above and downwards, pressing the material on the flat plate. The side of each plate with the Teflon foil must be facing the material. Once the upper plate has been placed correctly and it has been made sure that the separators (spacers) stay put into place, some heavy weight like a material tank can be placed on the upper plate in order to press the material at a constant rate, for a long enough period of time. At this point, it is important that the tank is not removed or disturbed within the necessary time period previously indicated.

3. Annotations

A) Injection

The application of the adhesive must be bubble-free. The adhesive should only be applied in the middle as a large ball. In this way, the adhesive can be applied bubble-free as far as possible.



Figure 50. Correct application of injected material

B) One-component- (1K) vs Two-component (2K) adhesives

With 1K adhesives, curing is largely prevented by the metal plates. Therefore it is necessary to put a non-stick paper on the plates and to apply on it. After the adhesive has hardened at the edge, the upper plate can be removed. The permeability of the paper allows curing to be achieved.

With 2K adhesives it is to be paid attention that the plates lay at least 24h in the standard climate, in order to prevent that these are damp. This could lead to the outgassing of PU adhesives. This means that no adhesive skin of sufficient quality can be produced.

C) Non-stick paper

In order to increase the efficiency and to guarantee the complete curing, permeable non-stick papers can be laid on the Teflon plates. This allows the device to be opened much faster and used for new adhesives. This also ensures that 1K adhesive comes into sufficient contact with moisture.

D) Curing time

- 1K adhesives: 2 weeks, lid can be opened after 24 hours
- 2K adhesives: 1 week, lid can be opened after 24 hours

As for the 2K components tested within this work, after three to four days both materials (SA and HCA) have achieved its final composition and could then be carefully removed and set for testing. A one week curing time ensures a correct curing for all, worst cases and is essentially very convenient for a guideline. However, having a good feeling on what to expect from each specific material can save up a considerable amount of time. Preparing a side, smaller amount of material that can be checked during the curing period can also help to know what is exactly going on at the right material preparation setup and understand when a sufficient amount of curing time has passed.

4. Release of the adhesive layer

After curing time, which depends on the type of adhesive, the adhesive layer can be safely released by pulling the two plates apart. In some cases, a small tool might be used as a lever. The use of the non-stick paper helps to release the layer in a much safer manner.

5. Sampling

For subsequent tests (e.g. tensile test, DMA) can be performed by water jet trimming or molding. When molding, however, care must be taken that the material (very brittle materials) is not damaged. In this case, water jet cutting is recommended.

At this final step, a previous layout with all specimens desired on the end material plate retrieved from this process helps enormously by the subsequent water jet cutting. As some specimens may present irregularities along the whole preparation process, it is recommended to collect as many material samples as possible out of the material plate, so the very best looking ones can be selected for test afterwards. Whenever a hole or a scratch is found at the surface of a specimen, it needs to be immediately discarded and cannot be further used for test validation.

After retrieving the samples from the material plate and prior to the testing, the dimensions of the selected samples need to be checked. Being the standardized process for specimen preparation a non-extraordinarily precise method, the dimensions of the resulting samples will slightly differ from the standardized ones. It is however not a problem at all, as long as the specimens are thoroughly measured after their preparation and the real dimensions are entered into the measurement program.

Achieving a regular thickness along the whole specimen length is also essential for a correct experiment performance and data collection. A caliper foot can be used to measure the thickness of the samples at different points, checking whether they are equal to one another.

3.3.3.2 Geometry of the specimens

A special characteristic specific to the TCE should be highlighted when describing the tested samples: the geometry of the specimen is not a result of the sample preparation process as followed for the two adhesive materials. Instead, a piece of the end-material was cut from a roll, complying with the geometry specifications for DMA experimentation [ISO 6721]. The differential dimension between the three materials is the thickness, as it can be seen in the geometries displayed below.

It is also important to highlight that the process to sample preparation of the adhesives cannot provide the exact geometry that is specified. Being it a manual process, some imperfections might occur at certain steps. These imperfections need to be accounted for by measuring the real dimensions that result from the sample preparation process. A caliper foot was therefore used to retrieve the real dimensions of the SA and HCA specimens with an accuracy of 0.01mm. The width and thickness of the two adhesive samples need to be checked at several different points, as the surface of the press-plates might not be perfectly flat, making the thickness of the specimens slightly uneven.

The sketches below describe the real geometry of the tested samples, which were also addressed in the parametrization specifications of each test into the measurement software.

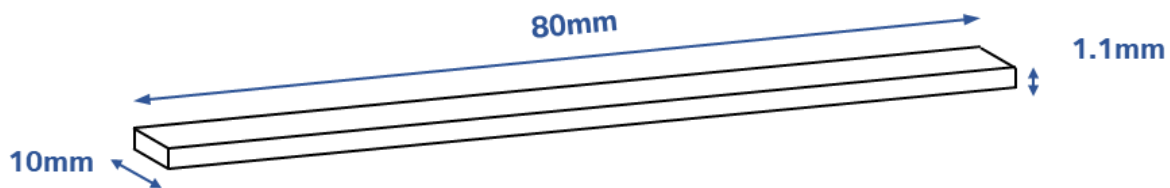


Figure 52. Geometry of the TCE sample

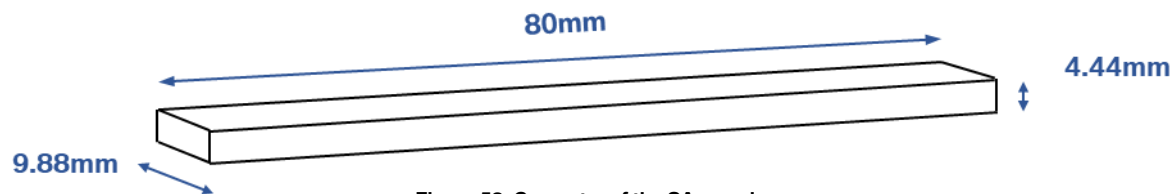


Figure 53. Geometry of the SA sample



Figure 51. Geometry of the HCA sample

4. ANALYSIS OF RESULTS

4.1 MODAL ANALYSIS

4.1.1 Overview

The study of the vibrational behavior of the cell module could successfully be addressed by means of the MA impact testing experiments performed in the climatic chamber. Each experiment had a duration of 90 to 120 minutes. Following the point-by-point with door opening strategy, specifically designed for such kind of test, the analysis of the hammer impacts was done during the measurement itself, which ended up in a very efficient way to perform the experiment.

However, the initial desire to control the humidity levels was not feasible. By the opening of the door, air comes in the chamber and the RH levels become unmanageable. The effect of humidity would stay for further analysis.

Focus was given to the natural frequencies of vibration: the goal was to quantify these frequencies for each temperature scenario, and compare them as a function of temperature. To this end, the FRF and CF of all measurement points for each scenario are recorded using PAK.

The CF was useful during the experimentation to validate for the best impacts. On the other hand, the FRF, as the most important tool in modal analysis, allows to retrieve the values of the natural frequencies of vibration for each measurement point.

Twenty FRFs are collected at the end of each experiment, one at each measurement point. The analysis of variance (ANOVA) on the natural frequencies of all measurement points allow to compute the dispersion of the collected data. This was considerably helpful to illustrate how accurately each test was performed.

The results of the ANOVA are collected into a chart, which displays the value of the averaged natural frequency and its standard deviation for each scenario. Due to excessive dispersion found at the second and third natural frequencies of the cell module, only the first natural frequency has been successfully analyzed for all four tested scenarios.

Prior to address the results on the first natural frequency of vibration, the feasibility of the measurement strategy implemented for the EMA experiments was subjected to analysis.

4.1.2 Reality in the climatic chamber

The temperature inside the climatic chamber was successfully measured, monitored and recorded during the entire duration of each of the four experiments performed. The objective was to provide clear argumentation on the feasibility of the measuring strategy performed.

For size reasons, only a small representation of the collected data is included in this section. The one temperature scenario with the most risk to experience a major temperature change during testing is the coolest scenario, at -20°C . This is because this scenario would exhibit the highest heat exchange rate when the door is opened, as it is the temperature that differs the most with the room temperature found outside the climatic chamber, at around 23°C .

To this end, the processed temperature data collected over the time span of slightly more than an hour during the EMA measurement at -20°C is included. As a result of the pattern displayed, a portion of the measurement is sufficient for the explanation, which is also more convenient for size matters.

The complete temperature data collection at each of the four tests is found in the Appendix.

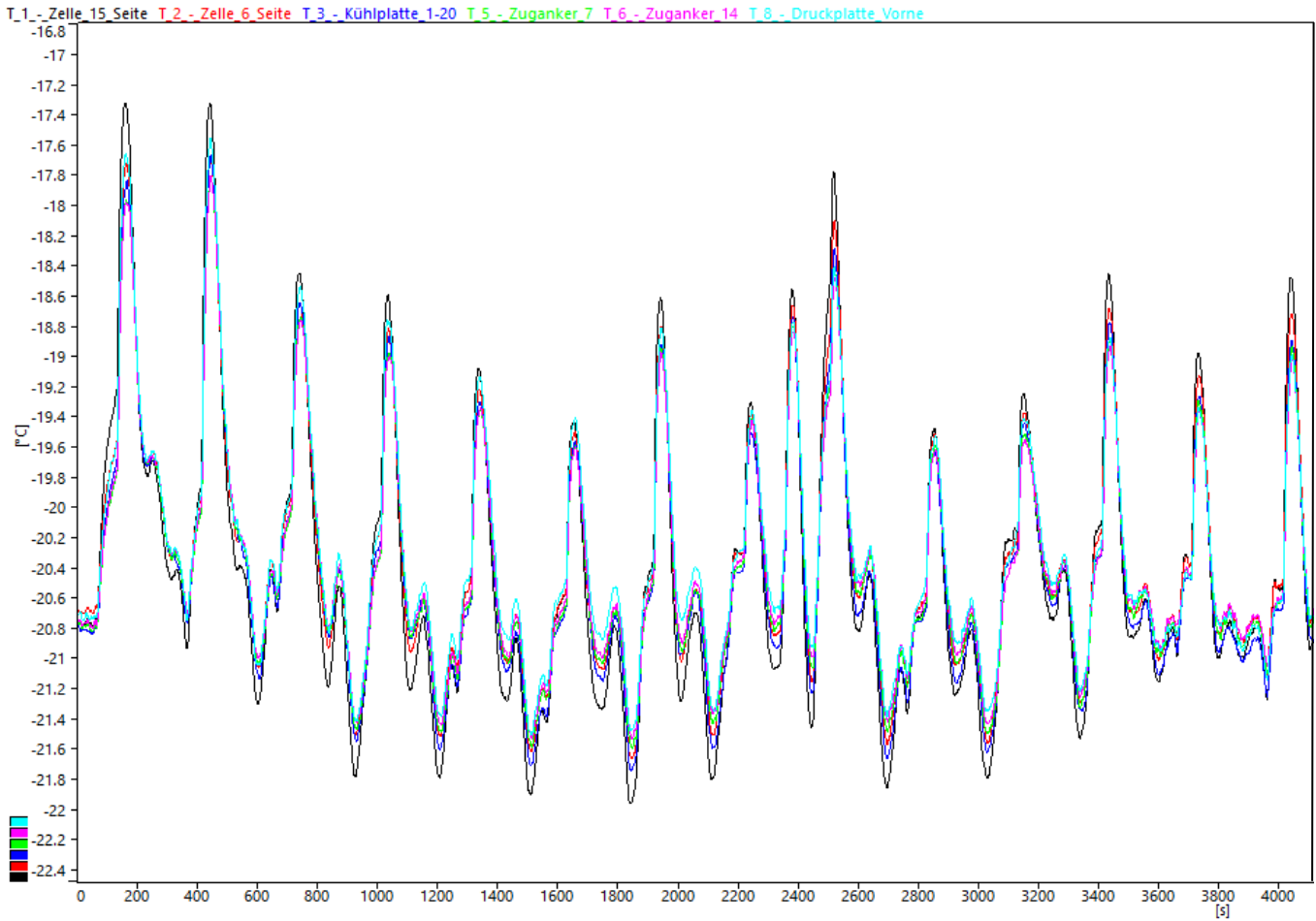


Figure 54. Temperature record inside the climatic chamber at the -20°C measurement

The temperature course over a period of more than an hour from the readings on six different thermocouples at the -20°C scenario shows a total deviation of less than 5°C when comparing the highest temperature and the lowest temperature recorded by any of the thermocouples over the analyzed measurement time. The maximum temperature is found around -17.2°C, whereas the coolest temperature was recorded around -21.8°C.

The sharp peaks show a rapid increase in temperature by the opening of the door. However, the temperature recovery by closing the chamber is almost equally quick. The time span between measurement points was intentionally set to 5 minutes (300s), which is the length of the pattern that is constantly repeated.

The data provided is very illustrative, as it shows that the longevity of the experiment do not have a negative impact on the steadiness of the temperature during the process. That asserts the feasibility of the measurement strategy to be implemented for longer tests. The readings of the type k thermocouples show a very similar temperature distribution on all areas of the cell module recorded. That illustrates an even heat loss or gain within the sampled areas of the module. The correct functionality of the thermocouples is ensured, as none of them show a different behavior.

When performing the experiments, the opening of the door occurred within a time span of one to two minutes, depending on the accuracy achieved and the feeling of the impacts. The rest of the time between measurement points, which was used for the analysis of the impacts was found to be sufficient for re-tempering. The temperature at the beginning of each measurement point can be said, with sufficient accuracy, to be the same for each point, and stays close to the -20°C area.

The thermocouple type k specifications show an accuracy of 1.5°C [FUEH19]. By accounting that the 5°C degree do not necessarily come from the same thermocouple, nor the same

measurement point, the characteristics shown of this measurement strategy are proven to be sufficiently accurate for the purposes of this work.

The analysis of the temperature data implemented with TurboLab do not show any drastic temperature drop or gain in any of the four tested scenarios. The analysis of the worst case-scenario shows little impact of the heat gain on the cell module’s test temperature during opening of the door. The collected data proves the applicability of the designed point-by-point with door opening measurement technique for all four studied scenarios.

4.1.3 First natural frequency of vibration

The initial hypothesis on the effect that temperature has on the mechanical behavior of the cell module is asserted by the analysis of the first natural frequency of vibration: the higher the operational temperature of the module, the more easily it will be excited by an external vibration. This is shown as an exponential decrease of the first natural frequency of vibration, as temperature is increased.

Prior to the analysis, the validity of the results needed to be confirmed. Following the condition on the natural frequencies of the supporting mechanism and the test frame, the test setup was found to be compliant with the characteristics of the module. A separation over 100Hz between the highest natural frequency of the test setup and that of the cell module was checked for all four scenarios [HOOP15]. Even for the lowest frequency scenario, at +40°C, the frequency separation is sufficiently large to confirm that the bearing mechanism and frame had no impact on the results.

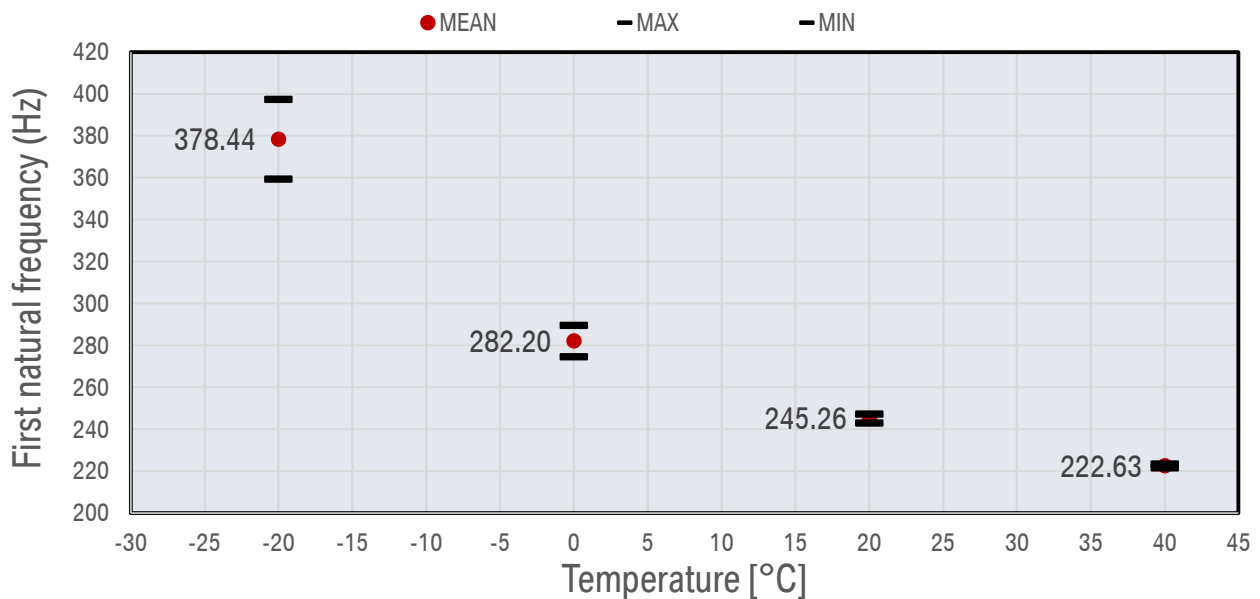


Figure 55. Distribution of the first natural frequency of the cell module over temperature

Temperature [°C]	Count	Sum	Average [Hz]	Variance	St. Abw. [Hz]	Max. [Hz]	Min. [Hz]
+40	19	4230	222,63	0,91	0,96	223,59	221,68
+20	19	4660	245,26	4,54	2,13	247,39	243,13
0	20	5644	282,20	56,80	7,54	289,74	274,66
-20	18	6812	378,44	362,14	19,03	397,47	359,41

Table 5. ANOVA on the first natural frequency at the four tested scenarios

The FRF (gain and phase) and CF analyzed for all temperature scenarios can be found in the Appendix. The results of the ANOVA on the first natural frequency at each of the four temperature scenarios are represented below.

The ANOVA on the first natural frequency results in a very appropriate way to illustrating the findings of the experiments. First of all, dispersion of the data is seen to increase as temperature goes down. This is due to the increase in the temperature difference between room temperature and that in the climate chamber. Whenever the door is open for test, the heat exchange between the chamber and the environment begins, which causes the module to experience a dynamic temperature change and ultimately causes the vibrating properties of the module to be altered during the experiment. It therefore makes sense that the largest dispersion is found at the smallest temperature, -20°C , as the heat exchange rate between the chamber and the environment is in this case the highest, due to the larger temperature difference between the two systems.

The exponential regression is worsened by the addition of the -20°C scenario. This is also explained due to the large deviation the measurement points have at this temperature, when compared to the other three scenarios.

The substantial change within the temperature range of interest for the first natural frequency of vibration suggests the enormous effect that the temperature of the environment has on the mechanics of cell modules. This information could be crucial for certain structural considerations of relevance at the design phase of the module architecture.

The analysis of the agent temperature has been quantified and illustrated. A further investigation on the second and third modes would be a direct complement to this work. It would be interesting to see whether the same behavior is found at higher frequencies.

4.1.4 Applications of the designed measurement strategies

The point-by-point with door opening technique has been proven to work for the purposes of this work. However, the other two designed techniques might have an application as well.

The measurement strategy with the door closed was discarded due to safety concerns. Its advantage is the temperature stability due to a minimal and irreparable heat loss or gain (that of the climatic chamber itself). That means that, if there was a way to safely implement this technique, the results provided would be the most accurate ones achievable. Some kind of automated measurement executed by automated machinery might be a possibility of implementation of this technique.

On the other hand, the sequential measurement with door opening has the advantage of being a mixture of the quickest and safest. Its disadvantage is the great heat loss or gain and the tempering time for long experiments. However, when the heat transmission is controlled and the measurement grid allow for a quick test, this technique is the most convenient measurement strategy to implement.

4.2 DMA

After a thorough understanding of the purposes of DMA and its foundations, the limitations of the measurement technique and equipment, as well as a rigorous visual analysis of the three materials committed to testing that conform the polymeric components present in a state-of-the-art cell module, some deliberation about the pattern of test results to be expected for each material can be pulled off.

Beginning with the TCE, some characteristics of its behavior can be immediately perceive: its foam-like structure, soft to the touch and ductile-elastic appearance at room temperature. After some stretch is applied, the material recovers its original form. Prior to testing, it was therefore classified as an elastomer. Its microstructure should therefore show a high organized bonding chain layout, to which stretching could be done due to the weak bonds that hold them. This whole idea made much sense as for its rubbery appearance.

With respect to the adherent components, the behavior of both the structural and the heat-conducting adhesives were initially more challenging to predict, as the appearance of these two-component (2K) glues could only be seen after the preparation process described earlier was already completed. Once the samples of the two components were prepared, some differences could be appreciated between the two. The SA showed a very soft and flexible behavior to bending, less resistance when subjected to torsion and a general more ductile and elastic appearance. On the other hand, the HCA stood out for its much harder and rigid presence, to which minimal or zero stretching could be done by simple handling. Their mechanical behaviors would be expected to differ, yet both of them were classified as thermoplastics. The SA should have its glass-transition temperature below room temperature, whereas the HCA behavior perceived at room temperature should be that of the area of performance prior to the glass-transition.

Although a quantitative analysis prior to the test is unreasonable to predict, the feeling experienced by playing around with the samples provides a modest idea on the test performance of each component. As mentioned several times in this document, the feeling obtained from a proactive attitude and essentially a wide experience at working with engineering materials clarifies most of the initial uncertainties and builds up the confidence needed for a proper decision making and a precise execution of the tasks. This needs to be an ability developed by any engineer which strives for precision, problem solving and flawless understanding of the job.

The analysis of results of the DMA experiments focused on the four magnitudes of interest: the storage modulus, the loss modulus and the resulting complex modulus and tan delta. Special attention was given to the storage modulus and tan delta, as for their ability to describe the material behavior as indicated in the theory.

As seen in the literature and from an engineering perspective, the higher the temperature, the softer the behavior of the polymeric material that can be expected. With these guidelines, the magnitude of the storage modulus is expected to decrease throughout the whole temperature range in the direction of temperature increase. This was the original premise by which the decision to test the properties of these three components was made. Once that is understood, the important point of study lies on how much these magnitudes will change, in a more quantitative level, throughout the temperature range of study.

The point is then to quantify these changes in the behavior of the materials and to focus on characterizing the magnitude of those changes and compare them between the materials. For this end, a normalized representation of the magnitudes of interest was found to be the most appropriate criteria. By working with relative values, a direct visualization of the magnitudes of these changes is provided, which is also independent on how high or low these magnitudes can go in absolute values.

The following subsections show the data collected and the further analysis of the curves carried out for each of the studied materials. The base value for the normalization of such magnitudes was set to the closest measurement point to 20°C, for each material. This idea allows to compare the behavior of the materials to their regular values found at room temperature. The base measurement point and its values of the four magnitudes of interest are highlighted in bold and red in each table.

Although the experiments were performed within a range from -50°C to +60°C, the analyzed data restricts the studied range by 10°C at each end, that is, from -40°C to 50°C. This is due to the transient phase a DMA experiment may exhibit due to the stabilization time during the heating at the beginning and end of the measurement. All magnitudes are collected within this range of interest, which is also closer to the one studied by means of EMA.

Along with the graphs, the ratio between the highest and the lowest value of storage modulus is computed, as it helps to better understand the impact of these results. From now on, this will be called the Highest-to-Lowest Ratio, or simply HL-Ratio. Additionally, the percentage change of the storage modulus is calculated, in order to visualize the maximum relative change of this magnitude within the temperature range of interest and for each material.

By the use of relative values, the comparison of value change among the three materials is straight-forward. That also applies for the tan delta, which is dimensionless by definition.

Two decimal values are found convenient for the description of the magnitudes presented, as a finer characterization would not result in better results, but in an unnecessarily more complex representation of the data. Calibration tolerances and the potential error carried through the whole measurement process due to the limitations of the equipment and the irregularities that may have occurred by the preparation of the samples do not stand for a finer measurement result, which is also not needed at all for the purpose of this analysis. The general idea of the considerable impact that the temperature has on these materials is what needs to be depicted from these analyses.

With regard to the graphs, a logarithmic scale is chosen for the case of the TCE and the SA normalized moduli in the y-axis [dimensionless, -], whereas a linear scale was established for the x-axis [Temperature, °C] for all graphs. Due to the substantial change in the values of the moduli, the logarithmic scale helps remarkably to understand the impact of the temperature on the three materials without having an enormous, inconvenient graph that is difficult to read. The changes in the magnitudes should therefore be interpreted as how quickly they jump into the adjacent lower decade. The slope of the graphic becomes more relevant for the higher section within the y-axis. On the other hand, the tan delta is displayed in linear scale for every case.

4.2.1 TCE

This rubbery material experienced the biggest change in magnitude throughout the entire measurement process. As initially speculated, its behavior mimics that of an elastomer and differs the most in comparison with the other two tested materials.

Measurement Point	T °C	E'	E''	IE*	Tan Delta
1	-40,6	79,98	34,18	71,81	0,24
2	-31,0	41,59	24,69	38,26	0,33
3	-21,0	16,31	15,02	16,02	0,51
4	-7,3	4,79	4,97	4,84	0,58
5	-0,9	3,03	3,14	3,05	0,58
6	14,6	1,27	1,30	1,28	0,57
7	19,7	1,00	1,00	1,00	0,56
8	26,1	0,79	0,76	0,79	0,54
9	38,9	0,51	0,44	0,49	0,49
10	51,3	0,36	0,27	0,34	0,41

Table 6. DMA data of interest from the TCE experiment

An important remark to make at this point is that the unique mechanical behavior of the TCE sample along with the measurement conditions did not provide such accuracy by data collection as seen on the SA and the HCA cases. Its DMA experienced more difficulties to work within the tolerances and parameters set for the experiment and therefore less measurement points and larger gaps between them are found by looking at the raw data included in the appendix. This ends up in a lesser accurate data than for the other two cases, yet not on an unacceptably imprecision that jeopardizes the validity of the results.

An interesting aspect from the data is that tan delta remains considerably stable from -20°C to +20°C. That suggest that no sharp behavioral transition occurs within the studied temperature range. Both the storage and the loss moduli decrease at a similar pace within this indicated range. The maximum tan delta is found somewhere between -10°C and +10°C. The data collected does not provide clearer insight to this end due to the big gaps between subsequent measurement points.

Looking at the E-Moduli, the curves follow an exponential decay, for which the stabilization occurs above room temperature, around 45°C. The largest decrease in the storage modulus occurs therefore at the very beginning, at which the magnitude decreases by a 50% in just an increase in temperature slightly smaller than 10°C.

As constitutive component of the tested cell module, the DMA suggests that the TCE may respond very differently under different environmental scenarios due to the significant impact of the temperature on its dynamic stiffness. These findings on the material shall be accounted when running operational experiments and for the simulation models, as the behavior of this component may differ drastically from the one considered at the design phase.

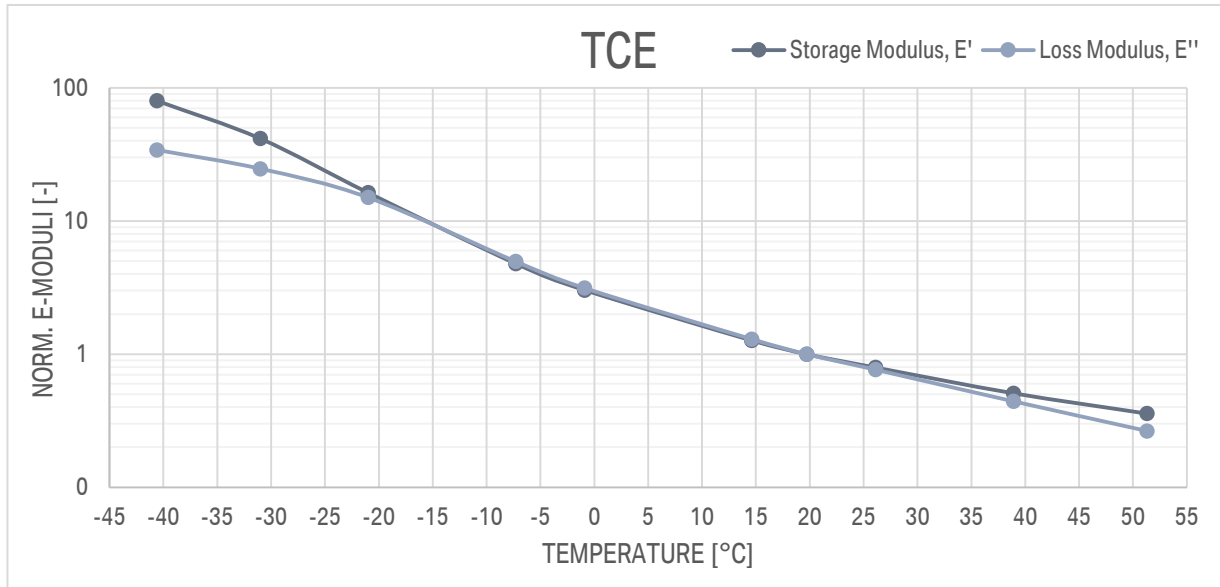


Figure 56. Normalized moduli over temperature for the TCE experiment

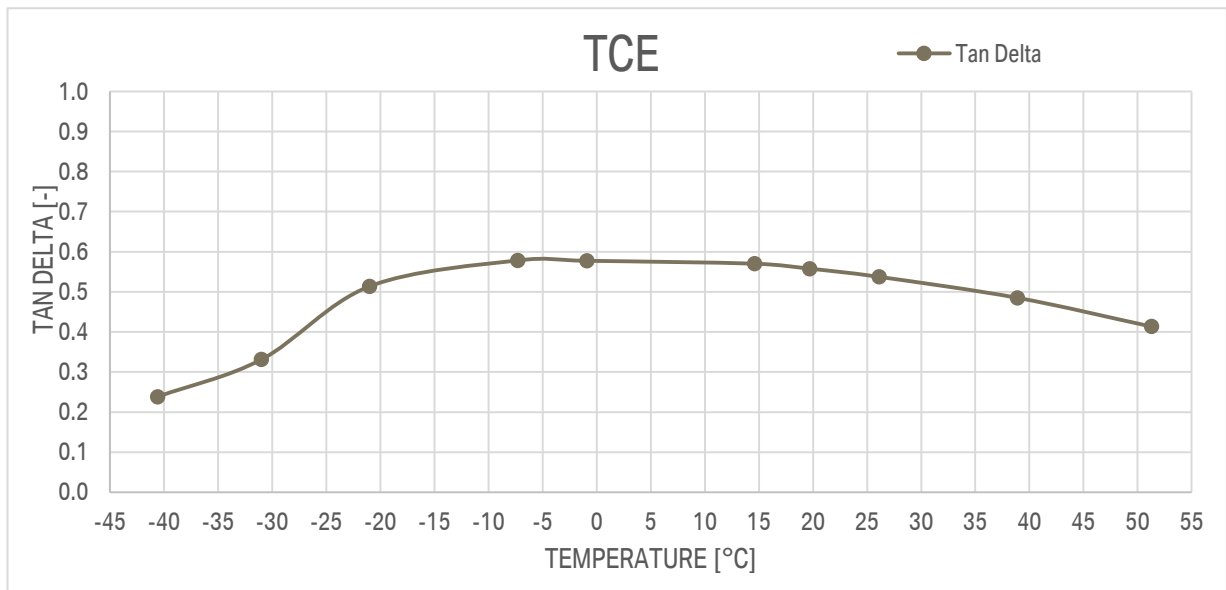


Figure 57. Tan delta over temperature for the TCE experiment

4.2.2 SA

The whole set of data included in the Appendix shows a maximum tan delta at -40°C, which can be stated as the glass-transition temperature. This cannot be seen in the graphs, as the transition does not occur inside the sampled temperature range, but slightly outside the lower end. As the material does not seem to collapse after this transition phase, a correct labeling would be to consider it a thermoplastic polymer that operates above its glass-transition temperature.

Table DMA	Measurement Point	T °C	E'	E''	E*	Tan Delta	7. data of
	1	-39,9	12,72	39,78	13,65	0,41	
	2	-29,9	5,27	14,65	5,57	0,37	
	3	-19,9	2,88	5,93	2,96	0,27	
	4	-9,9	1,92	3,00	1,95	0,21	
	5	-0,1	1,44	1,85	1,45	0,17	
	6	10,1	1,16	1,28	1,16	0,15	
	7	20,0	1,00	1,00	1,00	0,13	
	8	30,1	0,88	0,80	0,87	0,12	
	9	40,1	0,76	0,62	0,76	0,11	
	10	50,0	0,68	0,50	0,68	0,10	

interest from the SA experiment

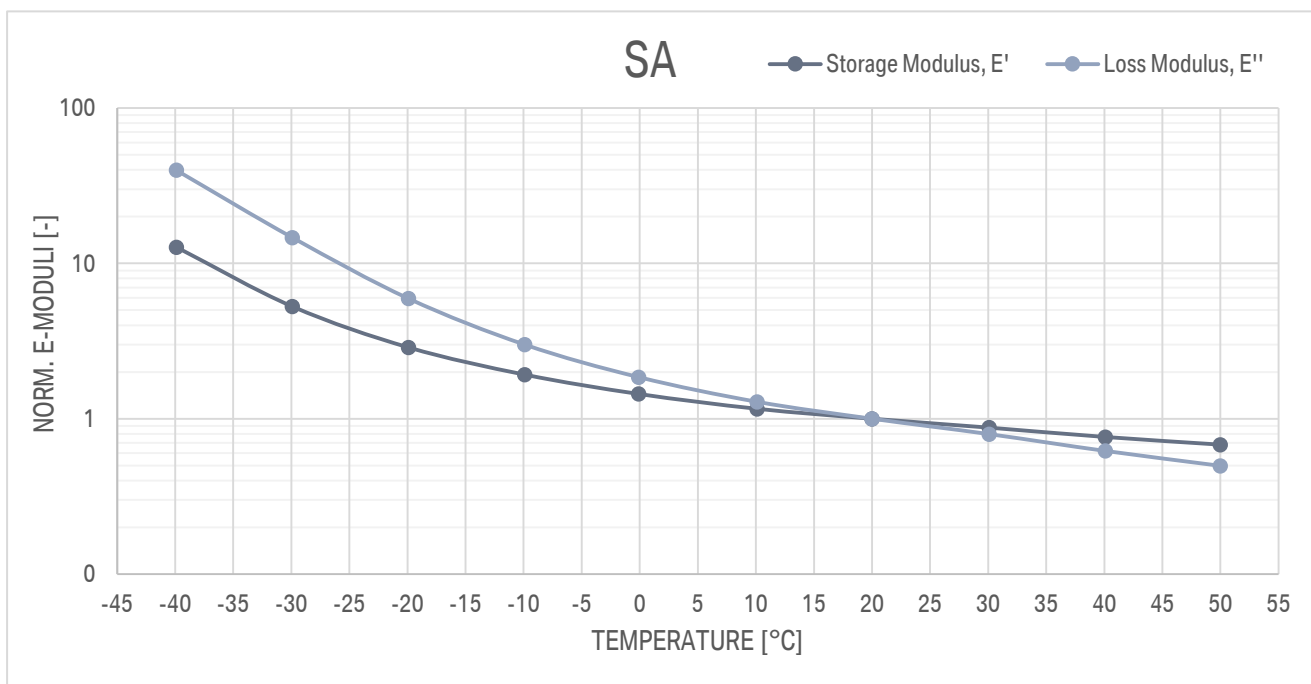


Figure 58. Normalized moduli over temperature for the SA experiment

Analysis of results

Within the first 10°C decay, the storage modulus is reduced by almost 60%. The performance of the material is highly altered in this area, which goes along with the transitional phase after the glass-transition temperature has been reached. The so-called “Plateau” will begin, however, earlier than for the case of the TCE. This suggests that the performance of this material will be found to be stable for a larger temperature range. Fair to say that it would be less problematic to have a material with such behavior when it comes to designing and selecting the components for a potential new cell module.

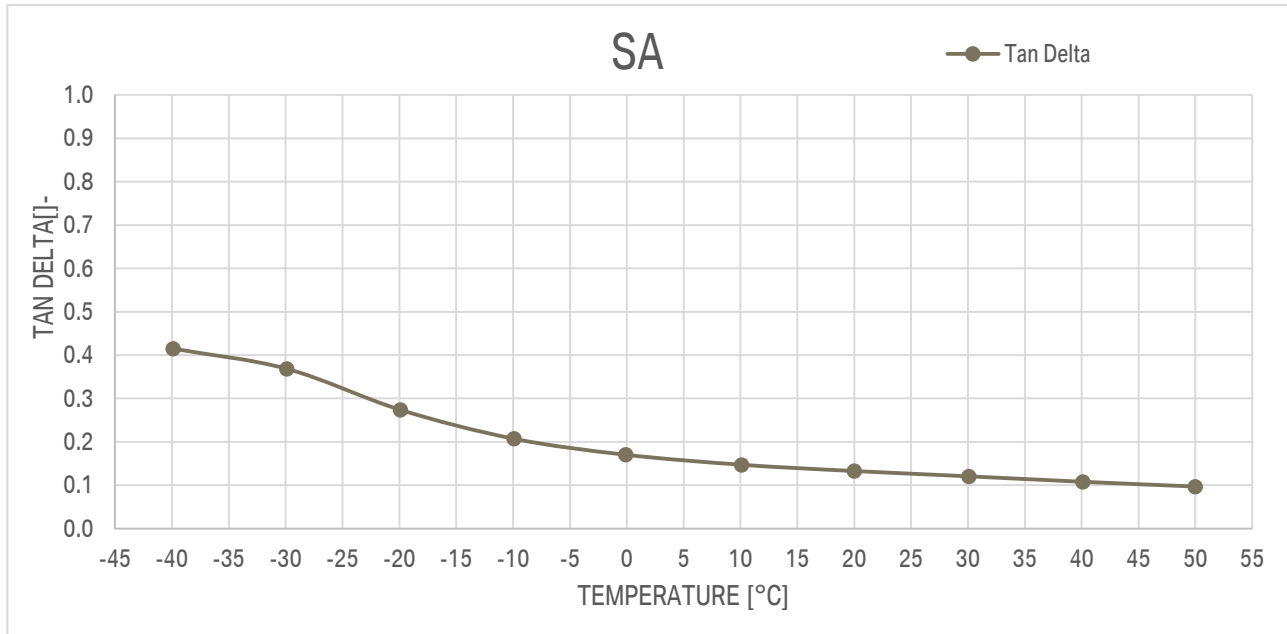


Figure 59. Tan delta over temperature for the SA experiment

4.2.3 HCA

As to some extent predicted from the appearances of the two glues, the performance of the HCA depicted from the analysis differs remarkably from that of the SA.

The glass-transition temperature is trickier to detect as it is for the SA. The raw data shows a maximum tan delta at the upper limit of the temperature range at which the experiment was carried out, slightly below the +60°C (around +57 to +58°C). That means that the glass transition is found outside the sampling rate of interest.

Measurement Point	T °C	E'	E''	IE*	Tan Delta
1	-39,7	2,53	0,62	2,49	0,04
2	-29,6	2,38	0,63	2,35	0,04
3	-19,8	2,20	0,66	2,17	0,05
4	-9,7	1,97	0,73	1,95	0,06
5	0,1	1,67	0,78	1,66	0,08
6	9,8	1,36	0,88	1,34	0,11
7	20,3	1,00	1,00	1,00	0,17
8	30,3	0,65	1,00	0,66	0,26
9	40,2	0,32	0,73	0,34	0,38
10	50,2	0,14	0,38	0,15	0,47

Table 8. DMA data of interest from the HCA experiment

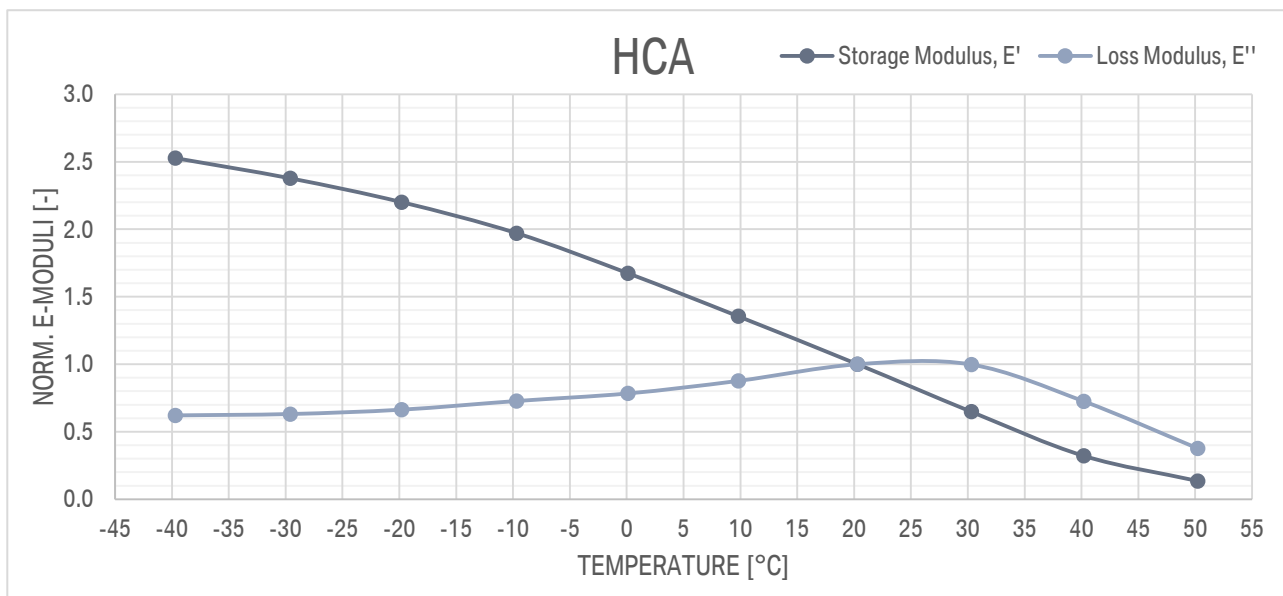


Figure 60. Normalized moduli over temperature for the HCA experiment

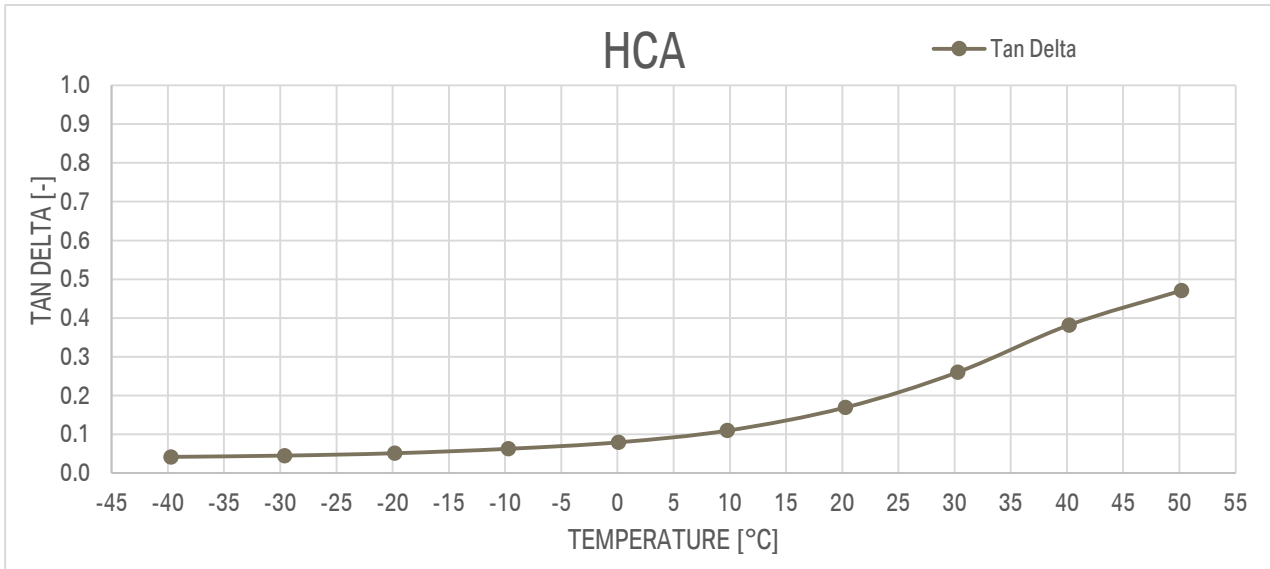


Figure 61. Tan delta over temperature for the HCA experiment

This suggests that the material exhibits a thermoplastic behavior, and that is also highly affected by the influence of temperature within the studied range. Speaking of relative values, the earlier mentioned 50% decay occurs nearby the +10°C area, already passed half of the range of interest. However, the magnitude of the storage modulus is by one decade higher than that of the SA, and more than 30 times higher in relation to the TCE. These comparisons are found normal when understanding the purposes of each material and their functions as components of the cell module.

4.2.4 General findings

Once the tests were finished, each sample was visually examined. No symptoms of fracture or some type of plastic deformation was found in any of the three materials, besides the marks at each end due to the contact force applied by the clamps to hold the specimen during the measurement. The samples looked exactly the same as they did prior to the experiments.

This is at first a good indicator of a correct execution of the tests and a proper choice of the parametrization for each specific case. However, no test can be ensured to be out of error, as only a visual inspection of the surface is possible, missing out potential irregularities that may have occurred in the inside of the samples during the measurement or at the sample preparation phase. The irregularities by data collection seen for the case of the TCE were further addressed to have had a negative impact on the reality studied. The repetition of the test under the same measurement parameters and conditions would allow for a direct comparison between similar tests and to find out whether an abnormality have occurred during one or more tests of the same material.

With the results available, very interesting conclusions have been retrieved. The whole data collection for each material can be found at the end of this document in the Appendix.

Component	H-L Ratio	Decay
TCE	223,54	99,55%
SA	18,69	94,65%
HCA	18,62	94,63%

Figure 62. Comparison of varying behavior of the three materials over temperature

The TCE experiences a higher order of change than the two adhesives. Nonetheless, the two other components also exhibit a varying mechanical behavior of certain degree within the temperature range of interest. This substantial change in the storage modulus suggests that these materials could have a potential impact on how the cell module handles vibrations under different operational conditions. Although the quantifiable impact is not possible to be addressed with such experimental analysis, the findings of these analyses provide valuable information to be accounted for at the structural design phase, with special prominence of the TCE. The results of these analyses should not be ignored by the simulation models either, for which a more direct implementation is to be provided.

4.2.5 Overview

With this data, the question on the impact of the temperature on the mechanics of the polymeric materials present in the studied cell module is clarified: within the temperature range of interest, the three cell module's components experience a significant change in their dynamic mechanical properties, which is seen even at temperatures not necessarily much wider apart from each other.

The results retrieved from the analysis of the DMA data show a substantial decrease in the magnitude of the storage modulus of all three material, with special prominence from the TCE. The stiffness of these polymers is highly affected by the influence of the environmental temperature and this can affect their in-service performance, depending on the temperature conditions in the surroundings. By higher temperatures, these materials might not possess the stiffness and rigidity for which they were designed, and this needs to be carefully considered at the design phase.

As for the dynamic E-Moduli, some other similar mechanical properties from this type of materials may be highly affected as well by the influence of temperature. A further investigation of the influence on other properties seem very interesting for a more complete description of the yet unknown in-service performance.

The temperature range of interest collects very valuable information from all three tests that can be addressed to the parameterization in some simulation tests for which the mechanical properties of these materials can be very relevant, as well as for some other types of experiments with a practical duty.

5. CONCLUSIONS

5.1 GENERAL FINDINGS

The impact that temperature, as described as one of the three main influencers that alter mechanical performance, has on the mechanics of a state-of-the-art cell module is successfully addressed within this work. The influence of the other two main factor, the SOC and the SOH, was entirely eliminated by the use of a “dummy-module”, in which no electric energy is stored.

The initial hypothesis on the qualitative effect that temperature has on the vibrating behavior of the studied cell module has been asserted by means of modal analysis. Within the temperature range imposed by mobility standards, which apply to the design specifications of such components in the automotive industry, the results show the differences in the vibrating dynamics that the cell module exhibit. The lower the temperature of the module’s environment, the stiffer the behavior that the studied polymeric components exhibit and less prone the module is to be excited. By higher temperatures, the opposite occurs and should be therefore the focus of study at the design phase. This is addressed by the natural frequencies of the module. This work has proven that the natural frequency of the first mode of vibration drops by an increase in temperature. The trend is seen within the whole temperature range of interest, without any discrepancy or exception within the measured temperatures.

A careful analysis of the components within the studied module exposed three elements with the potential of being greatly affected by the effect of temperature: a tolerance compensator foam, the TCE; and two adhesives, the SA and the HCA. The potential effect of temperature on the mechanical properties of these three elements was justified by polymer characterization and analyzed by means of DMA. The TCE was the element that displayed the greatest change in the measured magnitude of the dynamic modulus. The effect of temperature on the two adhesives is also considered to be very substantial.

The implementation of both techniques provided valuable information on the effect that the operational temperature has on the mechanical response and vibrating behavior of the cell module and of three specific components. The results are conclusive at both module and material level. The connection between the findings on both techniques is completely justified by the relationships between the dynamic properties of materials and the vibrating behavior of structures, as addressed by the theory. However, this connection does not imply that the behavioral changes experienced by the cell modules are entirely neither mostly justified by the effect of temperature on the dynamic stiffness of the three studied components. This work demonstrates how the changes in the mechanical properties of the three studied components, altered by the effect of temperature, could impact the vibrating behavior of the whole structure in a qualitative perspective.

The effects of the temperature on real modules could only be addressed by the testing of charged modules. The results of this work would surely complement the results of testing charged modules.

The findings in this work are believed to provide valuable information to many processes involved in the design phase of cell modules and potentially other components in an electric vehicle. The mechanical response of the polymeric materials present in a module under the influence of temperature should be of great consideration for the analysis of the vibrational behavior at the design phase, as clearly justified in this work. This effect on the mechanical magnitudes should be accounted for when approving the structural role of such polymeric materials within the module architecture.

5.2 WORK METHODOLOGY

5.2.1 Module level

The implementation of modal analysis by means of impact testing allowed for a successful examination of the effect of temperature within the range of interest. The chosen measurement configuration of parameters, software, equipment and the measurement grid allowed to quantify the differences on the natural frequencies at -20°C , 0°C , $+20^{\circ}\text{C}$ and $+40^{\circ}\text{C}$ through experimentation in a climatic chamber.

The roving hammer testing technique allowed to completely characterize the mode shapes of the studied module in all four temperature scenarios. The hammer size and tip selection ensured a proper excitation of all mode shapes of the module up to the maximum frequency of interest of 2.5kHz. The parameter configuration in PAK, as well as the design of the measurement grid had a positive impact on the accuracy of the results.

The design of test frame and supporting mechanism ensured a proper differentiation of the natural frequencies of the module from those of the setup, and showed no negative effect on the legitimacy of the results. The separation between the highest frequency of the entire setup and the lowest natural frequency of the module was found to be greater than 100Hz in all temperature scenarios [HOOP15].

Three measuring strategies for the EMA experiments in the climatic chamber were designed. The feasibility of the point-by-point with door opening strategy was validated for the studied temperature range and allowed to assert the qualitative frequency-temperature relationship of the modules. The use of thermocouples to record all variations of temperature during the measurements, and analyzed with TurboLab, showed a very small level of temperature dispersion during the measurements, absolutely acceptable for the purposes of the analysis.

5.2.2 Material level

Three polymeric materials were detected to be present in the cell module architecture in the form structural elements and the effect of the temperature was analyzed by means of DMA. All three materials were correctly analyzed within a temperature range of -40°C to $+50^{\circ}\text{C}$. The temperature-sweep experiments were performed under a tensile testing fashion and provided the magnitude of the dynamic E-Modulus along the whole range.

Prior to the experiments, some testing specimens were prepared for the SA and HCA cases. The experimental guidelines were proven to work, as the samples retrieved from the process were then correctly tested without showing any misbehavior.

5.3 RESULTS

5.3.1 Module level

The first natural frequency of the cell module was successfully analyzed at the four studied temperature scenarios. The values of the frequencies were computed by means of the analysis of variance (ANOVA) on the FRF of each measurement point: for each temperature, the total of the natural frequencies of each point were averaged and the dispersion calculated by means of the standard deviation.

The results show a steady decrease of the frequency as the temperature goes up. The degree of this decay can be most accurately approximated by a decreasing exponential curve.

The ANOVA shows a greater dispersion of the data as temperature goes down. Below 20°C, the standard deviation increases substantially, as seen in [Figure 51](#). This can be due to the greater loss of heat when performing the experiments at such extreme temperatures, at which the difference with the temperature outside the climatic chamber is maximum. The temperature scenario at -20°C shows a large degree of deviation, which worsens the regression adjustment of the other three measurements. This suggests that cooler temperatures might not be feasible to be tested with the technique elaborated in this work, due to an unacceptably high degree of dispersion of the data.

The initial hypothesis on the effect of temperature on the vibrating behavior of the cell module is asserted by these results. The module is more prone to exhibit resonance problems when the temperature of the environment increases. Following the trend, temperatures above 40°C could lead to serious mechanical damage and resonant failures when the road-induced vibrations are found to be near to 150Hz [HOOP15].

5.3.2 Material level

All three materials show a critical decrease in the magnitude of the storage modulus, with a prominent behavior for the TCE. The temperature range of analysis was shortened by 10°C at each end in relation to the temperature range of test, due to the transient phase that might occur at the beginning and at the end of a DMA experiment.

The highest and lowest values of the storage modulus are found at the lowest and highest temperatures, respectively. The three materials exhibit a continuous decay of this magnitude with no exception. The shape of these curves is found to be an exponential decrease with high decay and early stabilization at the TCE and SA and an exponential decrease with earlier stabilization and late, quick decay for the HCA. These are explanatory of the type of polymer these materials are classified to in relation to their thermal behavior.

In order to analyze the significance of the results, the high-to-low ratio was computed for all three materials, which indicates the ratio of the highest to the lowest storage modulus within the range of interest (value at the lowest temperature to the value at the highest temperature). The percentage of decay between the two extreme values was also computed. These two numbers are certainly a representative measure to illustrate the changing behavior by the effect of temperature.

The two adhesives exhibit very similar behavior in relative values: a decay of almost 95% and a high-to-low ratio of 18.69 for the SA and 18.62 for the HCA. The most remarkable behavior is displayed by the TCE, whose measurement magnitudes are one order above the other two materials. The high-to-low ratio reaches a value higher than 220, which can also be interpreted as a decay of over a 99.5%.

5.4 FURTHER WORK

An immediate complement to this work would be the repetition of the impact tests on the same module architecture that was used in this project, with the same testing equipment, parameters and measurement grid and at the same four temperature scenarios. The results of this second set of tests could confirm the results provided in this work, as well as the feasibility of the testing strategy when done by other operator. A third set of tests would eliminate any disbelief. The additional set of tests could validate the qualitative frequency-to-temperature relationship as proven with this work. A confirmation of the quantitative accuracy of the results might also be possible by performing further tests.

If more tests of the exact same component that was tested in this work were possible, a new set of tests performed on the used module could provide some insight on the fatigue and general degradation effects that the performed tests at extreme temperatures have on the modules and if their vibrating behaviors were to change. Being EMA a non-destructive test, the reutilization of the tested modules for further but similar testing would be feasible as a more inexpensive testing opportunity if no effect of degradation on the module's mechanics was showcased.

By carrying out the same impact tests on different module architectures, a positive source of results would confirm the validation of the here implemented experimental modal analysis as a successful technique to testing the vibrating behavior of cell modules, which would contribute to the robustness of the method.

The addition of a fifth temperature scenario at -40°C to the EMA set of tests would complete the operational temperature range covered by the Transportation of Dangerous Goods Standard [UNSE38]. The applicability of the impact testing strategy in the climatic chamber at this extreme temperature would need for confirmation. The results on the natural frequency of the first mode of vibration would result in the addition of a fifth point to the computed trend, which would end up in the validation or in a discrepancy with the expected position of this temperature by following the trend. The results on this temperature should display the lowest first natural frequency of all five scenarios.

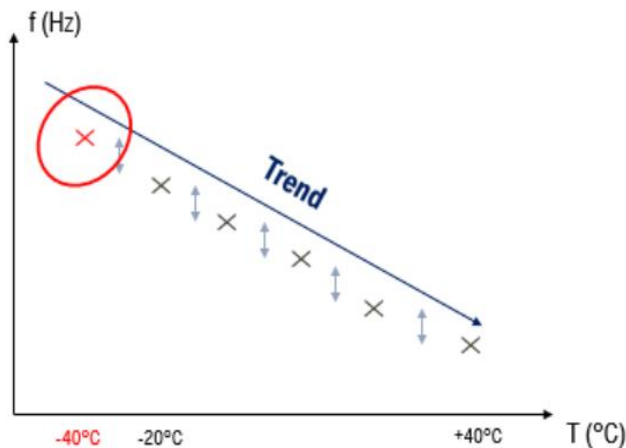


Figure 63. Expected result of the -40°C EMA test

The analysis of the temperature effect on the successive natural frequencies of the modules would clarify whether the exact same effects are also found at the higher frequencies. The analysis of the other natural frequencies retrieved from the collected data would explain how the whole block of frequencies varies with temperature. The displacement of the whole block along the frequency axis is the suggested hypothesis to his analysis, that is, the temperature have a similar effect on all excited set of frequencies.

A more accurate approach to describing the vibrating behavior of cell modules by means of modal analysis would imply the use of real, charged modules. In case the charged modules exposed the same sort of results, the here described method would serve as a less expensive way

to testing the vibrating behavior of real cell modules. Should there be a significant quantitative difference, the isolation test of the charged cells should also be included. DMA or some similar rheology test are for this purpose here suggested.

With respect to material experimentation, it would be interesting to analyze the effect of temperature on other mechanical properties for each material. The effect on the shear modulus (G) could provide more insight to this end, due to similar the relationship of this magnitude to energy transmission that the studied modulus has. This would be especially interesting for the behavior of the TCE, which exhibited the greatest change. The performance of DMA compression experiments is also desired to be addressed. The implementation of tensile testing on the three studied materials at some specific temperatures, for instance, the temperatures tested by means of EMA, would allow for a comparison between the static and the dynamic elastic moduli.

Extending the temperature range of the DMA to a certain degree would help to illustrate more accurately the transition phases of the materials. Even though this was not the initial goal of the DMA experiments performed, it would provide more information on how the material behaves, which could be accounted for at the design phase of the modules.

To complement the analysis of other module architectures, the polymeric materials present within these structures could also be tested by means of DMA, following the process implemented in this work.

As this work could not provide any insight on the effect of the relative humidity (RH) level on the vibrating response of cell modules, an investigation on this topic would complement the findings in this work. However, the designed point-by-point with door opening measuring strategy implemented for the EMA experiments would not work out for the study of the effect of RH. The closed door measuring mechanism would be more feasible to this end.

Finally, the likely volume variation experienced by certain components of the modules with the increase in temperature is also considered a potential explanation of the different vibrating behaviors seen at the module level. Therefore, the quantification and analysis of these structural changes is also considered a further study subject.

6. BIBLIOGRAPHY

- [AVIT01] Avitabile, P. "Experimental modal analysis - A simple non-mathematical presentation". Sound & Vibration Magazine, vol 35. University of Massachusetts. 2001.
- [BABO18] Babones, S. China Could Be The World's First All Electric Vehicle Ecosystem. [online] Forbes.com. 2018. Available at: <https://www.forbes.com/sites/salvatorebabones/2018/03/06/china-could-be-the-worlds-first-all-electric-vehicle-ecosystem/#33f85de2130f> [Accessed Aug. 2019].
- [BILL84] Billmeyer F. W., "Textbook of Polymer Science" 3rd edition, John Wiley and Sons. New York. 1984
- [BILO11] Bilošová, A. "Modal Testing". Techniká universita Ostrava. 2011. Available at: https://www.fs.vsb.cz/export/sites/fs/330/content/files/EMA_skriptaEN.pdf
- [DEAL83] Dealy, J. "Rheometers for molten plastics". Van Nostrand Reinhol. New York. 1983
- [ENGI19] Engineering ToolBox. "Young's Modulus of Elasticity for Metals and Alloys". 2014 [online] Available at: https://www.engineeringtoolbox.com/young-modulus-d_773.html [Accessed Aug 2019].
- [FERR80] J. Ferry, "Viscoelastic Properties of Polymers", 3rd ed., Wiley, New York. 1980
- [FFT19] FFT, F. "FFT". [online] Nti-audio.com. 2019. Available at: <https://www.nti-audio.com/de/service/wissen/fast-fourier-transformation-fft> [Accessed Aug. 2019].
- [GOWA15] Gowarikar, V.R. "Polymer Science", Second Edition. New Age International, New Delhi. 2015.
- [GUIL00] Guillaume P., "Modal Analysis", Technical Notes Research Groups Acoustics and Vibration, Vrije Universiteit Brussel, Pleinlaan 2, B-1050 Brussel, Belgium. 2000
- [HOOP14] Hooper, J. and Marco, J. "Characterising the in-vehicle vibration inputs to the high voltage battery of an electric vehicle". Journal of Power Sources, vol 245, pp 510-519. University of Warwick, Coventry, UK. 2014
- [HOOP15] Hooper, J. and Marco, J. "Experimental modal analysis of lithium-ion pouch cells". Journal of Power Sources. vol 285, pp 247-259. University of Warwick, Coventry, UK. 2015
- [JANC16] Janca A. "Small punch test evaluation methods for material characterization" Journal of Nuclear Materials. vol. 481, pp 201-213. 2016
- [KISS02] Kissel T., "Advanced polymer chemistry – a problem solving guide". European Journal of Pharmaceutics and Biopharmaceutics, vol 53. New York. 2002
- [KOKA10] Kokavezc, J. "Modalanalyse", Messtechnik der Akustik. Springer Berlin Heidelberg. 2010

Bibliography

- [KORT13] Reiner Korthauer, 2013, „Handbuch Lithium-Ionen Batterien“ (Springer Vieweg)
- [MCCA19] McCarthy, N. “Infographic: The Evolution Of U.S. Electric Vehicle Charging Points”. [online] Statista Infographics. 2019. Available at: <https://www.statista.com/chart/13466/the-evolution-of-us-electric-vehicle-charging-points/> [Accessed Aug. 2019].
- [MENA08] Menard, K. “Dynamic mechanical analysis”. Boca Raton, FL: CRC Press. 2008
- [MUDA12] Mudassir M., “Application of pilot models to study trajectory based manoeuvres”, AIAA Modelling and Simulation Technologies Conference. 2012
- [POPP18] Popp, H., Glanz, G., Alten, K., Gocheva, I., Berghold, W. and Bergmann, A. “Mechanical Frequency Response Analysis of Lithium-Ion Batteries to Disclose Operational Parameters”. Energies, vol 11No 3, pp 541. Vienna. 2018
- [POYN09] Poynting J. H., “The wave motion of a revolving shaft, and a suggestion as to the angular momentum in a beam of circularly polarized light”, Proceedings of the Royal Society, vol 82, p 546. London. 1909
- [UN38] European Union. “Recommendations on Transportation of Dangerous Goods, 5th revised edition”.
- [VPSO19] VP Solar. Electric cars market statistics. 2019 [online] Available at: <https://www.vpsolar.com/en/electric-cars-market-statistics/> [Accessed Aug. 2019].
- [XU16] Xu, J., Liu, B. and Hu, D. “State of Charge Dependent Mechanical Integrity Behavior of 18650 Lithium-ion Batteries”. Scientific Reports, vol 6 . Beijing 2016

7. APPENDIX

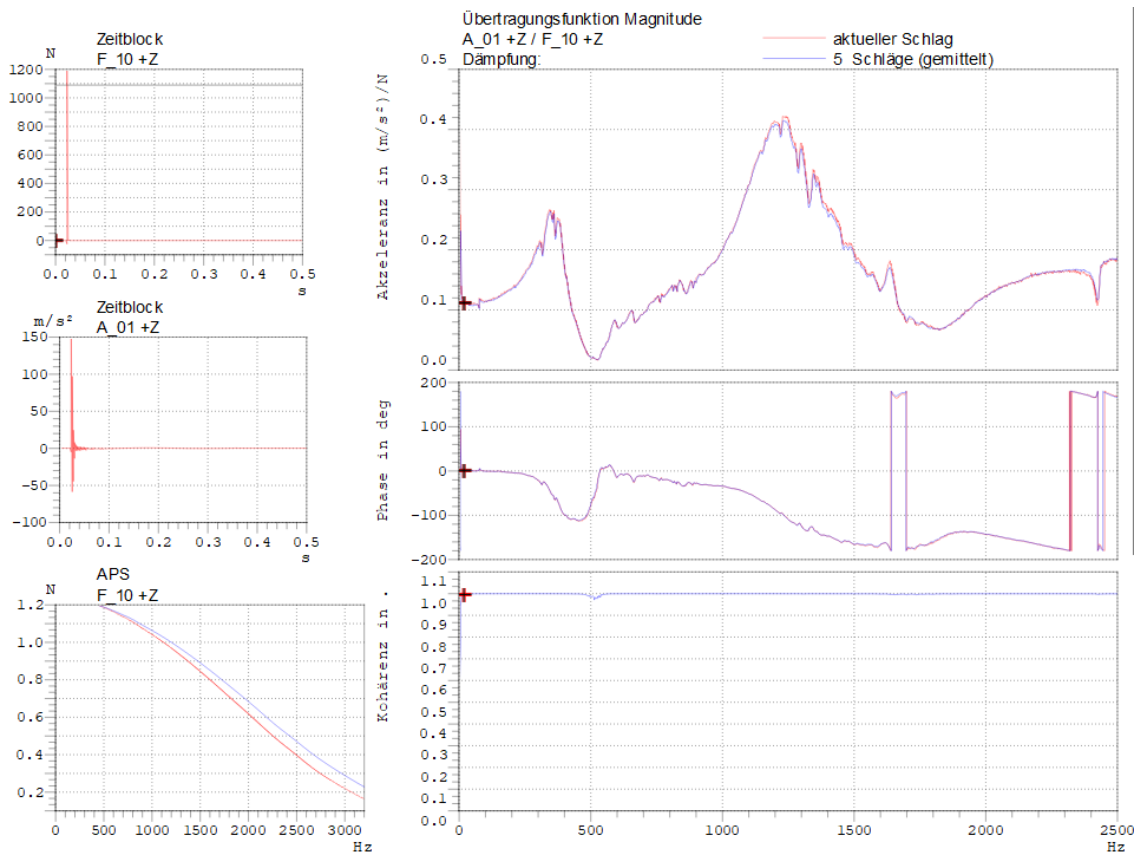


Figure 64. FRF and CF of the measurement at -20°C

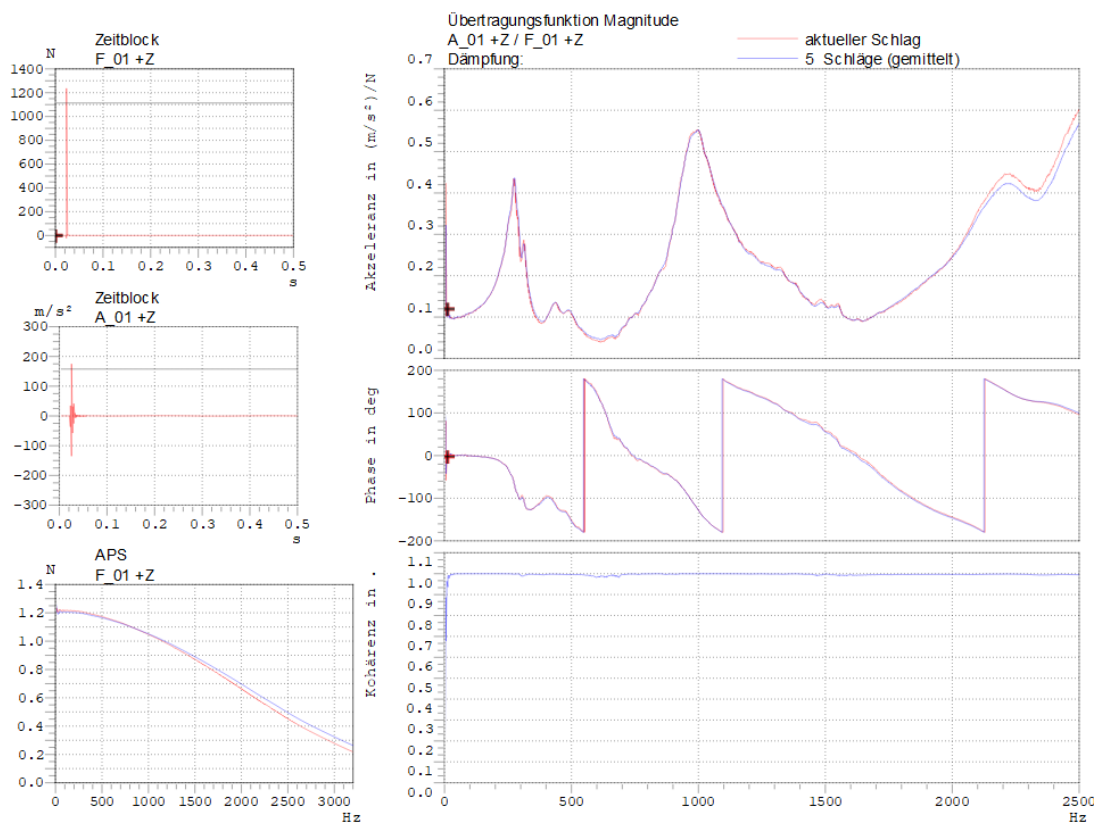


Figure 65. FRF and CF of the measurement at 0°C

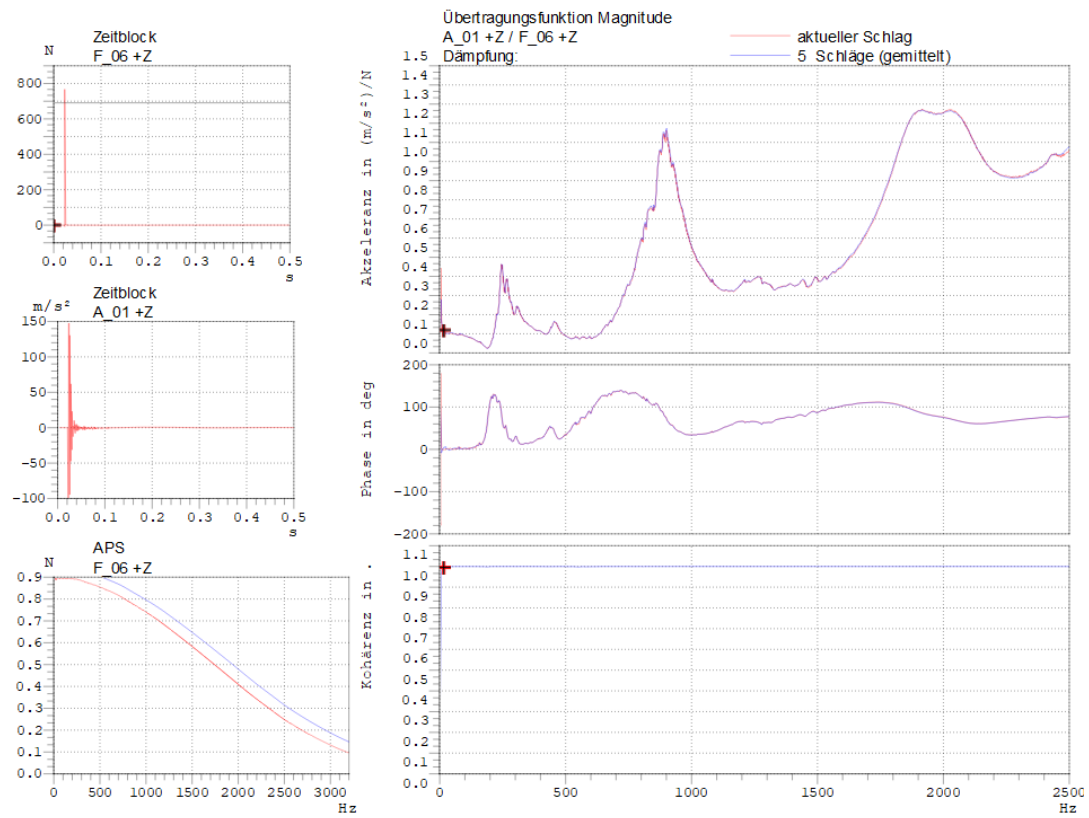


Figure 67. FRF and CF of the measurement at +20°C

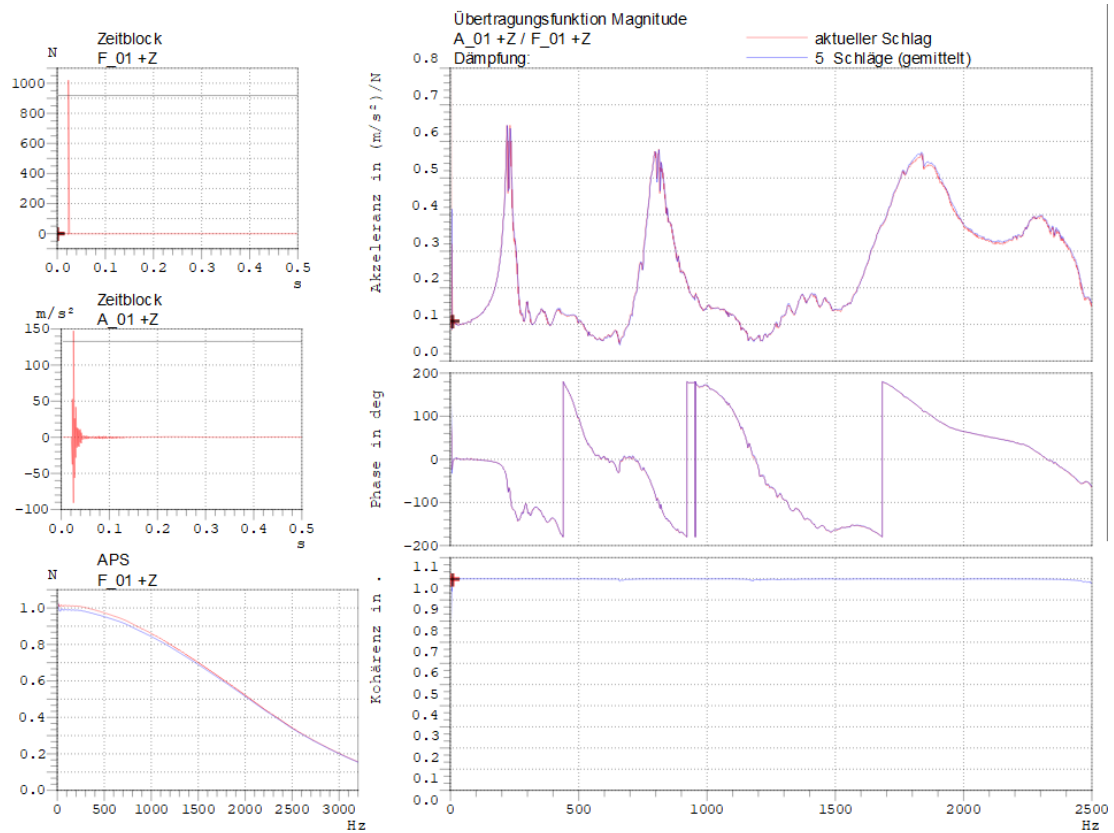


Figure 66. FRF and CF of the measurement at +40°C

Force Transducer		25N	
Type of Test		Tension	
		Temperature Sweep	
Frequency		10Hz	
Temperature	Range	-50°C to +60°C	
	Tolerance	2.0°C	
Heat rate		2.0K/min	
Temperature increment		2.0°C	
Preliminary temperature		1.0°C	
Soak time		300s	
Load between measurements		Remove load	
Sample / Specimen	Shape	Prismatic	
	Width	10mm	
	Thickness	1.1mm	
Static Load	Strain	1.00%	
	limit	18N	
	tolerance	0.10N	
	static average	100	
Dynamic Load	control time	1s	
	Strain	0.20%	
	Limit	7N	
	Tolerance	0.02%	
Contact Force	Static average	20	
	Force	0.10N	
	tolerance	0.06N	
	Max. displacement of Lo	10.0mm	
		Max. speed of cross bar	40.0mm/s

Table 9. DMA Parameters of the TCE experiment

Force Transducer		500N
Type of Test		Tension
		Temperature Sweep
Frequency		10Hz
Temperature	Range	-50°C to +60°C
	Tolerance	2.0°C
Heat rate		2.0°K/min
Temperature increment		2.0°C
Preliminary temperature		0.5°C
Soak time		1200s
Load between measurements		Remove load
Sample / Specimen	Shape	Prismatic
	Width	9,88mm
	Thickness	4.44mm
Static Load	Strain	0.30%
	Limit	350N
	Tolerance	0.03%
	Static average	100
	Control time	1s
Dynamic Load	Strain	0.30%
	Limit	150N
	Tolerance	0.01%
	Static average	40
Contact Force	Force	1.00N
	Tolerance	0.50N
	Max. displacement of Lo	5.0mm
	Max. speed of cross bar	40.0mm/s

Table 10. DMA parameters of the SA experiment

Force Transducer		500N
Type of Test		Tension
		Temperature Sweep
Frequency		10Hz
Temperature	Range	-50°C to +60°C
	Tolerance	2.0°C
Heat rate		2.0°K/min
Temperature increment		2.0°C
Preliminary temperature		0.5°C
Soak time		1200s
Load between measurements		Remove load
Sample / Specimen	Shape	Prismatic
	Width	10.13mm
	Thickness	4.15mm
Static Load	Strain	0.30%
	limit	350N
	Tolerance	0.03%
	Static average	100
	Control time	1s
Dynamic Load	Strain	0.30%
	limit	150N
	tolerance	0.00%
	static average	40
Contact Force	Force	1.00N
	Tolerance	0.50N
	Max. displacement of Lo	5.0mm
	Max. speed of cross bar	40.0mm/s

Table 11. DMA Parameters of the HCA experiment

Key Technical Data

NETZSCH

	EPLEXOR® 25 N	EPLEXOR® 100 N	EPLEXOR® 150 N	EPLEXOR® 500 N
Dynamic force range	± 25 N (50 N)*	± 100 N (200 N)*	± 150 N (300 N)*	± 500 N (1000 N)*
Static force range	150 N	150 N Optional: 1500 N	150 N Optional: 1500 N	500 N Optional: 1500 N
Dynamic strain	± 1.5 mm (3 mm)*	± 1.5 mm (3 mm)*	± 1.5 mm (3 mm)* Optional: ± 3 mm (6 mm)*	± 1.5 mm (3 mm)* Optional: ± 6 mm (12 mm)*
Static displacement	Up to 60 mm	Up to 60 mm	Up to 60 mm	Up to 60 mm
Frequency range	0.001 Hz to 100 Hz Optional ranges: 0.0001 to 200 Hz	0.001 Hz to 100 Hz Optional ranges: 0.0001 to 200 Hz	0.001 Hz to 100 Hz Optional ranges: 0.0001 to 200 Hz	0.001 Hz to 100 Hz Optional ranges: 0.0001 to 200 Hz
Temperature	RT to 500°C Optional**: -160°C to 500°C, RT to 1000°C/1500°C	RT to 500°C Optional**: -160°C to 500°C, RT to 1000°C/1500°C	RT to 500°C Optional**: -160°C to 500°C, RT to 1000°C/1500°C	RT to 500°C Optional**: -160°C to 500°C, RT to 1000°C/1500°C
HYGROMATOR®	Humidity range: 5% rH to 95% rH; Temperature range: 5°C to 95°C	Humidity range: 5% rH to 95% rH; Temperature range: 5°C to 95°C	Humidity range: 5% rH to 95% rH; Temperature range: 5°C to 95°C	Humidity range: 5% rH to 95% rH; Temperature range: 5°C to 95°C
UV accessory	Optional	Optional	Optional	Optional

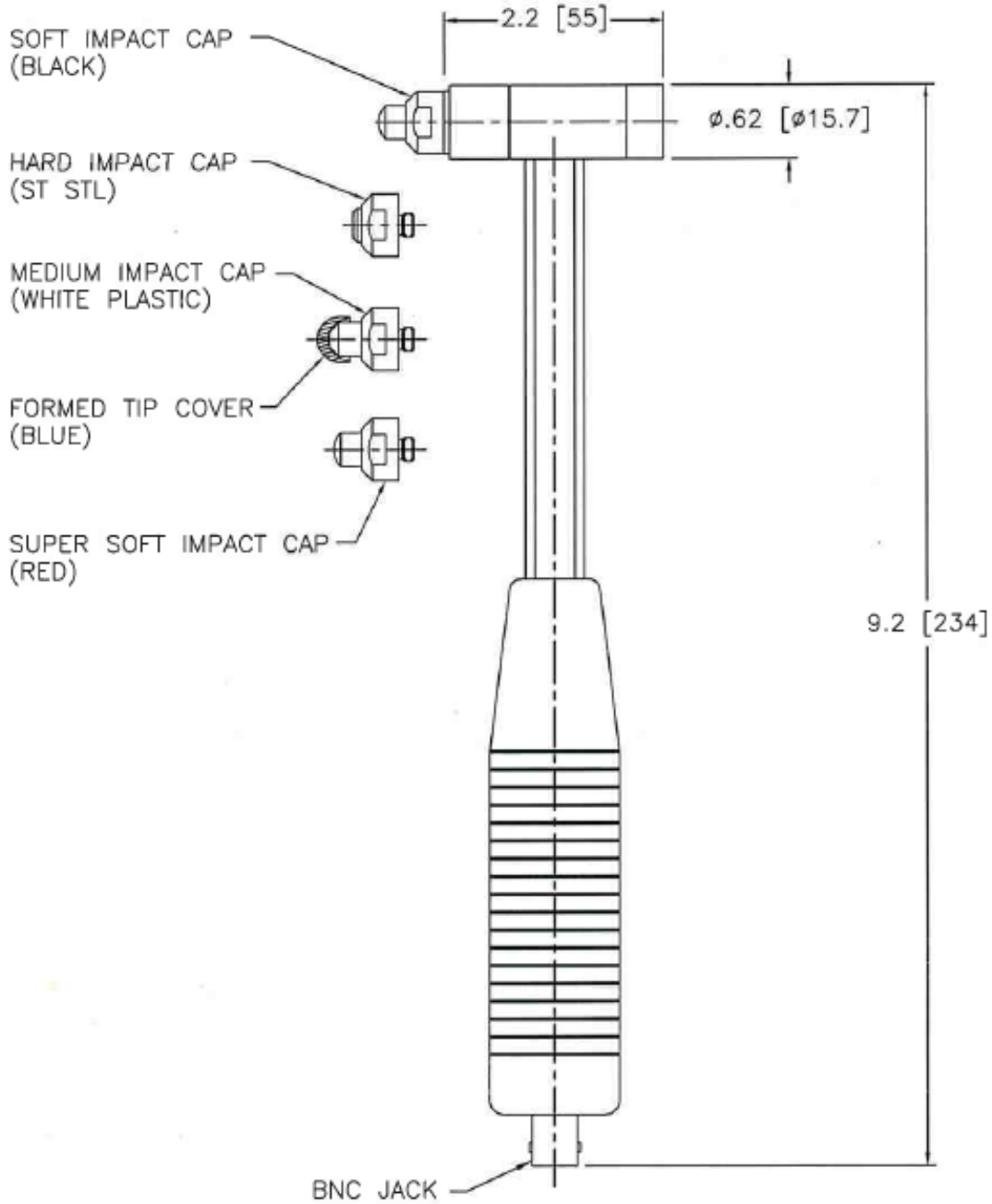
Figure 68. NETZSCH GABO EPLEXOR Series technical data

086-3020-95

PCB Piezotronics Inc. claims proprietary rights in the information disclosed herein. Neither it nor any reproduction thereof will be disclosed to others without written consent of PCB Piezotronics Inc.

REVISIONS

REV	DESCRIPTION	ECN	DATE	APP'D
E	REVISED PER ECN	22370	6/22/05	DM
F	UPDATED NOTES	25626	4/6/07	FB 4/6/07



UNLESS SPECIFIED TOLERANCES		DRAWN	MFG	PCB PIEZOTRONICS™	
DIMENSIONS IN INCHES	DIMENSIONS IN MILLIMETERS [IN BRACKETS]	87-JS 4/23/07	KY 4/23/07	3425 WALDEN AVE. DEPEW, NY 14043	
DECIMALS XX ±.03	DECIMALS X ±0.8	CHK'D EJS 4/23/07	ENGR CCR 4/23/07	(716) 684-0001 EMAIL: SALES@PCB.COM	
XXX ±.010	XX ±0.25	APP'D EJS 4/23/07	SALES KCA 4/23/07	CODE	DWG. NO.
ANGLES ±2 DEGREES	ANGLES ±2 DEGREES	TITLE		52681	086-3020-95
FILLETS AND RADII .003 - .005	FILLETS AND RADII [0.07 - 0.13]	OUTLINE DRAWING MODALLY TUNED IMPULSE HAMMER		SCALE: .75x	SHEET 1 OF 1
DD011 REV. C 01/21/03					

Figure 69. Engineering drawing of the Piezotronics 086C03 Impact Hammer


Model Number 086C03	ICP® IMPACT HAMMER		Revision: L ECN #: 32387
Performance	ENGLISH	SI	OPTIONAL VERSIONS Optional versions have identical specifications and accessories as listed for the standard model except where noted below. More than one option may be used. T - TEDS Capable of Digital Memory and Communication Compliant with IEEE P1451.4 TLD - TEDS Capable of Digital Memory and Communication Compliant with IEEE 1451.4
Sensitivity(± 15 %)	10 mV/lbf	2.25 mV/N	
Measurement Range	± 500 lbf pk	± 2224 N pk	[1]
Resonant Frequency	≥ 22 kHz	≥ 22 kHz	
Non-Linearity	≤ 1 %	≤ 1 %	[1]
Electrical			
Excitation Voltage	20 to 30 VDC	20 to 30 VDC	[1]
Constant Current Excitation	2 to 20 mA	2 to 20 mA	
Output Impedance	<100 ohm	<100 ohm	[1]
Output Bias Voltage	8 to 14 VDC	8 to 14 VDC	
Discharge Time Constant	≥ 2000 sec	≥ 2000 sec	
Physical			NOTES: [1] Typical. [2] See PCB Declaration of Conformance PS068 for details.
Sensing Element	Quartz	Quartz	SUPPLIED ACCESSORIES: Model 081B05 Mounting Stud (10-32 to 10-32) (2) Model 084A08 Extender - Steel, 0.6" Diameter (1) Model 084B03 Hard Tip- Hard (S.S) (1) Model 084B04 Hammer Tip- Medium (White Plastic) (1) Model 084C05 Hammer Tip- Soft (Black) (2) Model 084C11 Hammer Tip- Supersoft (Red) (2) Model 085A10 Vinyl Cover For Medium Tip (Blue) (2) Model HCS-2 Calibration of Series 086 instrumented impact hammers (1)
Sealing	Epoxy	Epoxy	
Hammer Mass	0.34 lb	0.16 kg	
Head Diameter	0.62 in	1.57 cm	
Tip Diameter	0.25 in	0.63 cm	
Hammer Length	8.5 in	21.6 cm	
Electrical Connection Position	Bottom of Handle	Bottom of Handle	
Extender Mass Weight	2.6 oz	75 gm	
Electrical Connector	BNC Jack	BNC Jack	
			Entered: <i>JH</i> Engineer: <i>SJS</i> Sales: <i>ggm</i> Approved: <i>EB</i> Spec Number:
			Date: <i>2/24/10</i> Date: <i>12/8/09</i> Date: <i>2/17/10</i> Date: <i>2/17/10</i> 15273
<p>All specifications are at room temperature unless otherwise specified. In the interest of constant product improvement, we reserve the right to change specifications without notice.</p> <p>ICP® is a registered trademark of PCB Group, Inc.</p>			<p>PCB PIEZOTRONICS™ VIBRATION DIVISION 3425 Walden Avenue, Depew, NY 14043</p> <p>Phone: 716-684-0001 Fax: 716-685-3886 E-Mail: vibration@pcb.com</p>

Figure 70. Data sheet of the Piezotronics 086C03 Impact Hammer

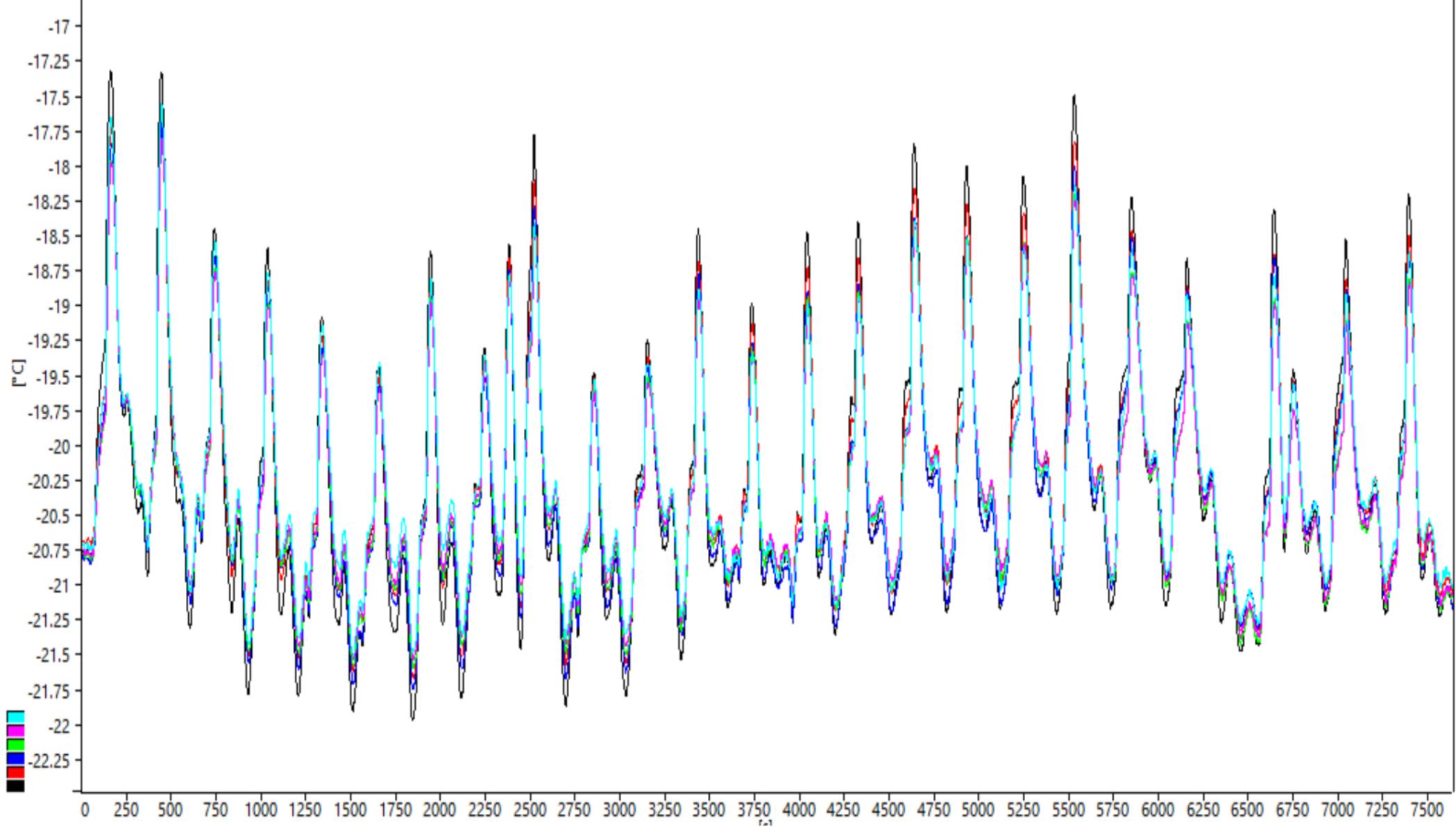


Figure 71. Temperature data record of the EMA experiment in the climatic chamber at -20°C

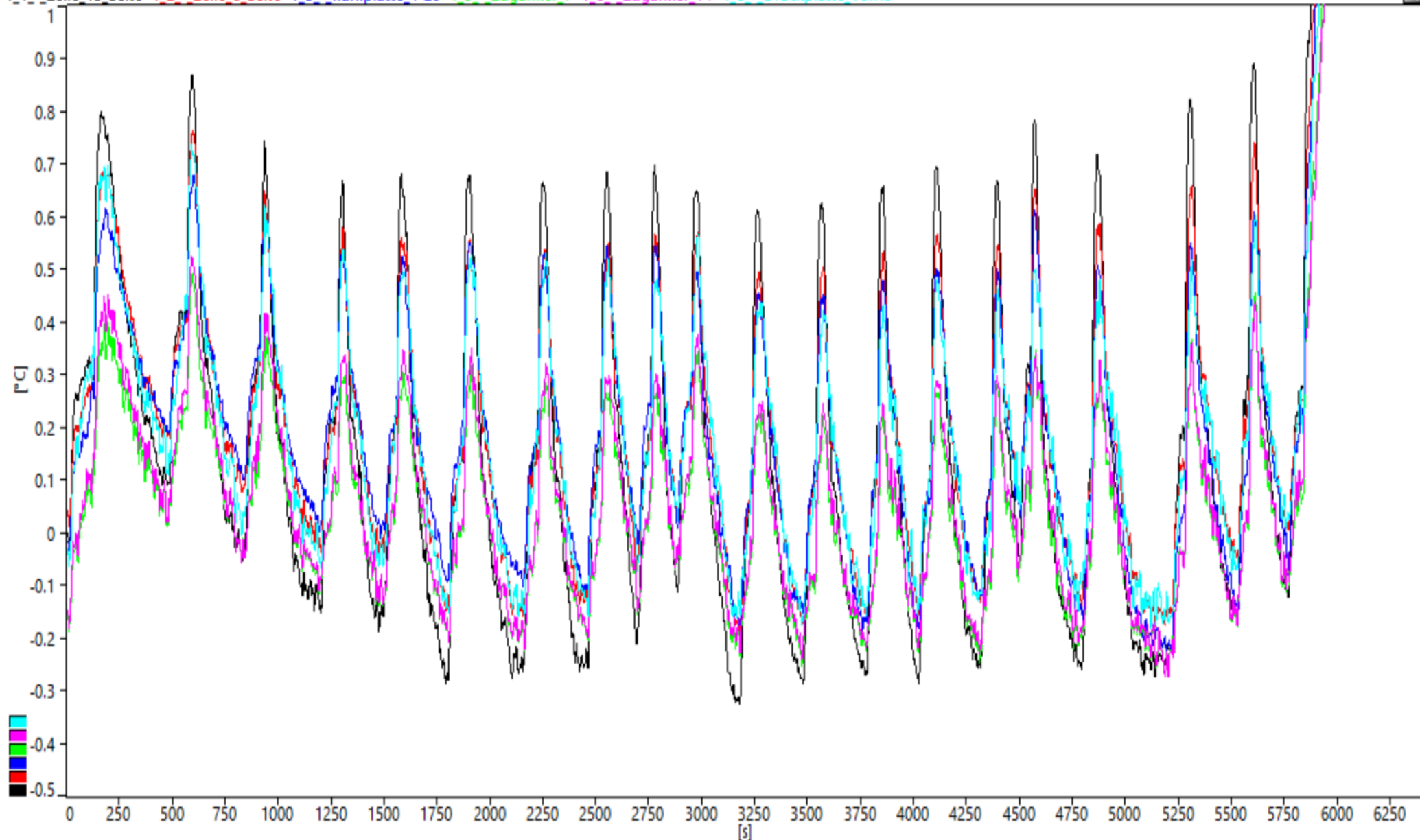


Figure 72. Temperature data record of the EMA experiment in the climatic chamber at 0°C

T 1 - Zelle 15 Seite T 2 - Zelle 6 Seite T 3 - Kühlplatte 1-20 T 5 - Zuganker 7 T 6 - Zuganker 14 T 8 - Druckplatte Vorne

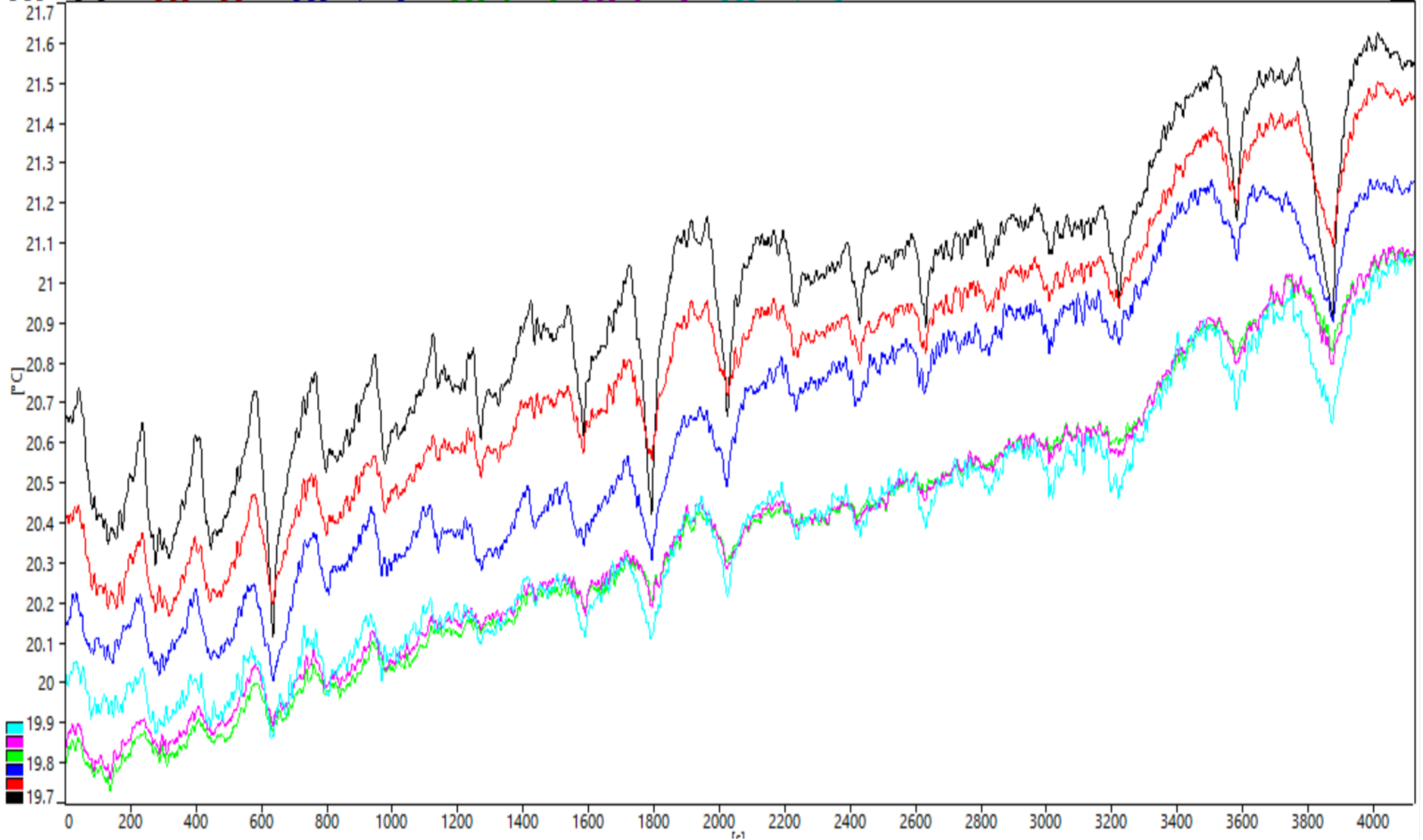


Figure 73. Temperature data record of the EMA experiment in the climatic chamber at +20°C

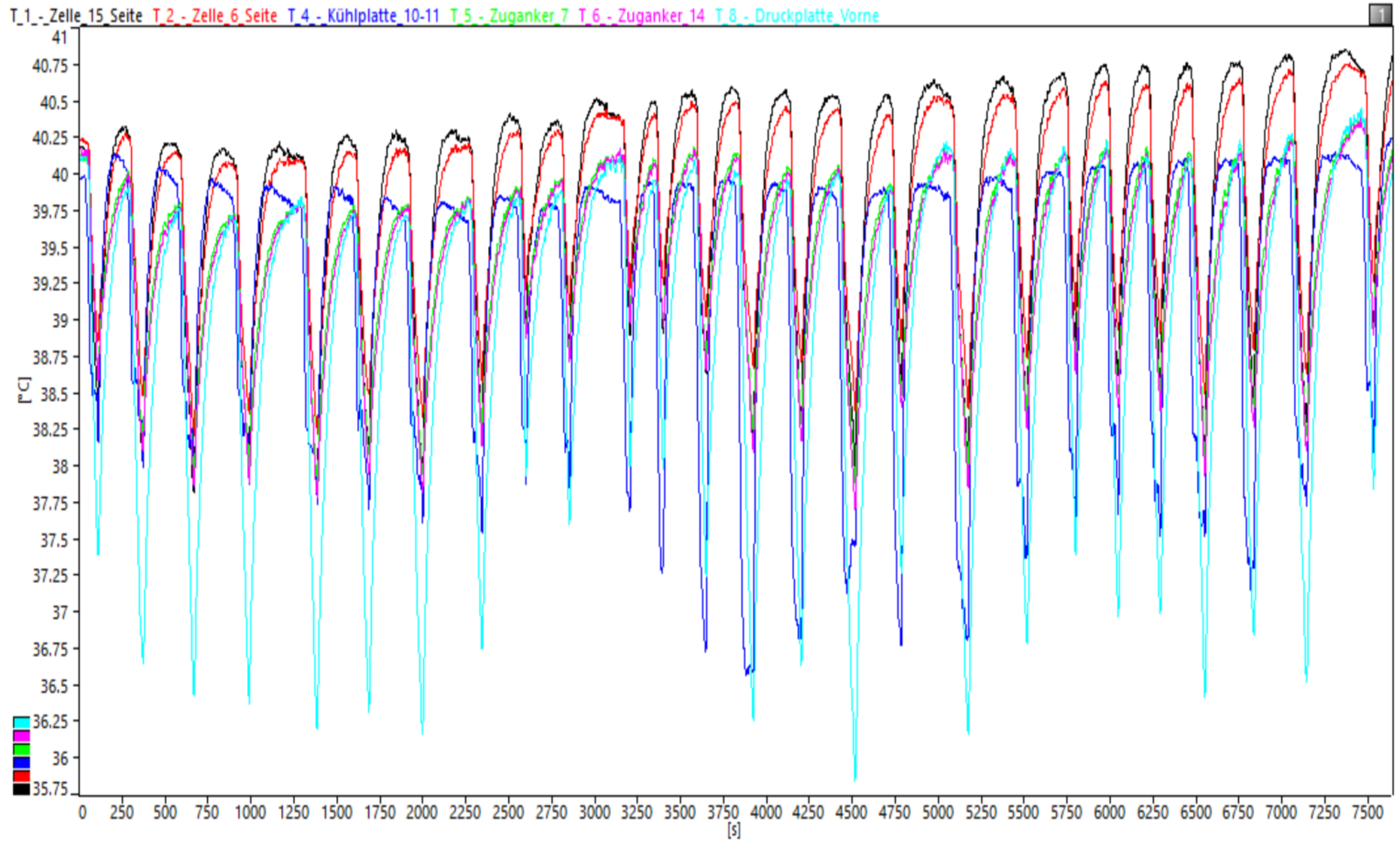


Figure 74. Temperature data record of the EMA experiment in the climatic chamber at +40°C

Meas. Point	F stat	Strain stat	Stress stat	Lo	Lm	F dyn	Strain dyn	Stress dyn	delta Time	T	E'	E''	IE*I	tan delta	F cont
	N	-	-	-	-	N	-	-	s	°C	-	-	-	-	N
1	-16,935	0,9945	55,6950	0,9594	0,9593	6,984	0,7119	76,8997	0,00	-48,9	121,7500	39,0335	108,0169	0,1788	-0,1088
2	-16,728	0,9939	55,0135	0,9611	0,9611	7,038	0,7494	77,4943	62,17	-48,1	116,4011	38,8932	103,4089	0,1864	-0,1369
3	-16,189	0,9935	53,2416	0,9616	0,9615	6,978	0,7873	76,8398	74,77	-46,6	109,7040	38,2433	97,6039	0,1944	-0,1334
4	-13,755	0,9942	45,2369	0,9622	0,9622	7,048	0,9044	77,6050	60,62	-43,9	96,0793	36,8290	85,8070	0,2138	-0,1392
5	-10,497	0,9969	34,5224	0,9626	0,9626	6,540	1,0028	72,0117	73,13	-40,6	79,9826	34,1751	71,8089	0,2383	-0,1506
6	-8,554	0,9952	28,1305	0,9632	0,9631	5,799	0,9998	63,8546	73,06	-38,5	70,8714	32,3365	63,8680	0,2545	-0,1826
7	-6,385	0,9923	21,0000	0,9638	0,9637	5,169	1,0546	56,9233	72,87	-35,9	59,5698	29,5282	53,9770	0,2765	-0,1641
8	-4,493	0,9972	14,7776	0,9644	0,9644	4,273	1,0537	47,0502	72,81	-33,1	48,9149	26,6874	44,6538	0,3043	-0,1802
9	-3,373	0,9947	11,0915	0,9653	0,9652	3,468	0,9982	38,1877	73,02	-31,0	41,5851	24,6922	38,2579	0,3312	-0,1975
10	-2,401	0,9988	7,8955	0,9659	0,9659	2,878	1,0178	31,6937	76,42	-28,4	33,4182	22,2820	31,1384	0,3719	-0,1922
11	-1,326	0,9978	4,3616	0,9652	0,9652	1,834	0,9997	20,1947	144,70	-23,5	20,9514	17,5722	20,2009	0,4678	-0,1424
12	-1,129	0,9954	3,7116	0,9678	0,9678	1,454	0,9994	16,0066	76,21	-21,0	16,3124	15,0244	16,0162	0,5137	-0,1978
13	-0,905	0,9984	2,9759	0,9696	0,9696	1,087	0,9997	11,9693	89,93	-18,0	11,9799	11,9518	11,9732	0,5564	-0,1954
14	-0,741	0,9976	2,4367	0,9718	0,9718	0,804	0,9997	8,8502	96,18	-14,8	8,7731	9,1034	8,8526	0,5787	-0,1951
15	-0,472	0,9969	1,5508	0,9716	0,9716	0,439	0,9996	4,8331	224,66	-7,3	4,7925	4,9698	4,8351	0,5784	-0,1480
16	-0,463	0,9987	1,5219	0,9770	0,9770	0,355	1,0008	3,9038	85,27	-4,4	3,8644	4,0153	3,9007	0,5795	-0,1960
17	-0,416	0,9966	1,3669	0,9810	0,9810	0,278	1,0004	3,0560	105,13	-0,9	3,0291	3,1360	3,0548	0,5774	-0,1981
18	-0,363	0,9992	1,1945	0,9837	0,9837	0,204	0,9997	2,2416	165,69	4,4	2,2243	2,2995	2,2424	0,5766	-0,1817
19	-0,270	0,9979	0,8893	0,9854	0,9854	0,116	0,9998	1,2757	297,88	14,6	1,2692	1,2976	1,2760	0,5702	-0,1416
20	-0,294	1,0004	0,9663	0,9931	0,9931	0,103	1,0000	1,1340	72,88	17,0	1,1309	1,1438	1,1340	0,5641	-0,1823
21	-0,304	1,0000	1,0000	1,0000	1,0000	0,091	1,0000	1,0000	76,51	19,7	1,0000	1,0000	1,0000	0,5577	-0,1995
22	-0,299	0,9977	0,9817	1,0062	1,0062	0,082	1,0004	0,9017	87,63	22,6	0,9039	0,8930	0,9013	0,5510	-0,1992
23	-0,291	0,9989	0,9567	1,0114	1,0114	0,072	1,0003	0,7873	106,58	26,1	0,7939	0,7649	0,7871	0,5374	-0,1975
24	-0,222	0,9985	0,7304	1,0104	1,0104	0,045	0,9998	0,4938	382,50	38,9	0,5089	0,4425	0,4940	0,4850	-0,1439
25	-0,235	0,9985	0,7737	1,0188	1,0188	0,042	1,0001	0,4578	72,77	41,3	0,4731	0,4046	0,4578	0,4770	-0,1708
26	-0,247	0,9923	0,8113	1,0268	1,0267	0,038	0,9994	0,4219	72,67	43,7	0,4388	0,3635	0,4221	0,4621	-0,1867
27	-0,249	0,9995	0,8199	1,0348	1,0348	0,036	1,0000	0,3913	72,77	46,3	0,4090	0,3279	0,3913	0,4471	-0,1893
28	-0,254	0,9984	0,8344	1,0427	1,0426	0,033	0,9999	0,3639	73,62	48,6	0,3827	0,2958	0,3639	0,4311	-0,1975
29	-0,253	0,9979	0,8334	1,0497	1,0497	0,031	1,0007	0,3384	84,07	51,3	0,3578	0,2652	0,3382	0,4133	-0,1960
30	-0,209	0,9968	0,6861	1,0498	1,0498	0,024	0,9999	0,2590	411,31	60,2	0,2743	0,2021	0,2590	0,4108	-0,1553

Table 12. DMA test data of the TCE experiment

Meas. Point	F stat.	Strain stat	Stress stat	Lo	Lm	F dyn.	Strain dyn	Stress dyn	delta Time	T	E'	E''	IE*	tan delta	F cont.
	N	-	-	-	-	N	-	-	s	°C	-	-	-	-	N
1	-48,999	0,9957	8,6194	0,9856	0,9856	74,295	1,0011	30,9893	0,00	-50,8	29,4629	77,9244	30,9534	0,3509	-1,0608
2	-46,015	0,9988	8,0945	0,9860	0,9860	66,724	1,0117	27,8313	131,29	-47,7	26,0474	72,1606	27,5104	0,3676	-0,9656
3	-41,918	1,0093	7,3739	0,9866	0,9866	57,855	1,0097	24,1320	45,91	-45,8	22,5073	65,1644	23,9016	0,3842	-0,7935
4	-35,760	1,0060	6,2906	0,9868	0,9868	48,381	1,0096	20,1801	54,47	-43,8	18,7244	56,4005	19,9895	0,3997	-0,8411
5	-30,507	1,0022	5,3665	0,9871	0,9871	39,976	1,0102	16,6743	59,56	-41,9	15,4066	47,6124	16,5069	0,4101	-0,8631
6	-26,392	1,0028	4,6426	0,9874	0,9874	33,010	1,0084	13,7690	57,46	-39,9	12,7229	39,7841	13,6550	0,4149	-0,7679
7	-22,895	1,0017	4,0275	0,9877	0,9877	26,960	1,0089	11,2454	65,17	-37,8	10,3891	32,4131	11,1465	0,4140	-0,8484
8	-20,402	1,0076	3,5890	0,9880	0,9881	22,462	1,0071	9,3690	57,26	-35,9	8,6877	26,7506	9,3034	0,4086	-1,0535
9	-18,239	1,0074	3,2083	0,9884	0,9884	18,730	1,0060	7,8125	58,83	-33,9	7,2773	21,8607	7,7660	0,3986	-1,0461
10	-16,536	1,0061	2,9089	0,9888	0,9888	15,856	1,0056	6,6138	56,86	-32,0	6,1907	17,9860	6,5771	0,3855	-0,9839
11	-14,980	1,0111	2,6352	0,9891	0,9891	13,423	1,0048	5,5989	62,41	-29,9	5,2747	14,6481	5,5726	0,3685	-1,1120
12	-13,918	1,0045	2,4484	0,9895	0,9896	11,564	1,0039	4,8234	58,21	-27,9	4,5744	12,0709	4,8046	0,3501	-0,9912
13	-12,765	1,0097	2,2455	0,9899	0,9899	10,022	1,0037	4,1804	62,56	-25,9	3,9902	9,9195	4,1652	0,3299	-1,0388
14	-11,938	1,0074	2,1000	0,9903	0,9903	8,875	1,0022	3,7019	57,41	-24,1	3,5580	8,3394	3,6938	0,3110	-1,1450
15	-11,184	1,0028	1,9673	0,9907	0,9907	7,959	1,0028	3,3197	54,11	-21,9	3,2048	7,0730	3,3104	0,2928	-0,8887
16	-10,499	1,0086	1,8469	0,9911	0,9911	7,097	1,0014	2,9603	66,52	-19,9	2,8763	5,9338	2,9562	0,2737	-0,9436
17	-10,027	1,0032	1,7638	0,9916	0,9916	6,448	1,0012	2,6897	60,67	-17,9	2,6244	5,0917	2,6865	0,2574	-0,9839
18	-9,708	1,0104	1,7078	0,9920	0,9920	5,915	1,0010	2,4673	58,72	-16,0	2,4162	4,4261	2,4649	0,2431	-1,1047
19	-9,258	1,0104	1,6286	0,9925	0,9925	5,424	1,0009	2,2625	62,06	-13,9	2,2227	3,8408	2,2606	0,2293	-0,9473
20	-8,760	1,0098	1,5410	0,9929	0,9929	5,036	1,0009	2,1007	57,06	-12,0	2,0686	3,4023	2,0989	0,2182	-1,0535
21	-8,313	0,9950	1,4624	0,9934	0,9933	4,670	1,0010	1,9481	65,92	-9,9	1,9223	2,9990	1,9460	0,2070	-0,9729
22	-8,072	1,0075	1,4199	0,9938	0,9938	4,389	1,0006	1,8305	55,51	-7,9	1,8101	2,7089	1,8295	0,1986	-1,0718
23	-7,680	1,0081	1,3510	0,9943	0,9943	4,112	1,0006	1,7149	63,28	-5,9	1,6986	2,4325	1,7140	0,1900	-0,9473
24	-7,515	1,0021	1,3220	0,9947	0,9947	3,884	1,0003	1,6202	56,81	-3,9	1,6071	2,2180	1,6196	0,1831	-1,0498
25	-7,193	1,0073	1,2653	0,9952	0,9952	3,662	1,0011	1,5276	62,07	-1,9	1,5160	2,0102	1,5259	0,1759	-0,9253
26	-7,050	1,0077	1,2402	0,9957	0,9957	3,483	1,0008	1,4530	55,96	-0,1	1,4439	1,8532	1,4519	0,1703	-1,0718
27	-6,820	1,0039	1,1996	0,9963	0,9963	3,261	1,0011	1,3603	141,53	5,3	1,3529	1,6602	1,3589	0,1628	-1,1450
28	-7,259	1,0003	1,2769	0,9971	0,9971	3,141	1,0005	1,3103	25,22	5,9	1,3046	1,5654	1,3096	0,1592	-1,2768
29	-7,230	1,0017	1,2718	0,9975	0,9975	3,065	1,0048	1,2784	25,36	6,4	1,2680	1,4947	1,2723	0,1564	-1,3244
30	-6,296	1,0102	1,1075	0,9975	0,9975	2,911	1,0005	1,2141	57,26	8,1	1,2104	1,3828	1,2136	0,1516	-0,9546
31	-6,172	1,0036	1,0857	0,9980	0,9980	2,786	1,0010	1,1622	57,27	10,1	1,1588	1,2849	1,1611	0,1471	-1,0278
32	-6,029	1,0033	1,0605	0,9984	0,9985	2,681	1,0003	1,1181	56,41	12,1	1,1162	1,2056	1,1178	0,1433	-0,9436
33	-5,937	1,0109	1,0444	0,9989	0,9989	2,598	0,9999	1,0835	56,31	14,1	1,0826	1,1434	1,0837	0,1401	-0,9729
34	-5,817	1,0022	1,0232	0,9992	0,9993	2,527	1,0001	1,0542	59,47	16,1	1,0534	1,0922	1,0541	0,1376	-0,9693
35	-5,718	1,0043	1,0058	0,9996	0,9996	2,457	1,0000	1,0248	60,86	18,1	1,0246	1,0414	1,0249	0,1349	-0,9876
36	-5,685	1,0000	1,0000	1,0000	1,0000	2,397	1,0000	1,0000	57,02	20,0	1,0000	1,0000	1,0000	0,1327	-1,0644

37	-5,527	1,0076	0,9723	1,0003	1,0003	2,334	1,0000	0,9734	62,92	22,2	0,9737	0,9572	0,9734	0,1304	-0,9766
38	-5,483	1,0034	0,9646	1,0007	1,0007	2,281	0,9999	0,9514	58,06	24,0	0,9521	0,9192	0,9515	0,1281	-0,9729
39	-5,370	1,0042	0,9446	1,0011	1,0011	2,214	1,0001	0,9236	64,02	26,2	0,9244	0,8737	0,9235	0,1254	-0,9619
40	-5,260	1,0081	0,9253	1,0014	1,0015	2,155	1,0003	0,8988	59,07	28,1	0,8997	0,8341	0,8986	0,1230	-0,9656
41	-5,172	1,0024	0,9098	1,0019	1,0019	2,096	0,9994	0,8742	58,62	30,1	0,8761	0,7958	0,8748	0,1205	-0,9766
42	-5,147	1,0103	0,9053	1,0023	1,0023	2,036	0,9998	0,8493	61,52	32,2	0,8511	0,7559	0,8495	0,1178	-1,0205
43	-5,011	1,0123	0,8815	1,0028	1,0028	1,974	0,9997	0,8234	61,01	34,3	0,8254	0,7173	0,8237	0,1153	-0,9839
44	-4,894	1,0081	0,8609	1,0032	1,0032	1,919	1,0000	0,8004	57,72	36,1	0,8024	0,6816	0,8005	0,1127	-0,9693
45	-4,828	1,0027	0,8493	1,0037	1,0037	1,870	1,0000	0,7801	58,91	38,1	0,7822	0,6499	0,7801	0,1102	-0,9510
46	-4,810	1,0054	0,8461	1,0041	1,0041	1,824	1,0001	0,7606	60,37	40,1	0,7628	0,6202	0,7606	0,1079	-1,0352
47	-4,689	1,0043	0,8248	1,0045	1,0046	1,779	1,0009	0,7422	61,02	42,2	0,7439	0,5911	0,7416	0,1054	-0,9656
48	-4,656	1,0110	0,8190	1,0050	1,0050	1,738	1,0002	0,7249	60,52	44,1	0,7273	0,5661	0,7248	0,1033	-0,9876
49	-4,594	1,0010	0,8081	1,0054	1,0054	1,703	1,0004	0,7103	57,00	46,0	0,7125	0,5443	0,7100	0,1014	-0,9619
50	-4,524	1,0079	0,7958	1,0058	1,0059	1,665	1,0003	0,6943	59,57	48,0	0,6968	0,5219	0,6941	0,0994	-0,9656
51	-4,506	1,0042	0,7926	1,0064	1,0064	1,625	0,9997	0,6780	60,17	50,0	0,6809	0,4974	0,6782	0,0969	-1,0498
52	-4,455	1,0107	0,7836	1,0068	1,0069	1,592	0,9991	0,6642	58,91	51,9	0,6677	0,4794	0,6649	0,0953	-1,0315
53	-4,337	1,0103	0,7630	1,0073	1,0073	1,560	1,0011	0,6505	64,62	54,2	0,6528	0,4540	0,6498	0,0923	-0,9583
54	-4,345	1,0064	0,7643	1,0078	1,0078	1,527	0,9993	0,6370	57,12	56,1	0,6404	0,4376	0,6374	0,0907	-1,0352
55	-4,275	1,0009	0,7521	1,0083	1,0083	1,501	1,0006	0,6261	60,82	58,1	0,6287	0,4206	0,6257	0,0888	-1,0059
56	-4,272	1,0062	0,7514	1,0088	1,0088	1,474	1,0005	0,6150	61,46	60,2	0,6178	0,4017	0,6147	0,0863	-1,0425

Table 13. DMA test data of the SA experiment

Meas. Point	F stat.	Strain stat.	Stress stat.	Lo	Lm	F dyn.	Strain dyn.	Stress dyn.	delta Time	T	E'	E''	IE*I	tan delta	F cont.
	N	-	-	-	-	N	-	-	s	°C	-	-	-	-	N
1	-349,832	0,5175	2,2704	0,9907	0,9893	149,951	0,7298	1,8839	0,00	-50,7	2,6089	0,6419	2,5745	0,0416	-1,0169
2	-349,953	0,4654	2,2712	0,9914	0,9900	149,975	0,7303	1,8842	112,78	-48,9	2,6066	0,6416	2,5723	0,0417	-0,9619
3	-349,920	0,4757	2,2710	0,9916	0,9902	149,949	0,7346	1,8839	71,47	-46,0	2,5911	0,6317	2,5569	0,0413	-1,1560
4	-349,964	0,4743	2,2713	0,9918	0,9903	149,946	0,7398	1,8838	58,81	-43,7	2,5728	0,6281	2,5389	0,0413	-0,8484
5	-349,880	0,4775	2,2707	0,9919	0,9905	149,976	0,7461	1,8842	57,27	-41,7	2,5515	0,6217	2,5179	0,0412	-0,9912
6	-349,949	0,4786	2,2712	0,9921	0,9906	149,959	0,7533	1,8840	58,02	-39,7	2,5271	0,6212	2,4938	0,0416	-0,8118
7	-349,978	0,4874	2,2714	0,9922	0,9908	149,946	0,7612	1,8838	58,66	-37,7	2,5006	0,6182	2,4677	0,0418	-0,9583
8	-349,931	0,4905	2,2711	0,9924	0,9910	149,981	0,7701	1,8843	59,76	-35,8	2,4723	0,6180	2,4398	0,0423	-1,0974
9	-349,971	0,4989	2,2713	0,9925	0,9911	149,952	0,7793	1,8839	62,97	-33,8	2,4426	0,6167	2,4105	0,0427	-1,1450
10	-349,967	0,5100	2,2713	0,9927	0,9913	149,937	0,7903	1,8837	67,83	-31,7	2,4087	0,6202	2,3772	0,0436	-0,6068
11	-349,898	0,5112	2,2708	0,9929	0,9915	149,970	0,8008	1,8841	59,25	-29,6	2,3774	0,6313	2,3465	0,0449	-1,1011
12	-350,165	0,5171	2,2726	0,9931	0,9917	149,945	0,8113	1,8838	59,97	-27,8	2,3463	0,6279	2,3158	0,0453	-1,0864
13	-349,956	0,5354	2,2712	0,9932	0,9920	149,971	0,8237	1,8842	58,27	-25,5	2,3113	0,6397	2,2814	0,0468	-1,0315
14	-350,015	0,5422	2,2716	0,9934	0,9922	149,971	0,8360	1,8841	59,51	-23,7	2,2775	0,6441	2,2481	0,0479	-1,1926
15	-349,931	0,5495	2,2711	0,9936	0,9924	149,933	0,8498	1,8837	57,67	-21,6	2,2397	0,6543	2,2110	0,0494	-1,0461
16	-349,905	0,5679	2,2709	0,9938	0,9926	149,943	0,8649	1,8838	58,32	-19,8	2,2008	0,6637	2,1728	0,0510	-0,6837
17	-349,978	0,5865	2,2714	0,9940	0,9928	149,950	0,8815	1,8839	60,61	-17,7	2,1596	0,6738	2,1323	0,0528	-0,6764
18	-349,982	0,5962	2,2714	0,9942	0,9931	149,968	0,8991	1,8841	61,97	-15,9	2,1175	0,6815	2,0909	0,0545	-1,1450
19	-349,901	0,6182	2,2709	0,9944	0,9934	149,950	0,9190	1,8839	60,32	-13,7	2,0714	0,6941	2,0456	0,0567	-0,7496
20	-349,920	0,6363	2,2710	0,9947	0,9936	149,952	0,9407	1,8839	61,81	-11,8	2,0235	0,7115	1,9987	0,0595	-0,5702
21	-349,978	0,6698	2,2714	0,9949	0,9940	149,965	0,9657	1,8841	62,12	-9,7	1,9713	0,7277	1,9475	0,0625	-0,5885
22	-349,960	0,7014	2,2713	0,9951	0,9943	149,938	0,9943	1,8837	66,12	-7,5	1,9143	0,7347	1,8915	0,0649	-0,5922
23	-349,909	0,7276	2,2709	0,9955	0,9947	145,776	0,9957	1,8315	61,32	-5,4	1,8585	0,7440	1,8366	0,0677	-1,2621
24	-349,934	0,7853	2,2711	0,9957	0,9951	141,074	0,9968	1,7724	64,31	-3,3	1,7966	0,7567	1,7759	0,0713	-0,9912
25	-349,923	0,8253	2,2710	0,9961	0,9956	135,969	0,9966	1,7082	59,91	-1,0	1,7319	0,7701	1,7124	0,0752	-1,1011
26	-349,858	0,8853	2,2706	0,9965	0,9962	131,261	0,9951	1,6491	60,23	0,1	1,6744	0,7838	1,6561	0,0792	-1,3720
27	-305,767	0,9823	1,9844	0,9966	0,9965	121,106	0,9974	1,5215	144,53	5,8	1,5409	0,8114	1,5253	0,0891	-0,5775
28	-292,481	0,9862	1,8982	0,9974	0,9973	113,107	0,9981	1,4210	58,27	7,9	1,4367	0,8467	1,4236	0,0997	-1,0828
29	-277,859	0,9853	1,8033	0,9981	0,9980	106,600	0,9961	1,3393	52,67	9,8	1,3554	0,8765	1,3443	0,1094	-1,4781
30	-253,184	0,9826	1,6432	0,9986	0,9985	101,477	0,9982	1,2749	51,25	11,4	1,2862	0,9063	1,2771	0,1192	-1,1011
31	-239,499	0,9924	1,5544	0,9992	0,9991	96,874	0,9987	1,2171	48,02	13,1	1,2259	0,9262	1,2186	0,1278	-1,2512
32	-214,395	0,9874	1,3914	0,9995	0,9994	92,428	0,9960	1,1612	49,51	14,8	1,1714	0,9459	1,1657	0,1366	-1,1853

33	-182,785	0,9892	1,1863	0,9995	0,9994	87,604	0,9955	1,1006	57,72	16,7	1,1091	0,9709	1,1055	0,1481	-1,3903
34	-162,733	0,9955	1,0561	0,9996	0,9996	82,925	0,9978	1,0418	59,26	18,8	1,0456	0,9907	1,0441	0,1603	-1,0571
35	-154,082	1,0000	1,0000	1,0000	1,0000	79,596	1,0000	1,0000	50,22	20,3	1,0000	1,0000	1,0000	0,1692	-1,1706
36	-132,438	1,0000	0,8595	0,9999	0,9999	74,567	1,0000	0,9368	67,57	22,5	0,9345	1,0144	0,9369	0,1836	-0,7972
37	-119,767	1,0062	0,7773	1,0002	1,0002	69,677	0,9987	0,8754	58,02	24,5	0,8720	1,0213	0,8765	0,1982	-1,2255
38	-105,485	1,0127	0,6846	1,0003	1,0003	64,160	0,9967	0,8061	59,51	26,5	0,8018	1,0234	0,8088	0,2160	-0,7899
39	-91,976	1,0148	0,5969	1,0005	1,0005	58,509	1,0002	0,7351	57,41	28,4	0,7254	1,0161	0,7350	0,2370	-0,9619
40	-79,301	1,0155	0,5147	1,0006	1,0006	52,639	1,0011	0,6613	57,92	30,3	0,6484	0,9979	0,6606	0,2604	-1,3354
41	-68,186	1,0245	0,4425	1,0008	1,0008	46,617	0,9995	0,5857	58,17	32,3	0,5715	0,9647	0,5860	0,2856	-1,0828
42	-57,734	1,0175	0,3747	1,0009	1,0009	40,704	1,0004	0,5114	61,21	34,3	0,4949	0,9147	0,5112	0,3127	-0,9180
43	-49,365	1,0339	0,3204	1,0011	1,0012	35,535	1,0034	0,4464	59,85	36,3	0,4276	0,8544	0,4450	0,3381	-0,9290
44	-42,607	1,0271	0,2765	1,0013	1,0014	30,864	1,0005	0,3878	59,48	38,4	0,3697	0,7901	0,3876	0,3616	-0,7533
45	-37,324	1,0324	0,2422	1,0016	1,0017	27,048	1,0022	0,3398	57,17	40,2	0,3213	0,7254	0,3391	0,3820	-1,2805
46	-31,861	1,0360	0,2068	1,0018	1,0019	23,325	1,0045	0,2930	58,30	42,1	0,2745	0,6533	0,2918	0,4026	-0,8338
47	-26,970	1,0358	0,1750	1,0021	1,0022	19,888	1,0102	0,2499	60,67	44,2	0,2311	0,5779	0,2474	0,4232	-0,6068
48	-22,672	1,0312	0,1471	1,0025	1,0026	16,640	1,0036	0,2091	60,97	46,2	0,1933	0,5043	0,2083	0,4414	-1,1011
49	-18,773	1,0317	0,1218	1,0028	1,0029	13,962	1,0014	0,1754	60,16	48,3	0,1615	0,4373	0,1752	0,4580	-1,0498
50	-15,643	1,0406	0,1015	1,0032	1,0033	11,778	1,0011	0,1480	59,10	50,2	0,1357	0,3776	0,1479	0,4709	-0,9583
51	-13,380	1,0327	0,0868	1,0035	1,0036	9,921	1,0003	0,1246	60,42	52,2	0,1139	0,3235	0,1246	0,4805	-0,9619
52	-11,682	1,0407	0,0758	1,0039	1,0040	8,407	1,0010	0,1056	59,61	54,2	0,0962	0,2769	0,1055	0,4869	-0,8155
53	-10,327	1,0283	0,0670	1,0042	1,0043	7,121	1,0005	0,0895	60,47	56,3	0,0814	0,2360	0,0894	0,4902	-0,9253
54	-9,415	1,0201	0,0611	1,0045	1,0046	6,091	0,9996	0,0765	59,31	58,2	0,0697	0,2022	0,0766	0,4907	-0,8484
55	-8,701	1,0338	0,0565	1,0048	1,0049	5,231	0,9995	0,0657	58,71	60,2	0,0599	0,1730	0,0658	0,4882	-0,9802

Table 14. DMA test data of the HCA experiment